Molecules Involved in Purkinje Cell Dendritic Development and Spinocerebellar Ataxias

Inauguraldissertation

Zur

Erlangung der Würde eines Doktors der Philosophie

vorgelegt der

Philosophisch-Naturwissenschaftlichen Fakultät

der Universität Basel

von

Qinwei Wu

Basel, 2020

Genehmigt von der Philosophisch-Naturwissenschaftlichen Fakultät

auf Antrag von

Prof. Josef Kapfhammer
Prof. Markus Rüegg
Prof. Beat Schwaller

Basel, den 15. September 2020

Dekan
Prof. Martin Spiess

Table of Contents

List of Abbreviations

ARCA	Autosomal recessive cerebellar ataxia
Ca	Calcium
CACNA1G	Calcium voltage-gated channel subunit alpha1 G
Car8	Carbonic anhydrase related protein 8
CB6	B6CF1, mouse strain
CELSR2	Cadherin EGF LAG seven-pass G-type receptor 2
CF	Climbing fiber
CGN	Cerebellar granule cell
CNS	Central nervous system
Cpd	Compound
DAG	Diacylglycerol
DCN	Deep cerebellar nuclei
DHPG	(RS)-3,5-Dihydroxyphenylglycine
DIV	Days *in vitro*
DRAK2	DAP kinase-related apoptotic kinase 2
E	Embryonic day
EA2	Episodic ataxia type 2
EGL	External granule layer

FHM	Familial hemiplegic migraine
FVB	Friend leukemia virus B, mouse strain
ITPR1	Inositol 1,4,5-Trisphosphate Receptor Type 1
G protein	Guanine nucleotide-binding protein
GABA	Gamma-aminobutyric acid
GAP	GTPase-activating protein
GFP	Green fluorescent protein
GPCR	G protein coupled receptor
GRM1	Glutamate metabotropic receptor 1
IGL	Internal granule layer
IP3	Inositol 1,4,5 trisphosphate
INPP5A	Inositol polyphosphate-5-phosphatase A
KCNC3	Potassium voltage-gated channel subfamily C member 3
KCND3	Potassium voltage-gated channel subfamily D member 3
LTD	Long term depression
MCHR1	Melanin-concentrating hormone receptor 1
mGluR1	Metabotropic glutamate receptor, type 1
ML	Molecular layer
Mwk	Moonwalker
P	Postnatal day

PB	Phosphate buffer
PC	Purkinje cell
PCL	Purkinje cell layer
PCR	Polymerase chain reaction
PF	Parallel fiber
PKC	Protein kinase C
PLC	Phospholipase C
PMA	Phorbol-12-myristate-13-acetate
PP2A	Protein phosphatase 2A
PPP2R2B	Protein phosphatase 2 regulatory subunit B beta
PRKCG	Protein kinase C gamma
RAR	Retinoic acid receptor
RGS8	Regulator of G protein signaling 8
RORα	RAR-related orphan receptor alpha
SCA	Spinocerebellar ataxia
SPTBN2	Spectrin beta, non-erythrocytic 2
STK17B	Serine/threonine-protein kinase 17B
TBP	TATA-Box binding protein
TRE	Tetracycline response element
TRPC3	Transient receptor potential cation channel, type 3

tTA	Tet TransActivator
UBC	Unipolar brush cell

Summary

Spinocerebellar ataxias (SCAs) are a group of hereditary neurodegenerative diseases which are caused by diverse genetic mutations in a variety of different genes. The genetic background of SCAs can be classified into two groups: Group I repeat expansion SCAs, are caused by dynamic repeat expansion mutations, such as SCA1 and SCA7, and Group II conventional mutation SCAs are caused by mutations in specific genes, such as Protein Kinase C gamma (PKCγ) in SCA14. In the moment it is still unclear by which mechanisms the genetic mutations cause the disease. Several genes have been identified to be dysregulated in SCAs, but it is not well understood how these genes contribute to the pathogenesis of the disease.

An important open question is whether there are some key genes which are dysregulated in both Group I and Group II types of SCAs. Such genes might help us to pinpoint potential pathological mechanisms shared by all SCAs. As a starting point of my thesis I have compared microarray data from published SCA1 and SCA7 mouse models (both Group I) and a transgenic mouse model of SCA14 from our own lab (Group II) with a constitutive activation of the PKCγ kinase (PKCγ S361G mice). With this comparison, I have identified three potential key molecules (RGS8, STK17B and INPP5A) dysregulated in all three SCA mouse models. Recently, INPP5A has been reported to contribute to neuropathology of SCA17, supporting our concept of key molecules being involved in SCA pathogenesis.

In this thesis, the potential key molecules RGS8 and STK17B have been studied in more detail and their role for Purkinje cell dendritic development and for SCA pathogenesis has been explored. We showed that RGS8 is specifically expressed in Purkinje cells in the mouse cerebellum. Further studies showed that increased expression of RGS8 in Purkinje cells is associated with an increased activity of the mGluR1-PKCγ signaling pathway. Functional experiments showed that RGS8 overexpression could protect Purkinje cells from the negative effects of mGluR1 activation on dendritic growth. Our results indicate that RGS8 is an important

mediator of mGluR1 pathway dysregulation in Purkinje cells and it is well known that abnormal mGluR1 signaling is found in several different types of SCAs.

STK17B is one of the molecules downstream of PKCγ signaling. STK17B is strongly expressed in Purkinje cells starting at early postnatal development. The expression of the STK17B protein was reduced in dissociated cerebellar cultures of SCA14 S361G mice in parallel with a reduction of the dendritic tree size of Purkinje cells in this mouse model. We showed that PMA treatment induced a strong decrease of STK17B expression in Purkinje cells. As STK17B is known to be a substrate and phosphorylated by PKCγ, we overexpressed the phosphorylation mimetic form of STK17B(S351D) in Purkinje cells. We found that overexpression STK17B(S351D) in Purkinje cells did indeed inhibit dendritic growth of Purkinje cells. The regulation of its expression and our functional studies suggest that STK17B downregulation in the SCA14 mouse model might be a protective reaction protecting Purkinje cells from the constant activation of PKCγ signaling in the SCA14 PKCγ S361G mouse model.

Our findings show that the study of molecules with a common dysregulation in SCAs caused by mutations in different genes is a fruitful strategy to learn more about the pathological mechanisms causing SCAs.

Chapter 1: Background

1.1 Spinocerebellar ataxias (SCAs)

1.1.1 SCAs overview

Spinocerebellar ataxias (SCAs) are a heterogeneous group of the autosomal dominantly inherited progressive disorders with degeneration and dysfunction of the cerebellum (Durr, 2010; Klockgether et al., 2019; Seidel et al., 2012). The name of these disorders, “spinocerebellar ataxias”, consists of two terms. The word “spinocerebellar” is associated with the involvement of the “spinocerebellum”, yielding the typical pattern of the ataxia. The word “ataxia”, coming from the Greek word “a taxis”, means “lack of order” and it denotes a clinical syndrome of incoordination. So far, there are more than 40 genetically distinct subtypes of SCA. The names of each subtype are followed by progressive numbers that represent the chronological order by which the disease locus or the causative gene of this subtype was identified. The genetic background of SCAs can be classified into two groups: Group I repeat expansion SCAs, such as SCA1 and SCA2 which are caused by dynamic repeat expansion mutations, typically polyglutamine repeat expansions, and Group II conventional mutation SCAs (non-repeat expansion SCAs), which are caused by nonsense mutations, missense mutations, deletions or insertions, such as SCA5 or SCA14. In general, signs and symptoms can develop in patients with SCA at any time from childhood to late adulthood, but most common is the adult-onset (Durr, 2010; Klockgether et al., 2019; Seidel et al., 2012). Previous studies have shown that the age of onset of Group II conventional mutation SCAs is earlier than that of SCAs due to polyglutamine repeat expansions (Durr, 2010; Klockgether et al., 2019). The clinical features of all SCAs include progressive loss of balance and coordination, accompanied by slurred speech. The mobility and communicative skills of individuals with SCA are reduced and many SCAs lead to premature death. As the name suggests, pathological changes of SCA occur primarily in the nervous system and the cerebellum is the principal affected part of the brain. Purkinje cell

degeneration, which leads to cerebellar atrophy, occurs in most SCAs (Durr, 2010; Klockgether et al., 2019; Seidel et al., 2012).

1.1.2 Group I repeat expansion SCAs

Group I repeat expansion SCAs are primarily caused by CAG repeat expansion mutations in the traditional open reading frames that encode stretches of pure glutamine in the respective disease proteins, such as Ataxin-1 protein in SCA1, Ataxin-2 protein in SCA2 and Ataxin-7 protein in SCA7. The mutations of the causative genes underlying the polyglutamine in SCA normally hold about 100 CAG repeats (Durr, 2010). Repeat expansions can also occur in non-coding regions. For example, SCA12 is caused by a CAG repeat expansion in the 5'UTR non-coding region of the *PPP2R2B* gene, which encodes the regulatory subunit B beta isoform (PR55β) of protein phosphatase 2A (PP2A) (Holmes et al., 1999). The PP2A is a trimeric enzyme that has been shown to be involved in many cellular functions (Millward et al., 1999) and the region of the CAG repeats is associated with the putative promoter region of *PPP2R2B* gene. The repeat expansion appears to increase the transcription of this variant from the promoter region and may influence the function of PP2A in brain, although the exact role of PR55β is not so clear with respect to the regulation of PP2A activity (Holmes et al., 1999). Non-coding expansions are not only CAG repeats. In contrast to translated CAG repeat expansions, in SCA10 patients the repeat of the *ATXN10* gene in intron 9 consists of an expansion of the pentanucleotide ATTCT repeat and comprises up to 4500 repeats (Alonso et al., 2006; Matsuura et al., 2000). These mutations suggest that the pathogenic mechanism of SCA10 should not only be considered as a loss of function but also as a gain of function. This large expansion could have effects on the transcriptional level or post-transcriptional steps (Klockgether et al., 2019; Matsuura et al., 2000). These studies show that the repeat mutations in the intronic regions or non-coding regions may primarily cause diseases at the transcriptional or regulatory level.

In Group I repeat expansion SCAs, polyglutamine-related SCAs are more widely studied than other types of SCA, and they belong to the class of polyglutamine diseases, such as Huntington's disease (Havel et al., 2009; Ortega and Lucas, 2014). Expanded CAG repeats occur in polyglutamine diseases, which produce abnormally long polyglutamine proteins that are associated with pathogenesis. Although the normal proteins also have glutamine stretches, they are in the right range and only long glutamine tract leads to severe disease symptoms (Klockgether et al., 2019). In this context, the disease-associated proteins often lead to an aggregation or accumulation that is deposited and increases the burden in cells (Wang et al., 2013). However, pathology of polyglutamine-related SCAs is more complicated and not only depends on toxic aggregation of the mutated proteins. Since glutamine has been reported to support conformational changes of normal proteins, the disease-associated proteins with polyglutamine repeats may lose the correct biological protein conformation which changes their interaction with the usual targets and may also lead to inappropriate interactions with other endogenous proteins (Ju et al., 2014; Lim et al., 2008). In SCA1, Ataxin-1 is a transcription co-factor that interacts with numerous other proteins, including the transcriptional repressor protein that helps to regulate gene expression. The disease-associated polyglutamine Ataxin-1 protein has the ability to alter its normal conformational state (Lam et al., 2006). Instead of interacting with normal target proteins in the correct conformational state, the mutant Ataxin-1 protein can also interact with transcriptional repressor proteins, such as Capicua, which influences global gene expression (Fryer et al., 2011; Ingram et al., 2016; Lam et al., 2006). In addition, many important cellular signal transduction pathways are disrupted because many proteins are accumulated and become deposited in the cell nuclei (Havel et al., 2009). For example, in SCA3, a mutated Ataxin-3 protein is aggregated to neuronal nuclear inclusion bodies. A large number of proteins, including transcriptional factors, are associated with Ataxin-3 (Seidel et al., 2010). Intracellular aberrant protein aggregation and inclusion body formation indirectly or directly interferes with membrane transport, e.g. an increased cargo load, which increases the pathological load on neurons (Wang et al., 2013).

1.1.3 Group II conventional mutation SCAs

Group II conventional mutation SCAs have been studied recently as more and more types of SCA caused by conventional mutations in certain genes have been identified. These mutations offer researchers the opportunity to identify key pathways related to the pathogenic mechanism of SCAs and Purkinje cell degeneration.

SCA5, as a representative of the Group II type of SCA, was a relatively early identified and is caused by conventional mutations of the *SPTBN2* gene (Ikeda et al., 2006), which encodes for the Beta-III spectrin protein highly expressed in cerebellar Purkinje cells (Ohara et al., 1998). The mutated Beta-III spectrin protein causes progressive motor deficits and cerebellar degeneration in an SCA5 mouse model. Since endogenous Beta-III spectrin interacts with metabotropic glutamate receptor 1 (mGluR1), Beta-III spectrin mutant protein interferes with cell signaling by changing the mGluR1 localization and inducing dysfunction of mGluR1 at the dendritic spines of Purkinje cells (Armbrust et al., 2014). mGluR1 is encoded by *GRM1* gene. Missense mutations of *GRM1* were first reported to lead to an ataxia phenotype in mice (Rossi et al., 2010). Later, *GRM1* has been identified as the causative gene of autosomal recessive cerebellar ataxia (ARCA) in humans (Guergueltcheva et al., 2012). Recently, SCA44 has been found to be caused by heterozygous dominant mutations of *GRM1* gene that cause different phenotypes. Truncation mutations of the *GRM1* cause a dominant negative effect in juvenile-onset ataxia phenotypes, and point mutation of the *GRM1* with increased receptor activity leads to an adult-onset cerebellar ataxia phenotypes (Watson et al., 2017).

The alteration of calcium channel is believed to be an important factor in the pathology of SCAs. SCA6, which is caused by a CAG repeat expansion in the *CACNA1A* gene, encoding the voltage-gated calcium channel subunit alpha 1A, belongs to the Group I type of SCA (Zhuchenko et al., 1997), but there are also a number of point mutations of *CACNA1A* in SCA6 patients (Alonso et al., 2003; Du and Gomez, 2018). Overlapping phenotypes have been reported for SCA6 caused by missense mutations, episodic ataxia type 2 (EA2) and familial hemiplegic migraine (FHM). The causative gene of EA2 and FHM is also *CACNA1A*, previously

called *CACNL1A4* (Ophoff et al., 1996). Similar to SCA6 involving calcium channels, many genes causing Group II conventional mutation SCAs have been found to be involved in the regulation of the calcium equilibrium. SCA15 (Hara et al., 2008), also known as SCA16 (Iwaki et al., 2008), is caused by a heterozygous mutation in the *ITPR1* gene and by deletions involving the *ITPR1* gene. *ITPR1* gene encodes inositol 1,4,5-trisphosphate receptor type 1, mediating intracellular calcium release. The ITPR1 protein had a decreased expression in lymphocytes of the patient, suggesting a loss of function or a haploinsufficiency of ITPR1 (Novak et al., 2010; Van De Leemput et al., 2007). SCA29 is also related to the *ITPR1* gene, but has different single-nucleotide variants in ITPR1. The clinical feature of SCA29 differs significantly from SCA15. The SCA29 missense mutations of ITPR1 are localized in the functional domain that refers to coupling or regulatory events and phosphorylation sites to influence the regulation of ITPR1 signaling (Huang et al., 2012). The causative gene for SCA41 is *TRPC3*, which encodes the short transient receptor potential channel 3, which also regulates intracellular calcium (Fogel et al., 2015; Prestori et al., 2020). The causative gene for SCA42 is *CACNA1G*, which encodes voltage-dependent T-type calcium channel subunit α1 G, which is highly expressed in the cerebellum. The mutated CACNA1G protein causes a shift of the current-voltage and steady-state activation curves with a higher slope factor of the inactivation curve of the Cav3.1 channels (Coutelier et al., 2015). The SCA42 mouse model shows an adult-onset ataxic phenotype going together with cerebellar Purkinje cell loss, similar to the reported phenotype in SCA42 patients. The voltage-dependence of T-type Ca^{2+} channels is altered with the expression of the mutant CACNA1G protein in Purkinje cells (Hashiguchi et al., 2019).

Some genes causing SCAs are also linked to potassium channels, suggesting their importance in pathogenesis of SCAs. *KCNC3*, the causative gene of SCA13 encodes the voltage-gated potassium channel subfamily C member 3 (Khare et al., 2017; Waters et al., 2006). Although the mutant KCNC3 protein was shown to have a relatively normal membrane trafficking, electrophysiological experiments have shown a reduced inactivation and sensitivity to the actin depolymerizer latrunculin B (Khare et al., 2018). SCA19, also known as SCA22, is caused by mutations in the *KCND3* gene (Lee et al., 2012), which encodes voltage-gated potassium channel

subfamily D member 3 (Duarri et al., 2012). A dominant negative effect on protein biosynthesis and voltage-dependent gating of Kv4.3 potassium channels of SCA19/22 mutants has been proposed based on the study of biophysical and biochemical properties of the mutant KCND3 protein. The mutant KCND3 protein showed a loss of function electrophysiological profile. KCND3 mutants have also increased protein degradation and obstruction of membrane trafficking (Hsiao et al., 2019). It is expected that the associated pathways or channels associated with the genes of the conventional mutations will be found and it will eventually be possible to understand how the mutations induce the SCAs.

1.1.4 SCA14

The clinical manifestations of Spinocerebellar ataxia type 14 (SCA14) mainly include ataxia, oculomotor disturbance and dysarthria. In some cases, a psychological syndrome or cognitive deficit may also occur. Lifespan is relatively normal in SCA14 patients, and the onset may extend from childhood to late adulthood. The *PRKCG* gene has been identified as the causative gene for SCA14, located on chromosome 19q (Koht et al., 2012; Newton, 1995). The *PRKCG* gene encodes protein kinase C gamma (PKCγ), which is mainly expressed in the brain and is strongly expressed in cerebellar Purkinje cells (Barmack et al., 2000; Hirai, 2018; Moriya and Tanaka, 1994). This expression pattern supports the marked loss of cerebellar Purkinje cells observed in a post-mortem study (Wong et al., 2018). To date, more than 40 mutations of *PRKCG* gene have been identified in SCA14 patients (Figure 1.1). Although changes of kinase activity have been found based on functional studies of PKCγ mutant proteins expressed in cell lines, the pathogenesis of SCA14 is still unclear. Loss-of-function, gain-of-function and dominant-negative-function have been suggested, but none of them can explain the pathology sufficiently. PKCγ knockout mice show a relative normal cerebellar development and function making a simple loss of function explanation unlikely (Abeliovich et al., 1993). Indeed, inhibition of PKCγ activity by pharmacological inhibitors in cerebellar organotypic slice culture may even promote Purkinje cell dendritic development (Schrenk et al., 2002). The hypothesis of a toxic gain-of-function has been suggested as the aggregation of PKCγ has been observed in some studies and induces a toxic effect

on the cells. For the H101Y PKCγ mutation it has been reported that the H101Y PKCγ transgenic mouse has an ataxic phenotype with altered morphology and loss of Purkinje cells. H101Y PKCγ protein leads to a reduction in total PKC enzyme activity (Zhang et al., 2009). In addition to the reduction of kinase activity of PKCγ mutations, several PKCγ mutants with increased kinase activity have been found (Adachi et al., 2008). PKC activator PMA does induce a reduction of the dendritic growth of Purkinje cells, suggesting that increased kinase activity could be an explanation for some of the cases. In our previously published S361G PKCγ transgenic mouse model of SCA14, Purkinje cells had severe morphological abnormalities similar to the inhibition of dendritic growth induced by PMA treatment. These findings support the concept that increased kinase activity of PKCγ is involved in SCA14 pathogenesis (Ji et al., 2014; Shimobayashi and Kapfhammer, 2017). More recently, a PKCγ mutant has been reported to be caused by the PKCγ(R76X), which produces a short peptide with a pseudosubstrate domain that served as a pan-PKC inhibitor. It is believed that the PKCγ(R76X) peptide functions in a dominant negative manner by inhibiting PKC activity and causing the death of Purkinje cells (Shirafuji et al., 2019).

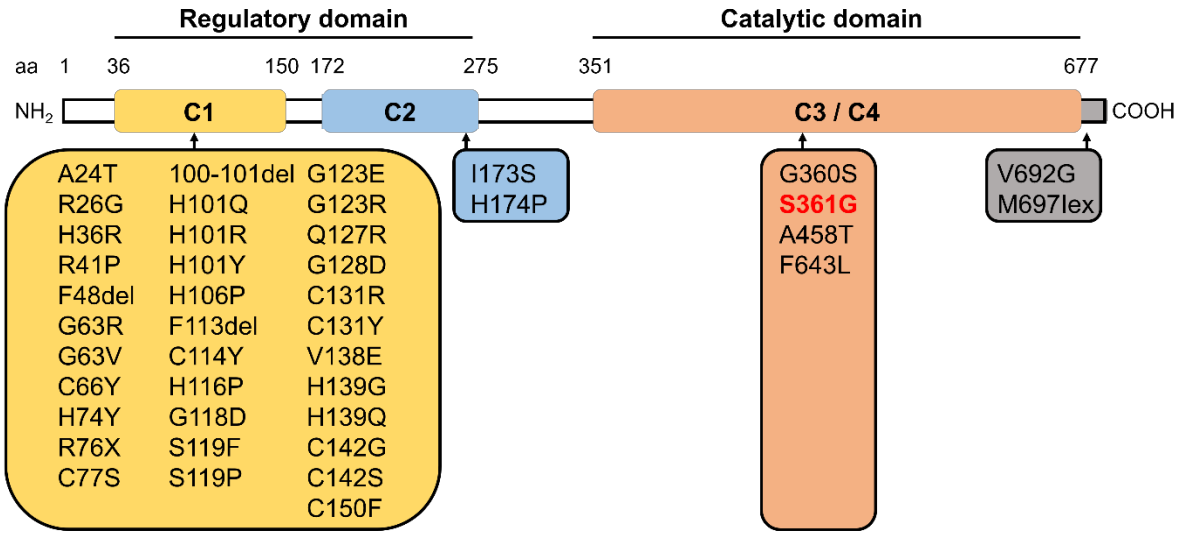

Figure 1.1 All reported SCA14-associated mutations in PKCγ are listed.

In this study the transgenic mouse model of S361G in the kinase domain of PKCγ is used.

1.2 Cerebellar Purkinje cell (PC) development

1.2.1 Cerebellum

The cerebellum is an important part of the body's motor control systems. It is also known as the little brain, which occupies only about 10% of the volume of the entire brain, but about half of all the neurons in the brain are located in the cerebellum (Azevedo et al., 2009; Yamazaki et al., 2019). The cerebellum receives input from motor regions and integrates the information for refining movements.

The cerebellum is located in the posterior cranial fossa behind the brain stem, pons and medulla (Figure 1.2A and B). It is separated from the inferior portion of the occipital lobes by the cerebellar tentorium and is composed of an outer layer of gray matter, an inner layer of white matter and the deep cerebellar nuclei (DCN). The cerebellum is connected to the rest of the brain by three cerebellar peduncles called the inferior, the middle and the superior cerebellar peduncle which anchor to the dorsal part of the brain stem. The adult cerebellum is divided into three main anatomical regions along the mediolateral axis: Hemispheres, Paravermis, and Vermis. According to conserved foliation patterns, 10 lobules are formed along the sagittal axis of the cerebellum (Figure 1.2A). The cerebellum can also be divided into three functional regions (Klein et al., 2016; White and Sillitoe, 2013): Vestibulocerebellum, Spinocerebellum and Cerebrocerebellum (also called Pontocerebellum) (Figure 1.2B).

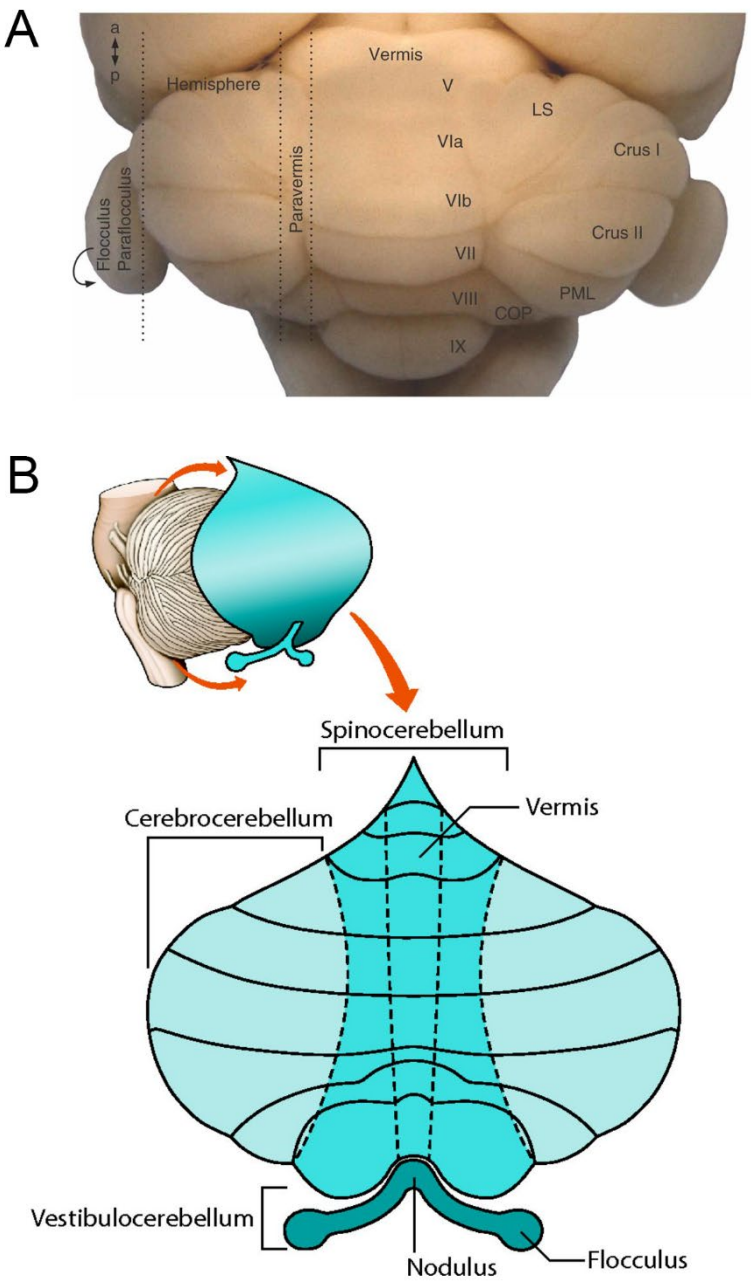

Figure 1.2 Anatomy and three functional regions of the cerebellum.

(A) The adult cerebellum is divided into three major anatomical regions: hemispheres, paravermis, and vermis. 10 lobules are divided and indicated (labelled roman numerals) in the cerebellum. LS, lobulus simplex; PML, paramedian lobule; COP, copula pyramidis; a, anterior; p, posterior. The image is adapted from (White and Sillitoe, 2013). **(B)** The cerebellum can be divided into three functional regions:

The vestibulocerebellum (lobules IX/X), the oldest part of the cerebellum, receives its input from the vestibular nuclei of the brain stem. The spinocerebellum (vermis and paravermis) receives its inputs directly from the spinal cord. The cerebrocerebellum (lateral parts of the hemispheres), the largest and newest part of the cerebellum, receives its input mainly from the cortical areas of cerebrum. The picture is adapted from (Klein et al., 2016).

The Vestibulocerebellum, phylogenetically the oldest part of the cerebellum, consists of the flocculonodular lobe that receives vestibular and visual input. The Purkinje cells of this region project their axon directly back to the vestibular nuclei. It is responsible for balance, eye movements and vestibular reflexes. The Spinocerebellum consists of the vermis and the adjacent intermediate zone of the cerebellum. It receives somatosensory input from brain stem motor centers. The output runs via the deep cerebellar nuclei. This functional region is responsible for integration of the sensory input to maintain balance and command movements. The Cerebrocerebellum (or Pontocerebellum), the largest part of cerebellum, consists of the lateral hemispheres and projects via the dentate nuclei. Input from the motor areas of cerebral cortex reach the cerebellum through the pontine nuclei (afferents). The cerebellar cortex of the Cerebrocerebellum projects to the dentate nuclei and continues into the red nucleus and returns to the cerebral cortex via the ventral lateral nucleus of the thalamus (efferents). This functional subdivision supports the motor functions of the cortex with regard to the arrangement and timing of movements (Klein et al., 2016; White and Sillitoe, 2013).

The cerebellum is thought to have very specific functional roles due to its regular internal circuitry in the cerebellar cortex, which consists of three layers called the molecular layer, the Purkinje layer and the granule cell layer (Figure 1.3A and B). Within the cerebellum, there are several different types of cells, and the five most important cell types are Purkinje cells, granule cells, basket cells, stellate cells and Golgi cells. Out of these, the granule cells are the only excitatory neurons releasing the neurotransmitter glutamate and exciting the synapses to which they connect. The

other four types of cells are all inhibitory neurons, like the Purkinje cell mentioned above. It means that the primary output of the cerebellar cortex is inhibitory. In addition, there are several other types of cells in cerebellum. Unipolar brush cells (UBC) are a class of excitatory glutamatergic interneurons that are mainly present in the granule cell layer. Lugaro cells are primary sensory interneurons that are found under the Purkinje cell layer. The candelabrum cells are distributed throughout the cerebellar folia and the soma of candelabrum cells is squeezed between the cell bodies of Purkinje cells (Lainé and Axelrad, 1994). Glial cell types are also present in the cerebellum. Bergmann glia are unipolar astrocytes, associated with the organization of the molecular layer. They develop large processes in the plane of dendrites of Purkinje cells and their cell bodies are found in the Purkinje cell layer. Astrocytes are present in the granule cell layer. Oligodendrocytes are found in the granule cell layer and in the white matter of the cerebellum. All these cells occupy their place in the three-layer structure that is repeated throughout the cerebellum (Bihannic and Ayrault, 2016; Cerminara et al., 2015).

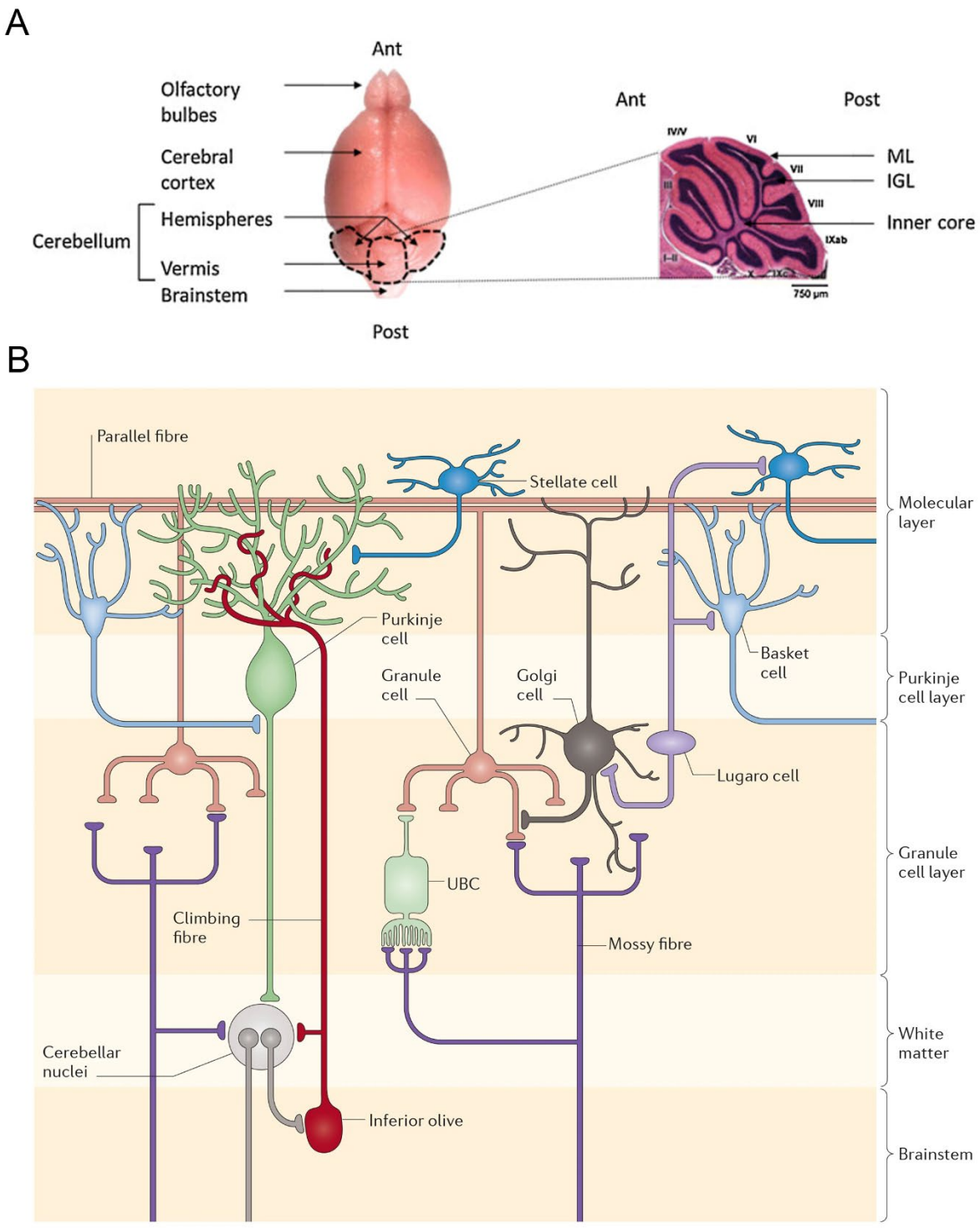

Figure 1.3 The cerebellar cytoarchitecture of rodents.

(A) The cerebellum and its compartmentations (dashed outline) are shown in a mouse brain. The cerebellar vermis is divided by the anatomical midline and the 10 cerebellar lobules (labeled I-X) are indicated in the picture (right side). Ant, Anterior;

IGL, Internal granule layer. The picture is adapted from (Bihannic and Ayrault, 2016). **(B)** The regular internal circuit in the cerebellar cortex comprising the molecular layer, the Purkinje layer and the granule cell layer. UBC, unipolar brush cell. The picture is adapted from (Cerminara et al., 2015).

The molecular layer consists mainly of the dendrites of the Purkinje cells and the parallel fibers with some inhibitory interneurons, mainly basket cells and stellate cells, which are loosely distributed between the Purkinje cell dendritic ramifications and the axons of the parallel fibers (Bihannic and Ayrault, 2016; Cerminara et al., 2015).

The Purkinje cell layer consists of the cell bodies of Purkinje cells, which are the output neurons of the cerebellar cortex. Purkinje cells are very large, and the diameter of the cell body can be as much as 80 micrometers and they have one of the most widely branched dendritic trees in the brain. The large dendritic trees of Purkinje cells enter the molecular cell layer where they form an interface and receive the synapses from the parallel fibers (Napper and Harvey, 1988), which are derived from the granule cells. Only the Purkinje cells project out of the cerebellar cortex. The Purkinje cell axon projects to the deep cerebellar nuclei and release GABA as an inhibitory neurotransmitter. Dendritic trees of Purkinje cells also receive the excitatory inputs from the climbing fibers, which originate from the inferior olivary nucleus (Bihannic and Ayrault, 2016; Cerminara et al., 2015).

The granule cell layer is the densest neuronal region in the cerebellum and is mainly formed by granule cells which are the most abundant neurons of the brains. Mossy fibers are the important excitatory input to the cerebellum and synapse on the granule cells. The granule cell sends an axon up through the Purkinje cell layer into the molecular cell layer. This axon then divides into two long fibers forming a T-shaped axon, forming the parallel fibers, which synapse on the dendritic spines of Purkinje cells. The Golgi cells are GABAergic inhibitory interneurons and form inhibitory synapses with the granule cells. They also receive the excitatory synaptic

inputs from mossy fibers that form the cerebellar glomerular synapses (Bihannic and Ayrault, 2016; Cerminara et al., 2015).

The deep cerebellar nuclei are the output structure of the cerebellum and project to many parts of the brain. They also send a feedback projection to the inferior olive and can suppress this signal at the subcortical level (Binda et al., 2020; D'Angelo and Casali, 2013).

The feedforward excitatory chain refers mainly to mossy fiber and granule cells. The mossy fibers, which originate in brain stem and spinal cord nuclei, have their terminals in the granule cell layer and excite granule cells and Golgi cells. In addition, they have a collateral branch sending the same information directly to the deep cerebellar nuclei. Golgi cells are also activated by parallel fibers and thus provide both feed-forward and feedback regulation to granule cells. The axons of granule cells form the parallel fibers in the molecular layer and send the excitatory signal to the highly branched dendritic tree of Purkinje cells and other cells in the molecular layer. Basket cells and stellate cells, which are also activated by parallel fibers, inhibit the excitatory inputs on Purkinje cells and participate in the regulation during the integration of information. The dendrite of a Purkinje cell is innervated by a single excitatory climbing fiber derived from the cells of the inferior olive in the brainstem, and one climbing fiber can activate a Purkinje cells. The output of Purkinje cells projects to the cells of the deep cerebellar nuclei and then to the cerebral cortex, the brainstem and the spinal cord. Purkinje cells send out inhibitory signals and inhibit the spontaneous activity of the deep cerebellar nuclei, which in the final step send out excitatory signals and regulate the output of the cerebellum. Therefore, the inhibitory loop includes inhibition by Golgi cells in the granule cell layer, inhibition by basket cell and stellate cells in the molecular layer, and inhibition by Purkinje cells (Binda et al., 2020; D'Angelo and Casali, 2013) (Figure 1.4).

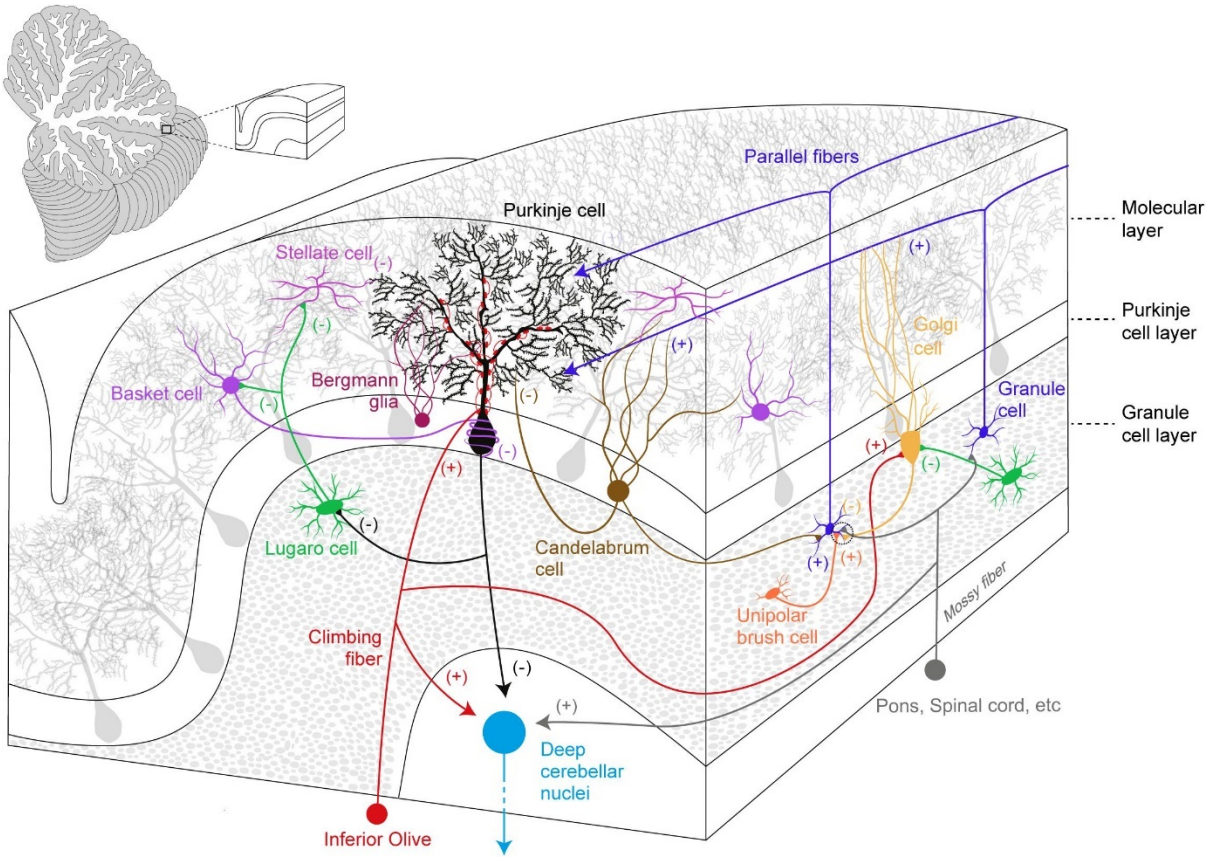

Figure 1.4 Wiring diagram of the cerebellar neuronal circuit organization.

The mossy fibers are exciting granule cells and send an axon collateral directly to the cells of the deep cerebellar nuclei. The mossy fiber indirectly sends excitatory signals to Purkinje cells. Parallel fibers formed by axons of granule cells send the excitatory signals directly to the Purkinje cells. Basket cells and stellate cells participate in the regulation of Purkinje cells during the integration of information. Climbing fibers originating from the cells of the inferior olive and also activate Purkinje cells and deep cerebellar nuclei. Purkinje cells project onto the cells of the deep cerebellar nuclei and inhibit them. The picture is adapted from (Binda et al., 2020).

1.2.2 PC growth and development

In the cerebellum, Purkinje cells are cells which have a large and highly branched dendritic tree. During development, one of the most important processes in Purkinje cells is dendritic growth (Figure 1.5) (Sotelo, 2004). Purkinje cells are originally produced in the ventricular zone from embryonic day 11 to 13. During this period, many molecular signals and environmental cues are involved in the regulation of dendritic development. The thyroid hormone L-3,3',5-triiodothyronine (T3) plays an important role for growth and branching of Purkinje cell dendritic arbors, and directly regulates Purkinje cell differentiation via activation of the thyroid hormone receptors (Heuer and Mason, 2003; Oppenheimer and Schwartz, 1997). After Purkinje cells are born they have a bipolar shape in the migratory period. Immature Purkinje cells then enter a process of dendritic regression (Sotelo and Dusart, 2009; Sotelo, 2004). During this phase in rodents, bipolar cells retract their primitive processes and extend many short protrusions. Development of Purkinje cells in this period is slow with little expansion of the dendritic tree. This phase continues up to postnatal day 6 or 7 in mice (Altman, 1972). When parallel fibers first appear in the immature molecular layer of the cerebellum, Purkinje cell development enters into a phase of rapid dendritic expansion (Armengol and Sotelo, 1991). RAR-related orphan receptor alpha (RORα) regulates the early dendritic differentiation and is critical for the progression to the phase of rapid dendritic expansion of Purkinje cells (Boukhtouche et al., 2006). Synaptogenesis between Purkinje cell dendrites and parallel fibers appears during this time (Armengol and Sotelo, 1991). Later, dendritic tree expansion becomes restricted to a single sagittal plane by dendritic reconstruction during the third to the fourth week. Mature dendritic trees of Purkinje cells are first present after four weeks. The maturation of electrophysiological properties in Purkinje cells proceeds in parallel to the dendritic expansion (McKay and Turner, 2005). Purkinje cell dendritic growth is regulated by a variety of mechanisms including the action of growth factors, thyroid hormone, and further regulators controlling Purkinje cell development (Kapfhammer, 2004).

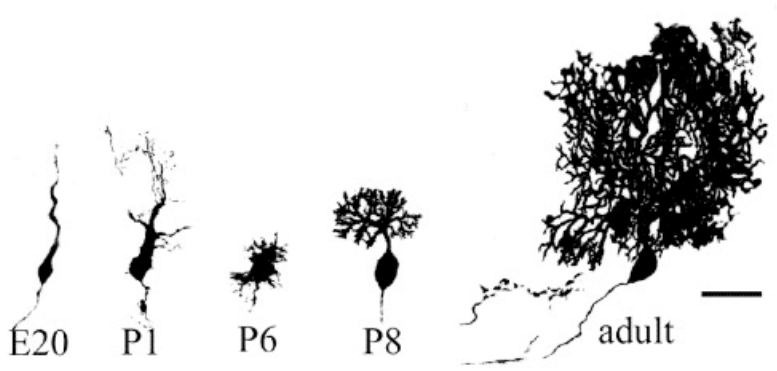

Figure 1.5 Morphological stages of Purkinje cell dendritic development from E20-Adult in rats.

Immature Purkinje cell enters a regression period up to P5. From P6 on, the ultimate dendritic tree is expanded. Scale bar: 55 μm. The image is adapted from (Sotelo, 2004).

Many molecules participating in the regulation of different stages of Purkinje cell development have been indenified, including dendritic growth, differentiation and maintenance. SCLIP protein is a member of the stathmin family and *SCLIP* mRNA is prominently expressed in Purkinje cells. SCLIP is an important factor that controls Purkinje cell dendritic growth during the early and later phases. In early steps of development of Purkinje cells, SCLIP is involved in dendrite formation. In the later stages of differentiation, it regulates dendritic elongation and branching (Poulain et al., 2008). Celsr2 protein is distributed in postnatal Purkinje cells (Shima et al., 2002) and controls dendritic morphogenesis implying a role of adhesion molecules for maintenance of dendritic branches of Purkinje cells (Shima et al., 2004). TRPC3 is mainly distributed in the cerebellar Purkinje cell layer during the stage of dendritic growth and functions in both dendritic growth and survival of Purkinje cells (Becker et al., 2009). TRPC3 is highly expressed in the soma and dendrites of Purkinje cells during the postnatal development of the cerebellum (Becker et al., 2009; Huang et al., 2007), and the high level of TRPC3 expression continues to the period of adulthood, suggesting that TRPC3 may also regulate the growth and refinement of dendritic trees of Purkinje cells in the cerebellar cortex during adulthood (Becker et

al., 2009). Beta-III spectrin has been identified to play a critical role in the organization of the dendritic tree and the development of dendritic spines of Purkinje cells. Beta-III spectrin knockout mice have defects of the ordered dendritic arborization, particularly a loss of monoplanar organization, a decreased dendritic diameter, a reduction of the density of dendritic spines and a reduced number of synapses in Purkinje cells. Purkinje cells from Beta-III spectrin knockout mice also show strongly reduced dendritic areas compared to wildtype cells in dissociated cultures (Gao et al., 2011). Carbonic anhydrase related protein 8 (Car8) is abundantly expressed in Purkinje cells and is important for synaptogenesis and maintenance of synaptic morphology and function in the cerebellum (Hirasawa et al., 2007). Car8 has been recently identified as a novel regulator of Purkinje cell dendritic development (Shimobayashi et al., 2016).

mGluR1, a subtype of the group I mGluRs, is most strongly expressed in Purkinje cells starting during the embryonic period (Catania et al., 1994; Göres et al., 1993; Lein et al., 2007; Shigemoto et al., 1992). Although no marked abnormality in cerebellar anatomy of mGluR1 deficient mice was found, the Purkinje cell dendritic arbors were found to be smaller and have a reduced complexity of Purkinje dendritic branches (Alba et al., 1994). In dissociated cultures of rat cerebellar Purkinje cell and granule cells, pharmacological inhibition of mGluR1 by application of the subtype-selective antagonist of group I metabotropic glutamate receptors 7-(hydroxyimino)cyclopropa[b]chromen-1a-carboxylate ethyl ester (CPCCOEt),reduced the number of surviving Purkinje cells and the size of their dendritic arbors. These findings have been confirmed by rat *in vivo* experiments via local injections of LY367385, a highly selective and competitive mGlu1a receptor antagonist, mGluR1 antisense oligonucleotides, or systemic administration of CPCCOEt (Catania et al., 2001). In contrast, in cerebellar organotypic slice cultures derived from P8 mouse pups and maintained for 12 days, pharmacological inhibition of mGluR1 by (RS)-alpha-methyl-4-carboxyphenylglycine (MCPG), a competitive metabotropic glutamate receptor antagonist, had an only minor negative effect on Purkinje cell dendritic morphology (Adcock et al., 2004). These studies indicate that mGluR1 signaling is essential for Purkinje cell growth and survival particularly at earlier developmental stages. At later developmental stages, mGluR1 signaling has an

important regulatory function in the period of rapid dendritic expansion in cerebellar slice cultures. When mGluR1 signaling was induced by treatment with Dihydroxyphenylglycine (DHPG), a group I mGluR activator, a severe reduction of Purkinje cell dendritic growth was found (Sirzen-Zelenskaya et al., 2006).

Increased PKCγ activity was identified as a negative regulator for Purkinje cell dendritic development. Although many isoforms of PKC are expressed in the cerebellum, PKCγ is specifically and strongly expressed in Purkinje cells (Barmack et al., 2000; Huang et al., 1988; Kose et al., 1988). PKCγ expression is relatively low at birth and increases in the postnatal period (Hashimoto et al., 1988; Yoshida et al., 1988). PKCγ can be activated by binding of diacylglycerol (DAG) and Ca^{2+} (Saito and Shirai, 2002). In rat organotypic slice cultures, Purkinje cells were shown to grow increased dendritic trees with more ramified dendritic branches with treatment of a general PKC inhibitor, GF109203X (Metzger and Kapfhammer, 2000). Treatment of an inhibitor specific for conventional PKC isoforms, Gö6976 also promoted extensive branching of Purkinje cells (Schrenk et al., 2002). In slice cultures from PKCγ deficient mice, Purkinje cells were shown to have expanded dendritic trees with an increased number of dendritic branching points compared to wildtype mice (Schrenk et al., 2002). When Purkinje cells are treated by phorbol-12-myristate-13-acetate (PMA), an activator of PKC, a marked reduction of the dendritic trees was shown in either organotypic slice cultures or dissociated cerebellar cultures (Ji et al., 2014; Metzger and Kapfhammer, 2000; Schrenk et al., 2002; Shimobayashi and Kapfhammer, 2017).

1.2.3 SCA and PC development

As many molecules are involved in the regulation of Purkinje cell development, some of them, which are highly expressed in Purkinje cells, such as Beta-III spectrin, TRPC3, mGluR1 and PKCγ, have also been identified as causative genes of SCAs and are probably associated with pathogenesis of SCAs. SCA5 is caused by gene mutations of *SPTBN2* encoding Beta-III spectrin protein (Gao et al., 2011; Ikeda et al., 2006; Ohara et al., 1998). The mutant of Beta-III spectrin protein was strongly

expressed in Purkinje cells by immunofluorescence staining in a SCA5 mouse model with a phenotype of progressive cerebellar degeneration (Armbrust et al., 2014). The mutation Arg762His of TRPC3 has recently been identified to result in SCA41 (Fogel et al., 2015; Prestori et al., 2020). To date, no SCA41 disease-associated mouse model has reported, however, the moonwalker (Mwk) mouse mutant is caused by a different Trpc3 point mutation T635A and exhibits profound impairment of growth and differentiation of Purkinje cell dendrites (Becker et al., 2009). The TRPC3 Arg762His mutation was shown to have a similar phenotype to the mouse Mwk Trpc3 mutation in cell experiments (Fogel et al., 2015). In addition, disrupted regulation of TRPC3 has been reported in other SCAs. TRPC3 downregulation has been reported in Purkinje cells of a SCA1 mouse model before the onset of Purkinje cell degeneration (Lin et al., 2000). Failure of TRPC3 phosphorylation by mutant SCA14 mutant PKCγ has been shown in cellular assays (Adachi et al., 2008). Mutations of PKCγ causes SCA14 and in a mouse model of SCA14 expression of mutated PKCγ leads to dendritic abnormalities of Purkinje cells (Ji et al., 2014; Shimobayashi and Kapfhammer, 2017; Trzesniewski et al., 2019). SCA44 is caused by mutations of mGluR1 and missense mGluR1 mutants result in increased receptor activity (Watson et al., 2017). Activation of the mGluR1 signaling has been reported in the moonwalker mouse model (Becker et al., 2009). These findings provide a possible link between molecules regulating Purkinje cell development and pathogenesis of SCAs. This hypothesis has been confirmed for some molecules, such as RORα, which is not a causative gene of SCAs but plays an important role during the progression of disease. The expression of RORα is downregulated in Purkinje cells from the SCA1 mouse model and RORα mediated Purkinje cell development determines disease severity of SCA1 (Boukhtouche et al., 2006; Serra et al., 2006). These results suggest that mutations in or dysregulation of the molecules that play a role for Purkinje cell development may contribute to SCAs and cerebellar diseases.

1.3 Common dysregulated molecules

1.3.1 Dysregulated gene expression in SCAs

The normal cellar pathway for growth, development and differentiation depend on the accurate gene expression. Dysregulation of gene expression is an acknowledged characteristic of several SCAs and has been proposed to trigger the pathogenesis of SCAs (Carlson et al., 2009; Helmlinger et al., 2006). Several mutant SCA causing proteins are recognized as key factors associated with the regulation of gene expression and contribute to gene regulation on the transcriptional level. In some representative types of SCAs caused by polyglutamines, such as SCA1 and SCA7, the causative protein are ataxins, which interact with transcriptional regulators. Ataxin-1 can directly interact with Capicua, the mammalian homolog of Drosophila Capicua and modulate the repressor activity of Capicua in mammalian cells. However, in the Ataxin-1 with polyglutamine expansion, the binding to and the repressor activity of Capicua are changed. Capicua is a key transcriptional regulator and plays an important role in gene expression especially for developmental processes (Atkey et al., 2006). In SCA7, the Ataxin-7 protein plays a role for gene expression through its interaction with the co-activator SAGA complex, an extremely conserved complex involved in gene expression (Lee et al., 2001; Yvert, 2000). SAGA is influenced by the mutant Ataxin7 and clusters in a dysfunctional negatively charged SAGA complex, that is proposed to be involved in the pathogenesis of expanded polyglutamine diseases (McMahon et al., 2005).

Some SCA causative genes are directly responsible for gene expression regulation. The TATA-Box binding protein (TBP) is a general transcription factor and mutants of TBP cause a CAG repeat expansion resulting in SCA17 (Friedman et al., 2007). TBP contains polyglutamine regions and these regions play a role in the ability of TBP to promote or inhibit transcription by interaction with the regulators or by binding to the different promoter areas. Mutations of TBP cause reduced affinity for binding to the relative region of DNA (Friedman et al., 2008). These studies suggest that mutated proteins of SCAs can affect gene expression directly or indirectly by changing the activity of signaling proteins resulting in a dysregulation of transcription. Many

studies therefore have focused on the analysis of the gene expression on the global transcriptional level by the use of animal or cellular models and aimed to identify the genes with strongly altered expression. These genes are expected to pinpoint the pathways associated with SCAs.

1.3.2 Common molecular mechanism

Based on the global transcriptional data, several common molecules have been found from different mouse models with cerebellar ataxic phenotype, indicating potentially important pathways associated with pathogenesis of SCAs and cerebellar ataxia. For example, *staggerer* mice exhibit a characteristic severe cerebellar ataxia due to an underdeveloped cerebellar cortex and unaligned Purkinje cells (Steinmayr et al., 1998). Overlap based analysis of microarray data from the SCA1 mouse model (Serra et al., 2006) and *staggerer* mouse (Gold et al., 2003) was performed and many common genes have been identified (Table 1.1). These common molecules will provide a better understanding of the disease mechanisms of SCAs and cerebellar ataxia.

Table 1.1 The common genes between microarray sets of SCA1 and *staggerer* mice. Adapted from (Serra et al., 2006).

		Staggerer		SCA1[82Q]	
GENE	PROTEIN	Microarray	Q-PCR	Microarray	Q-PCR
Calb1	calbindin-28K, Ca^{+2} binding protein	⇓		⇓	
Itpr1	inositol 1,4,5-triphosphate receptor 1	⇓		⇓	⇓
Slc1a6	EAAT4, glutamate transporter	⇓		⇓	⇓
Pcp2 (L7)	GoLoco G protein modulatory domain	⇓		⇓	⇓
Rora	RAR-related orphan Receptor α	⇓		⇓	
Kit1	kit ligand	⇓			⇓
Pcp4	calmodulin inhibitor	⇓		⇓	⇓
Spnb3	brain-specific β-spectrin III	⇓		⇓	
Idb2	inhibitor of DNA binding 2	⇓		⇓	
Grm1	mGluR1 glutamate receptor subunit		⇓		⇓
Atp2a2	SERCA2, Ca^{+2}-transporting ATPase	⇓			⇓
Cals1	CARP, an Itpr1 binding protein	⇓		⇓	⇓
Homer2		⇔		⇔	

****Genes to which RORα binds to the promoter (Gold et al., 2003).

Calbindin 1, belongs to the calbindin family of calcium-binding proteins and is known as a Purkinje marker in the cerebellum (Andressen et al., 1993; Celio, 1990). Calbindin 1 is on the top the molecules found by overlapping data between SCA1 mouse model (Serra et al., 2006) and the *staggerer* mouse (Gold et al., 2003). Defects of calbindin D28K affect the physiology of Purkinje cell and the calcium pathway (Airaksinen et al., 1997; Vecellio et al., 2000) and loss of one copy of calbindin D28K causes enhanced ataxia of SCA1 mice (Vig et al., 2012). Although Calbindin 1 is identified as common molecule, highly expressed in Purkinje cells, relatively normal Purkinje cell development is found in calbindin null mutant mice. This may be due to the partial compensation by high levels of another calcium-binding protein, parvalbumin (Schmidt et al., 2007), which is also strongly expressed in cerebellar Purkinje cells (Airaksinen et al., 1997; Celio, 1990; Kosaka et al., 1993; Toyoshi et al., 1985).

Sptbn2, also known as brain-specific Beta-III spectrin encoded by *Spnb3* gene, is identified in the overlapping set of genes of SCA1 and *staggerer* mice (Serra et al., 2006). The dominant-negative mutations in the human homolog of *SPTBN2* lead to SCA5 (Ikeda et al., 2006). Beta-III spectrin plays a role in basic membrane protein trafficking and localization in Purkinje cells and mutations in Beta-III spectrin causes SCA5 (for review see Perkins et al., 2016).

mGluR1 is another common molecule from overlapping the data between SCA1 mouse model and the *staggerer* mouse, and abnormalities of mGluR1 signaling have been found in different mouse models, referring to molecules including mGluR1, Gαq, PLC, PKCγ, ITPR1 and TRPC3 (Aiba et al., 1994; Conquet et al., 1994; Hartmann et al., 2004; Jana Hartmann et al., 2008, 2011; Kano et al., 1998; Matsumoto et al., 1996; Miyata et al., 2001; Offermanns, Toombs, et al., 1997; Van De Leemput et al., 2007). Some of these molecules are known to cause SCAs or other disorder relating to the cerebellum. For example, PKCγ mutants, mentioned in the previous section, cause SCA14 (Ji et al., 2014; Shimobayashi and Kapfhammer, 2017; Trzesniewski et al., 2019) and PKCγ is downstream of mGluR1 signaling. SCA15 is caused by the mutation of ITPR1 (Hara et al., 2008), another downstream molecule of mGluR1. In SCA1, mGluR1, ITPR1, PKCγ and Homer3 have been found

to be downregulated on the transcriptional level (Lin et al., 2000; Serra et al., 2004, 2006) and for mGluR1 this reduction of expression has been confirmed on the protein level (Zu et al., 2004). Disruption of mGluR1 has been reported in the mouse models of SCA3 (Konno et al., 2014) and SCA5 (Armbrust et al., 2014). Mutations within *GRM1* coding for mGluR1 are relatively rare. Recently, SCA44 has been reported, with heterozygous dominant mutations in the *GRM1* gene showing typical phenotypes of SCA disease, but with different characteristics, possibly due to different functional changes in different mutants (Watson et al., 2017). The function of an mGluR1 truncation mutation was tested by cellular experiments and this mutation resulted in a decreased receptor activity and decreased downstream target phosphorylation, suggesting that a loss of function of this mutation interferes with downstream signaling of mGluR1 (Watson et al., 2017). These findings demonstrate an important role of mGluR1 signaling in Purkinje cells and show the relationship of altered mGluR1 signaling and SCA pathogenesis.

Evidence for enhanced mGluR1 signaling is also present in different types of SCA. For example, elevated calcium is reported in Purkinje cell in the SCA2 mouse model caused by $ATXN2^{Q58}$ (Liu et al., 2009) and mutant ataxin2 can interact with IP3R (Kasumu et al., 2012). Our previous study has reported increased IP3R1 (encoded by *ITPR1*, causative gene of SCA15 and SCA29) expression in an SCA14 mouse model (Shimobayashi et al., 2016). The two other SCA44 causing mGluR1 missense mutations showed increased receptor activity compared to the wild type mGluR1, suggesting that increased activity of mGluR1 leads to increased ligand sensitivity and ligand-independent activation, which is related to the fact that both missense mutations are closely located in the area of mGluR1 activation, resulting in excessive mGluR1 signaling by positive feedback with increased intracellular calcium levels (Watson et al., 2017). The *moonwalker* (Mwk) mouse model with severe ataxia and abnormal Purkinje cell development, is caused by the point mutations of TRPC3 (the causative gene of SCA41). This mutant TRPC3 can activate the cation channel, downstream of mGluR1 signaling (Becker et al., 2009; Sekerková et al., 2013). These studies suggest that increased mGluR1 pathway might also be associated with pathogenesis in some types of SCAs. Therefore, researchers have used the strategy of overlapping microarray data from different types of SCAs. In a previous

study, SCA1 and SCA7 mouse models have been used to identify 27 common molecules which could contribute to uncover potentially shared molecular mechanisms relating to the pathogenesis of SCAs (Gatchel et al., 2008).

1.4 Regulator of G-protein signaling 8 (RGS8)

Regulator of G-protein signaling 8 (RGS8) is one of the identified common genes in the study of SCA1 and SCA7 mice models (Gatchel et al., 2008). Although the detailed function of RGS8 is not known, there are many members of the RGS family, which are relatively well studied and may help us to better understand the possible function of RGS8.

1.4.1 RGS proteins

RGS proteins not only have a highly conserved structure in mammals, but are already present in lower eukaryotes, such as yeast. The SST2 protein of yeast is the homologoue of mammalian RGS protein, and its function can be replaced by mammalian RGS4 (Chan and Otte, 1982; Dohlman et al., 1995; Druey et al., 1996; Weiner et al., 1993). Until now, more than 30 RGS family members have been found in the human genome. They share a conserved RGS domain which is about 120-130 amino acids in length flanked by N-terminal and C-terminal domains of variable length, so the molecular weight range is variable from small size around 20kDa (e.g. RGS2, RGS10), medium size around 60kDa (e.g. RGS3, RGS9), and large size up to 160 kDa (De Vries et al., 2000; Hollinger and Hepler, 2002). The cellular distribution of RGS proteins is not well studied but it is assumed that most of them preferentially are present near the membrane because of their interaction with membrane proteins. The distribution of RGS proteins is related to and affected by the regulation of Gα-subunits. For example, RGS2 has a cytoplasmic or nuclear localization in HEK293 cells, but the localization will become plasma membrane associated when a Gα-subunit is expressed in the cells (Roy et al., 2003).

RGS proteins are classified into six sub-families according to the shared structure of the RGS domain forming the RZ, R4, R7, R12, RA and RL subfamily (Figure 1.6A) (Hollinger and Hepler, 2002; Ross and Wilkie, 2000). The RGS domain is a globular and mostly helical structure based on a four-helix bundle (helices 4–7) and a second subdomain composed of the N-terminal and C-terminal helices 1–3 and 8–9 (Figure 1.6B). The interaction of the RGS domain with the Gα-subunit depends on three nearby interhelix loops 3/4, 5/6 and 7/8. The residues, which are necessary for the overall structure and for the Gα contact sites, are most frequent on the front face of helices 2 and 3, on the back face of helices 6 and 7, and on loops 4/5 and 5/6. Sizable inserts are included in 4/5 and 6/7 loops, which may mediate the interaction of other regulatory molecules (Ross and Wilkie, 2000).

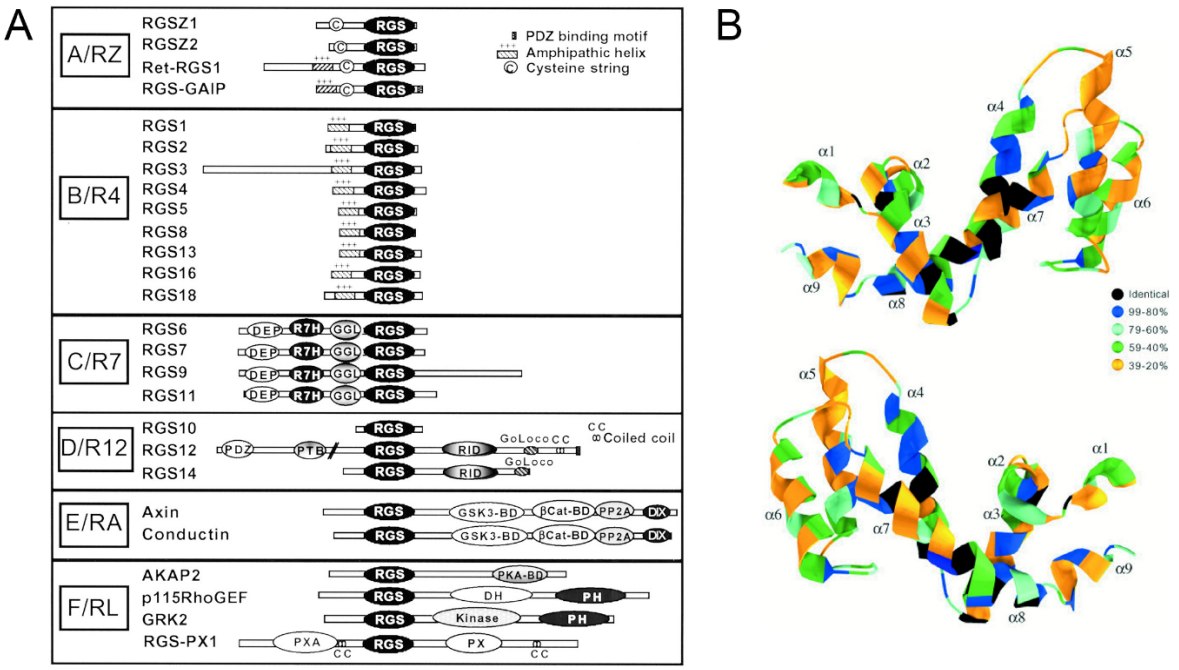

Figure 1.6 Structure and classification of RGS family proteins.

(A) RGS proteins are classified into six subfamilies according to the arrangement of RGS domain and relative motifs. The picture is adapted from (Hollinger and Hepler, 2002). **(B)** Top panel, conserved RGS domain structure from RGS4 is included in all members of RGS subfamilies. Identity at each position of RZ, R4, R7 and R12

subfamilies is shown. Bottom panel, same structure rotated by 180 degrees. The figure is adapted from (Ross and Wilkie, 2000).

1.4.2 RGS proteins play a role as GAPs

G protein coupled receptors (GPCRs) regulate cellular activity to adapt to the different cellular environment or internal stimuli. Guanine nucleotide exchange factor is an important protein after the steps of activation of GPCR and facilitates the replacement of GDP to GTP in the Gα-subunit of heterotrimeric G proteins. The phosphate of GTP can stabilize the Gα-subunit during a conformational change of heterotrimeric G proteins and the Gα-subunit is then dissociated from the dimeric Gβγ-subunit, and both of them are dissociated from the GPCR (Willars, 2006; Zhang and Mende, 2011). Next, the Gα-subunit and Gβγ-subunit interact with effector proteins. The Gα-subunit consists of the four main families Gαq/11, Gα12, Gαs and Gαi/o. All of them have an intrinsic GTPase activity and can hydrolyze GTP to GDP terminating the signaling. Afterward, the Gα-subunit and Gβγ-subunit reform into the heterotrimeric G protein (Willars, 2006; Zhang and Mende, 2011). The function of RGS proteins is the blockade of Gα signaling by preventing GTP binding to Gα or by limiting the period of GTP binding to Gα (Figure 1.7). Since the participation of RGS proteins can act as GTPase-activating proteins (GAPs), which dramatically accelerate the rate of Gα-GTP hydrolysis up to 1000-fold compared to the condition without RGS proteins. Accumulation of hydrolysis leads to reduction of the lifetime of the active Gα-GTP forms (Berman et al., 1996; Hepler et al., 1997; Hunt et al., 1996; Kozasa et al., 1998; N. Watson et al., 1996).

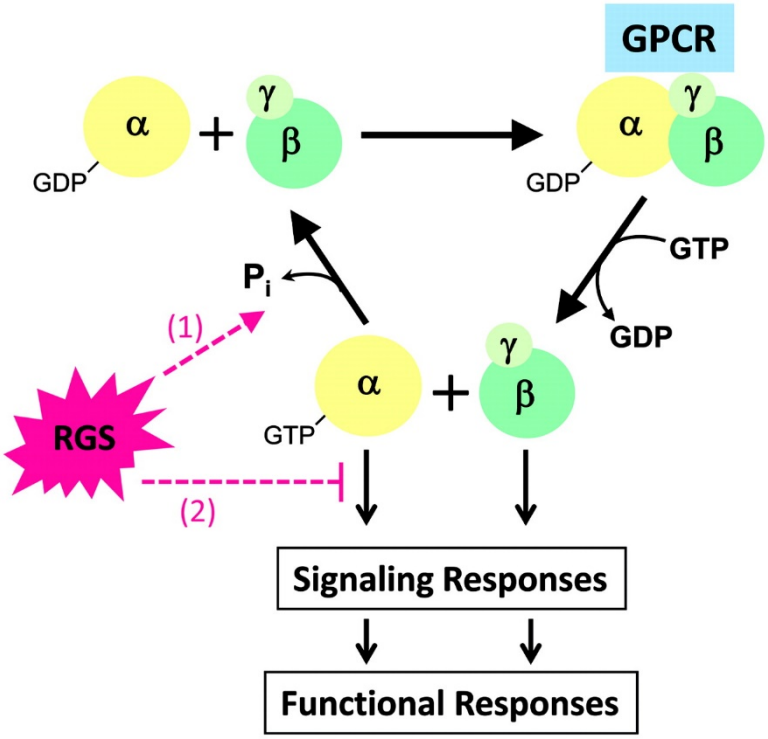

Figure 1.7 RGS proteins regulate G protein meditated signaling pathway.

RGS proteins accelerate Gα activity which reduces the duration of the Gα mediated downstream signaling by step (1). RGS protein bind to activated Gα, which may cause competitive inhibition with downstream effectors by step (2). The picture is adapted from (Zhang and Mende, 2011).

1.4.3 RGS tissue distribution

Although some RGS proteins have ubiquitous expression pattern, the main feature for most RGS family members is a specific tissue distribution or enriched expression in a particular cell type. The restricted tissue expression indicates the specificity of function for the relevant cell types (Grafstein-Dunn et al., 2001).

RGS2, RGS5 RGS12 and RGS16 are expressed ubiquitously or at least relatively widely in different types of tissue (Kurrasch et al., 2004). Expression of RGS2 is

strongest in the cardiovascular system and the brain. Similar to RGS2, RGS5 is widely expressed in many kinds of tissues with strong expression in the cardiovascular system and brain (Seki et al., 1998). RGS12 has a ubiquitous expression pattern, including bone, testis, spleen, heart, lung and brain (Snow et al., 1997; Yang and Li, 2007). RGS16 is widely expressed in the immune system, liver, heart and brain (Grafstein-Dunn et al., 2001; Kveberg et al., 2005; Patten et al., 2002). RGS19, also known as RGS-GAIP, is highly expressed in the liver, lung, heart with only weak expression in brain (De Vries et al., 1995; Ji et al., 2015).

Many RGS family members tend to have a tissue-specific expression pattern. Except for RGS18, which is more specifically expressed in platelets (Gagnon et al., 2002), tissues of the eye and organs of the immune system have relatively enriched expression of RGS proteins. RGS11 is prominently expressed in bipolar cells in the retina (Cao et al., 2012). RGS1 (Han et al., 2005) and RGS13 (Shi et al., 2002) have a selective expression in the cell types of the immune system, but relatively less expression in the other tissues. RGS10 is not only highly expressed in the immune system, but is also expressed in the brain (Gold et al., 1997; Haller et al., 2002).

Several RGS proteins have a selective expression in the heart, such as RGS3, RGS4, RGS6 and RGS14 (Hollinger et al., 2001; Ingi and Aoki, 2002; Li et al., 2016; Snow et al., 1997; Zhang et al., 1998). RGS4, RGS6 and RGS14 also have strong expression in the brain (Ahlers et al., 2016; Gold et al., 1997). These studies suggest that RGS proteins play an important role in the cardiovascular system and the nervous system. In contrast to the more general expression in the heart, RGS protein expression in the brain is enriched in particular brain regions or functional areas. For example, RGS7 is highly and selectively expressed in the brain stem, hippocampus, hypothalamus and amygdala (Hohoff et al., 2009; Larminie et al., 2004). One splice isoform of RGS9 is particularly expressed in striatum (Gold et al., 2007; Zhang et al., 1999). RGS17 is highly expressed in the cerebellum and also detectable in hippocampus and nucleus accumbens (Hayes and Roman, 2016; Mao et al., 2004). RGS20, also known as RGSZ1, is highly expressed in the caudate nucleus and the temporal lobe of the brain (Wang et al., 1998).

1.4.4 RGS function and diseases

RGS proteins has been reported in different kinds of diseases and human health issues relating to the heart. Fox example, RGS4 is associated with atrial fibrillation (Opel et al., 2015) and RGS6 is related to severe bradycardia (Yang et al., 2010). RGS3 overexpression protects against cardiac hypertrophy in mice (Liu et al., 2014) and RGS12 has been found association with pathological cardiac hypertrophy (Huang et al., 2016). RGS proteins cause different diseases relating to their expression in organs and cells. For example, since RGS12 is also expressed in skeletal muscle, RGS12 is implied in osteoporosis based on the finding that RGS12 conditional knockout mice exhibits abnormal bone mass (Yang et al., 2013). RGS5 plays a role in vascular remodeling (Manzur and Ganss, 2009). Downregulation of RGS5 is detected in hypertensive mouse models (Grayson et al., 2007). RGS18 knockout mice have reduced bleeding compared with wild-type mice due to hyper-responsive platelet activation, supporting its tissue-specific function (Alshbool et al., 2015). RGS16 knockout mice have increased expression of lipid metabolism and acid oxidation genes, higher rates of fatty acid oxidation in liver and elevated plasma β-ketone levels (Pashkov et al., 2011). Loss of RGS16 causes a dysregulation in circadian signaling in the suprachiasmatic nucleus. Attenuated food anticipatory activity and abnormal circadian locomotor rhythms were found in RGS16 knockdown mice (Hayasaka et al., 2011). RGS18 protein has been found to be elevated in amyotrophic lateral sclerosis patients (Häggmark et al., 2014).

RGS proteins have been shown to have important functions in the nervous system and been implied in nervous system diseases. RGS2 appears to be involved in synaptic development and the regulation of electrical activity in hippocampal neurons based on the study of RGS2 knockout mice (Hutchison et al., 2009). RGS2 is associated also associated with post-traumatic stress symptoms (Amstadter et al., 2009), suicide (Cui et al., 2008) and other disorders related to anxiety (Smoller et al., 2008; Yalcin et al., 2004). RGS4 can participate in the regulation of dopamine receptors (Min et al., 2012) and was shown to have a decreased expression in the frontal cortex of schizophrenic patients (Mirnics et al., 2001). RGS4 is also linked to the development Alzheimer’s disease (Emilsson et al., 2006) and Parkinson’s

disease (Ko et al., 2014). RGS11 is localized at the dendritic tips of ON-bipolar cells and it interacts with mGluR6 suggesting that this complex could serve as a regulator for light-evoked responses (Cao et al., 2012). RGS7 is associated with panic disorders according to genetic analysis (Hohoff et al., 2009). RGS9 splice isoform 2 regulates the dopamine receptor and plays a pivotal role in pathophysiology of L-dopa-induced dyskinesia (Gold et al., 2007). RGS5 is linked to schizophrenia symptom severity as suggested by genome-wide association studies (Campbell et al., 2008). RGS14 was identified as a risk gene for multiple sclerosis based on genome-wide association studies (Ryu et al., 2014).

RGS proteins are also linked to multiple diseases of the immune system. For example, RGS1 knockout mice exhibited abnormal B cell responses, exaggerated germinal center formation and partial disruption of the spleen (Moratz et al., 2004). RGS1 can be induced by interferonβ-1b to further reduce G-protein activation and immune cell migration (Croze et al., 2010) and has been associated with multiple sclerosis (Esposito et al., 2010), type 1 diabetes and celiac disease (Smyth et al., 2008). RGS10 expression is closely related to the severity of experimental autoimmune encephalomyelitis (Lee et al., 2016). Dysregulation of RGS10 in peripheral and central immune cells may be associated with the risk for age-related degeneration (Kannarkat et al., 2015). RGS13 is another immune-specific modulator and is increasingly expressed in the adult period. RGS13 knockout mice exhibit enhanced B cell responses (Hwang et al., 2013). RGS13 is regulated by p53 to modulate immune responses in B cells and mast cells (Iwaki et al., 2011). RGS16 knockout mice have an enhanced inflammatory response due to the accumulation of $CCR10^{+}$ T cells in the lung (Shankar et al., 2012).

In addition, RGS transcripts are dysregulated in cancer and RGS proteins may regulate the progression in different cancer types (Sethakorn and Dulin, 2013). RGS12 has been identified as a novel tumor suppressor gene in prostate cancer (Y. Wang et al., 2017). RGS17 has been found to be upregulated in prostate cancer and identified as a risk gene for the familial lung cancer susceptibility (Michael et al., 2009; You et al., 2009). Expression of RGS16 has been linked to pancreatic cancer, breast cancer and colorectal cancer (Carper et al., 2014; Liang et al., 2009; Miyoshi

et al., 2009). RGS11 and RGS20 may be involved in tumor metastasis. Several samples of lung adenocarcinoma had an upregulation of RGS11 (Yang et al., 2016). RGS20 had elevated expression levels in melanoma and breast tumors (Yang et al., 2016).

1.4.5 RGS8 introduction

RGS8 has been reported to be strongly expressed in rat cerebellar Purkinje cells and it appears to be enriched in brainstem and nucleus accumbens (Gold et al., 1997; Larminie et al., 2004; Osamu Saitoh et al., 2003; Osamu Saitoh and Odagiri, 2003). Since RGS8 is belonging to the R4 subfamily, its function is directly linked to Gq protein. RGS8 inhibits the M1 muscarinic acetylcholine receptor-Gq-mediated signaling in Xenopus oocytes (Itoh et al., 2006) and has a strong inhibitory function for Gαq- and Gαi/o-dependent receptor activity (Miyamoto-Matsubara et al., 2008). However, RGS8 was also demonstrated to function via direct interaction with the relative receptor. RGS8 is able to interact with the third intracellular loop of melanin-concentrating hormone (MCH) receptor 1 (MCHR1) and inhibits the calcium mobilization induced by melanin-concentrating hormone (Miyamoto-Matsubara et al., 2008). Increased RGS8 expression through the inhibition of the MCHR1 signaling in the hippocampal CA1 region may be related to the antidepressant-like behavior of RGS8 transgenic mice (Kobayashi et al., 2018). Although the expression of RGS8 protein has been reported in the hippocampal CA1 region, RGS8 knockout mice have normal brain development and no major abnormalities in other organs (Kobayashi et al., 2018; Kuwata et al., 2007). RGS8 is also expressed in testis, but RGS8 knockout mice are viable and fertile (Kuwata et al., 2007). Electroconvulsive seizures in rats caused an increase in RGS8 mRNA expression in the prefrontal cortex (Gold et al., 2002), suggesting a potential role for RGS8 in seizures. *RGS8* is transcriptionally downregulated in SCA1, SCA2 and SCA7, indicating a role in pathogenesis of SCAs (Dansithong et al., 2015; Gatchel et al., 2008). *RGS8* mRNA selectively interacts with ATXN2 and mutant ATXN2 reduced RGS8 expression in

the SCA2 mouse model (Dansithong et al., 2015). However, the exact physiological role of RGS8 in nervous system remains still unknown.

1.5 Serine/Threonine Kinase 17B (STK17B)

1.5.1 STK17B introduction

STK17B is another dysregulated molecule on the list of common genes between SCA1 and SCA7 mouse models (Gatchel et al., 2008). STK17B, also known as DAP kinase-related apoptotic kinase 2 (DRAK2), is located on chromosome 2 (2q32.3) and was first isolated from human placenta and liver cDNA libraries (Sanjo et al., 1998), belongs to the serine/threonine kinase family of the death associated proteins (DAP). STK17B is related to STK17A, also known as DRAK1, and both of them may constitute of a novel sub-family, which was originally thought to have the function of inducing apoptosis (Sanjo et al., 1998). STK17B protein structure includes a N-terminal autophosphorylation region and a C-terminal region, with a nuclear localization signal. Another putative nuclear localization signal has been reported in the kinase domain (Friedrich et al., 2005).

1.5.2 STK17B expression

STK17B has been reported to have a prominent expression in the brain, including the olfactory lobe, pituitary, superchiasmatic nuclei, ventricular zone and cerebellum (Mao et al., 2006). Although the the role of STK17B in brain is unclear, STK17B has been relatively well studied in immunology due to its expression in the immune system. STK17B is a key regulator for T cells with high expression in thymus, especially in T cells, and it is also highly enriches in lymph nodes, spleen and bone marrow (Gatzka and Walsh, 2008; Mao et al., 2006). Strong expression of STK17B has also been found in B cells of the spleen (Al-Qahtani et al., 2008; McGargill et al., 2004). In stably transfected Jurkat cells and COS7 cells, STK17B has been shown to be localized in the nucleus (Friedrich et al., 2005). By use of cells from different species, Myc-tagged STK17B also showed a nuclear localization in rat NRK, mouse

NIH3T3 and human Caco-2 cells (Kuwahara et al., 2006). In contrast, STK17B has been reported to have a cytoplasmic distribution in ACL-15, HeLa and WI-38 cells (Kuwahara et al., 2006).

1.5.3 STK17B function

STK17B is important for the induction of apoptosis. Overexpression of STK17B can cause increased apoptosis in NIH 3T3 cells (Sanjo et al., 1998), rat NRK cells and human colon carcinoma cells (Caco-2) cells (Kuwahara et al., 2006). Knockdown of STK17B in ACL-15 and NRK cells partially prevents apoptosis under UV-light (Kuwahara et al., 2006). Moreover, transgenic STK17B overexpression lead to severe β-cell apoptosis triggered by free fatty acids (Mao et al., 2008).

STK17B has also been demonstrated to have non-apoptotic functions in cells. Although overexpression of STK17B is able to induce apoptosis in some cell types (Kuwahara et al., 2006; Sanjo et al., 1998), overexpression of STK17B does not lead to apoptosis in COS-7 cells (Sanjo et al., 1998), suggesting that STK17B-induced apoptosis is depending on the cell type. A transgenic mouse model with overexpression of STK17B shows no obvious defects in most organs with only an increased spleen size (Mao et al., 2006). A STK17B-deficient mouse model also does not shown any phenotypes related to apoptosis and shows relative normal development (McGargill et al., 2004). The reason for the mild phenotypes might be related to the relatively small homology of STK17B with other family members and the lack of the classical C-terminal kinase domain that functions for promoting apoptosis (Friedrich et al., 2005). Indeed, STK17B has been shown to have non-apoptotic functions involving the modulation of T cell responses (Schaumburg et al., 2007) and the deletion of STK17B causes survival defects of T cells in situations of chronic autoimmune stimulation (McGargill et al., 2008).

The role of STK17B is closely related to the immune system. STK17B is a negative regulator of T cell activation via TCR signaling (Friedrich et al., 2005). The lack of this negative regulator of T cell activation causes increased probability for autoimmune diseases (Pentcheva-Hoang et al., 2009), STK17B knockout mice were expected to show some phenotypes related to the immune system, such as

autoimmunity or lymphadenopathy. However, STK17B knockout mice do not show such phenotypes and are not more vulnerable to autoimmune diseases. Surprisingly, STK17B knockout mice are even less susceptible to autoimmunity compared to wild-type mice (McGargill et al., 2004). This finding was supported by a later study showing that STK17B knockout mice have a dramatic resistance to autoimmunity (Ramos et al., 2008). In contrast, transgenic STK17B mice have an enhanced reactivity toward self-antigens and an increased susceptibility to experimental autoimmune encephalomyelitis (Gatzka et al., 2009). In addition, STK17B also plays a role in the maturation of B cells. STK17B shows increased expression during B cell maturation (Friedrich et al., 2005; McGargill et al., 2004) and enhances B cell positive in the germinal center reaction, which is critical for the generation of mature immune responses (Al-Qahtani et al., 2008).

STK17B is also linked to calcium mobilization and homeostasis. As STK17B has been found to regulate calcium flux in T cells (Friedrich et al., 2005; McGargill et al., 2004), later studies have further focused on STK17B participation in controlling calcium mobilization (Friedrich et al., 2007; Newton et al., 2011). Enhanced calcium responses have also been reported in T cells after STK17B knockdown (Newton et al., 2011). The dysregulated calcium mobilization can be rescued by the expression of wildtype STK17B in STK17B-deficient T cells (Friedrich et al., 2007). In the STK17B transgenic mouse model calcium responses in immature T cells were inhibited (Gatzka et al., 2009). These studies support the function of STK17B in regulating calcium responses and calcium influx is able to in turn regulate STK17B function through affection of its autocatalytic activity and phosphorylation (Newton et al., 2011).

Phosphorylation of STK17B is a key factor controlling its catalytic activity and biological functions. Ser12 autophosphorylation of STK17B has been shown to play an important role in T cell activation and the function of STK17B will be lost by introducing a Ser12Ala mutation (Friedrich et al., 2007). Transphosphorylation of STK17B mediated by protein kinase D is proposed to be dependent on calcium-induced reactive oxygen generation in the mitochondria of T cells under the condition of antigen receptor stimulation (Newton et al., 2011). STK17B is primarily distributed

in the nucleus of transfected Jurkat cells but can translocate to the cytoplasm after treatment with the protein kinase C (PKC) activators PMA and PHA in Jurkat cells (Friedrich et al., 2005). The nuclear distribution of rat STK17B can also be affected by the phosphorylation of Ser350 through PKC gamma, indicating the localization of STK17B might reflect its functional activity (Kuwahara et al., 2008).

Chapter 2: Aim of the project

2.1 Identification of key molecules of SCAs

Some molecules showing dysregulated expression both in SCA1 and in SCA7 have been identified implying they might be essential components of cerebellar development (Gatchel et al., 2008). Since there is also increasing evidence that abnormal Purkinje cell development may contribute to cerebellar ataxia and Purkinje cell degeneration (Becker et al., 2009; Serra et al., 2006), one important aim of this thesis is to search for key molecules, i.e. molecules which are dysregulated in different forms of SCAs. For defining our strategy for identifying key molecules, an assumption has to be made:

Assumption: The expression of key molecules is changed in different SCA mouse models.

The aim of this thesis is to identify and better characterize molecules with dysregulated expression in diverse SCA mouse models. We start with the SCA14 S361G mouse model from our own laboratory, for which dysregulated genes have been identified in a microarray screen. In order to identify candidate molecules, we will compare the transcriptional changes in SCA14 S361G mice with published data for dysregulated genes from SCA1 and SCA7.

2.2 The role of the key molecules in Purkinje cell development and pathogenesis of SCAs

The further aim of this project was to better characterize and study the function of the identified key molecules with a special focus on Purkinje cell dendritic development. Our central hypothesis is that the key molecules will be involved in controlling

Purkinje cell development, and that they will pinpoint the hypothetical shared pathways leading to pathogenesis of SCAs.

We assume that at the functional level, key molecules are involved in controlling Purkinje cell development and their dysregulation will cause dysfunction of some shared signaling pathways associated with pathogenesis of SCAs.

To investigate the role of key molecules for Purkinje cell development, we will examine the effects of an overexpression and if possible a knockdown or blockade of key molecules for Purkinje cell development by observing and analyzing dendritic tree expansion. The dysregulated key molecule will help us to identify the disrupted signaling pathways.

Chapter 3: RGS8 is regulating mGluR1 signaling in a mouse model of spinocerebellar ataxia

The following section is based on the work under revision in **Frontiers in Cell and Developmental Biology**. Some text, figures, the numbering of the figure legend and the title numbering have been adapted to this thesis**.**

3.1 Abstract

Spinocerebellar ataxias (SCAs) are a group of hereditary neurodegenerative diseases which are caused by diverse genetic mutations in a variety of different genes. In contrast, transcriptional dysregulation is a typical hallmark of all the different forms, and some molecules have been identified which have a similar dysregulation in different forms of the disease indicating that these genes may be involved in SCA pathogenesis. We have identified RGS8, a regulator of G-protein signaling, as one of the genes which is dysregulated in different mouse models of SCA. In the moment, little is known about the role of RGS8 for Purkinje cell dendritic development and function. We have studied the expression of RGS8 in the cerebellum in more detail and show that it is specifically expressed in mouse cerebellar Purkinje cells and that its expression was increased in a mouse model of SCA14. We further present evidence that RGS8 upregulation in the SCA14 mouse model is related to increased mGluR1-PKCγ signaling. RGS8 overexpression could protect Purkinje cells from the negative effects of mGluR1 activation on dendritic growth. Our results suggest that RGS8 is an important mediator of mGluR1 pathway dysregulation in Purkinje cells and can protect them from negative effects of mGluR1 overstimulation. These findings provide new insights in the role of RGS8 and mGluR1 signaling for the pathology of SCAs.

3.2 Introduction

Spinocerebellar ataxias (SCAs) are a heterogeneous group of progressive genetic disorders with degeneration and dysfunction of the cerebellum (Chen et al., 2005; Dansithong et al., 2015; Gatchel et al., 2008; Klockgether et al., 2019). The genetic background of SCAs can be classified into two groups: Group I, repeat expansion SCAs, are caused by dynamic repeat expansion mutations, such as SCA1 and SCA2, and Group II, conventional mutation SCAs (non-repeat expansion SCAs), are caused by mutations, deletions or insertions in specific genes, such as in beta-III Spectrin in SCA5 or in Protein Kinase C gamma (PKCγ) in SCA14 (Klockgether et al., 2019). Most

SCA mutations cause cerebellar damage and dysfunction typically resulting from Purkinje cell degeneration (Chen et al., 2005; Klockgether et al., 2019).

Due to the diversity of the affected genes it is not clear in the moment, whether there is a single disease mechanism causing the diverse forms. However, transcriptional changes in molecules that mediate the development of Purkinje cells are a hallmark of SCAs and determine the severity of the disease (Serra et al., 2006). The identification of molecules with transcriptional changes in different SCAs could reveal molecular mechanisms underlying the pathogenesis of SCAs. Previously, SCA1 and SCA7 mouse models have been chosen as the representatives of group I repeat expansion SCAs, and 27 molecules with transcriptional changes in both mouse models have been identified by using a microarray-based gene profiling strategy (Gatchel et al., 2008).

In the current study, we have used microarray data from an SCA14 mouse model (Shimobayashi et al., 2016) as a representative of Group II SCAs, and compared them with the common genes found in SCA1 and SCA7 (Gatchel et al., 2008) and genes found to be dysregulated in SCA2 (Dansithong et al., 2015). This approach identified RGS8 as the only molecule which was dysregulated in SCA1, SCA2, SCA7 and SCA14 mouse models. We studied the changes of RGS8 in the SCA14 mouse model in more detail and found that upregulation of RGS8 is associated with increased mGluR1 signaling. In addition, we present evidence suggesting that elevated RGS8 acts as a protective mediator of increased mGluR1 signaling.

3.3 Materials and methods

Animals

All experiments were carried out in accordance with the EU Directive 2010/63/EU for the care and use of laboratory animals, were approved by the veterinary office of the canton of Basel and permitted by Swiss authorities. FVB mice were used for primary cerebellar cell cultures. PKCγ knockout (KO) mice were constructed and generated by

CRISPR/Cas9-mediated gene editing technology in the Centre for Transgenic Models, University of Basel. The SCA14 conditional transgenic mice with FVB background used in this study have been described previously (Trzesniewski et al., 2019). Briefly, in order to generate a conditional transgenic mouse line to express the SCA14 associated human PKCγ(S361G) mutation specifically in Purkinje cells, transgenic mice including PKCγ(S361G) with Tetracycline Response Element (TRE) and GFP reporter were crossed with Pcp2-tTA transgenic mice which express the Tet-Transactivator under a Purkinje cell specific promoter.

Organotypic slice cultures

Organotypic slice cultures were made as described previously (Kapfhammer and Gugger, 2012). Mice were decapitated at postnatal day 8, and their brains were aseptically dissected. The cerebellum was separated in ice-cold minimal essential medium (MEM) supplemented with 1% glutamax (Gibco, Invitrogen) and sagittal slices of 350 µm thickness were cut with a McIlwain tissue chopper under sterile conditions. Cerebellar slices were separated, transferred onto a permeable membrane (Millicell-CM, Millipore), and incubated with incubation medium (50% MEM, 25% Basal Medium Eagle, 25% horse serum, 1% glutamax, 0.65% glucose) or Neurobasal medium (97% Neurobasal medium, 2% B27, 1% glutamax) under 5% CO_2 at 37° C. The medium was refreshed every 2 or 3 days.

Immunostainings

Immunohistochemistry was performed as described previously (Trzesniewski et al., 2019). For cerebellar sections, mice were sacrificed and perfused with 4% paraformaldehyde. Sagittal sections were cut with a cryostat (Leica) at 20 µm. Organotypic slice cultures were fixed after 7 days *in vitro* in 4% paraformaldehyde for 6–24 h at 4° C. Primary dissociated cerebellar cultures were fixed in 4% paraformaldehyde for 30 min at room temperature. All reagents were diluted in 100 mM phosphate buffer (PB). The sections or slices were incubated with primary antibody diluted in blocking solution (PB + 3% non-immune goat serum + 0.3%

TritonX-100) overnight at 4° C, dissociated cerebellar cultures for 1 h at room temperature. After washing with PB, the corresponding fluorescence-conjugated secondary antibodies were added to the slices in PB containing 0.1% Triton X-100 for 2 h at room temperature. The following primary antibodies were used: rabbit anti-Calbindin D-28K (1:500, Swant, Marly, Switzerland,); mouse anti-Calbindin D-28K (1:500, Swant, Marly, Switzerland); sheep anti-RGS8 (1:100, R&D Systems). The following secondary antibodies were used: goat anti-mouse Alexa 488 (1:500, Molecular Probes, Invitrogen); goat anti-rabbit Alexa 488 (1:500, Molecular Probes, Invitrogen); donkey anti-sheep Alexa 568 (1:500, Molecular Probes, Invitrogen). Stained slices or sections were mounted with Mowiol (Sigma-Aldrich, Buchs, Switzerland). The images were captured with an Olympus AX-70 microscope equipped with a Spot Insight digital camera or a Zeiss LSM700 upright confocal microscope.

Western blot and immunoprecipitation

Cerebellar slices were lysed with RIPA buffer in the presence of protease and phosphatase inhibitors. Samples were separated by SDS-PAGE and blotted on a nitrocellulose membrane. After blotting, membranes were incubated with 5% BSA in TBS for 1 h and incubated with the specific primary antibodies; After washing with TBS-T, membranes were incubated with HRP-labeled secondary antibodies. Proteins were visualized by ECL (Pierce, Thermo Scientific, Reinach, Switzerland). Alternatively, membranes were incubated with IRDye® Secondary Antibodies for 1 h. The proteins were quantified using C-Digit Western Blot software (LI-COR Biosciences, Bad Homburg, Germany). HEK293T cells were transfected with plasmids pCMV-mGluR1, pCMV-PKCγ-tGFP or pCMV-PKCγ(S361G)-tGFP using Lipofectamin 3000 (Invitrogen) according to manufacturer's instructions and incubated for 24-48 hours before harvest. tGFP trap agarose beads (Chromotek) were used for immunoprecipitation of tGFP-labelled PKCγ(S361G) or WT PKCγ proteins according to manufacturer's instructions. The following primary antibodies were used in this study: sheep anti-RGS8 (1:1000, R&D Systems), mouse anti-actin (1:2000, Millipore), rabbit anti-alpha Tubulin (1:1000, Proteintech), rabbit anti-phospho-PKC substrate

(1:1000, Cell Signaling), mouse anti-GAPDH (1:4000, Proteintech); rabbit anti-mGluR1 (1:1000, Cell Signaling); mouse anti-Gαq/11 (1:300, Santa Cruz); mouse anti-turboGFP (1:1000, Origene); rabbit anti-turboGFP (1:1000, Invitrogen); mouse anti-Myc (1:1000, Origene). The following secondary antibodies were used in this study: anti-sheep HRP conjugate antibody (1:1000, R&D Systems); anti-mouse HRP conjugate antibody (1:10000, Promega); anti-rabbit HRP conjugate antibody (1:10000, Promega); IRDye® 680LT Goat anti-Rabbit IgG Secondary Antibody (1:10000, LICOR); IRDye® 800CW Goat anti-Mouse IgG Secondary Antibody (1:10000, LICOR).

Microarray Study and Quantitative real-time PCR

The data of genes whose expression is commonly altered in SCA1 and SCA7 mouse models was used from published data (Gatchel et al., 2008). The data of top 50 genes in SCA2 mouse models was used from the study of Dansithong et al. (2015). The data from organotypic cerebellar slice cultures of SCA14 PKCγ(S361G) and control mice were previously established in the laboratory (Shimobayashi et al., 2016).

Plasmid construction

pCMV-Rgs8 and pCMV-mGluR1 vectors were from Origene (Rockville, MD, USA). Plasmid L7-green fluorescent protein (GFP) was previously described and a gift from Dr. Wolfgang Wagner (Wagner et al., 2011). Linearized pL7 vectors were produced by the restriction enzymes NotI and NcoI (New England BioLabs, Massachusetts, USA) and mouse *Rgs8* gene insert fragments were generated by Polymerase chain reaction (PCR). pL7-Rgs8-GFP were produced by In-Fusion HD Cloning Kits (Clontech, Mountain View, CA). The following primers were used for PCR: Rgs8 forward CAG GAT CCA GCG GCC GCA TGG CTG CCT TAC TGA TGC CA; Rgs8 Reverse CCC TTG CTC ACC ATG GTG CTG AGC CTC CTC TGG CTC TG. pCMV-PKCγ-tGFP, pCMV-PKCγ(S361G)-tGFP and pL7-PKCγ(S361G)-GFP were gifts from Dr. Etsuko Shimobayashi (Shimobayashi and Kapfhammer, 2017).

Primary cerebellar cell cultures and transfection

Primary cerebellar cell cultures were prepared from neonatal mice as described previously (Shimobayashi and Kapfhammer, 2017; Wagner, McCroskery, et al., 2011). Briefly, cerebella from postnatal day 0 mice were dissected, dissociated and plated on glass chambers coated with Poly-D-lysine. Indicated vectors were introduced into Purkinje cells by transfection with a Neon Transfection System (Thermo Fisher) using the following settings: Pulse voltage 1200 V, Pulse width 30 ms, Pulse number 1. Cells were incubated in incubation medium (90% Dulbecco's modified Eagle medium/F-12 nutrient-based medium, 1% N2 supplement, 1% glutamax, and 10% FBS). 2-4 hours after transfection, 500ul DFM supplemented 1% N2 and 1% glutamax was added to each well. After that, half of the medium was refreshed every 4 days. The media and supplements were from Life Technologies, Zug, Switzerland. Cells were kept in culture for two weeks before fixation. The following pharmacological compounds were added to the medium at 7 days *in vitro*: (S)-3,5-Dihydroxyphenylglycine hydrate (DHPG) (Sigma-Aldrich, St. Louis, Missouri, United States).

Quantification of Purkinje cell dendritic expansion and fluorescence intensity of immunostainings in dissociated cerebellar cultures

The quantification of Purkinje cell dendritic tree size was performed as previously described (Shimobayashi and Kapfhammer, 2017). The average value of control Purkinje cells was set as 1. In order to ensure a comparable growth environment, non-transfected Purkinje cells close to the Purkinje cells transfected with the indicated vectors from the same well were taken as control in this study. An image analysis program (ImageJ) was used to trace the outline of the Purkinje cell dendritic trees yielding the area covered by the dendritic tree. The mean fluorescence intensity of the Purkinje cell soma was calculated by ImageJ and the raw images were used for the fluorescence intensity analysis. The shown images were linearly adjusted in brightness and contrast. The data were analysed using GraphPad Prism software (San Diego, USA). The statistical significance of differences in parameters was assessed by the nonparametric two-tailed Mann–Whitney's test. Confidence intervals were 95%, statistical significance was assumed with $P < 0.05$.

3.4 Results

3.4.1 RGS8 is dysregulated in several SCAs

By comparing the transcriptional expression of various genes in SCA1 and SCA7 mouse models 27 common genes have been identified which were suggested to be involved in the pathogenesis of SCAs (Gatchel et al., 2008). We have now further compared these genes to transcriptional changes in a mouse model of SCA14 (Ji et al., 2014; Shimobayashi et al., 2016), and have identified 3 genes which were dysregulated in all three mouse models. Interestingly, these 3 molecules were strongly up-regulated in the SCA14 model but down-regulated in SCA1 and SCA7 models (Table 3.1 and Figure 3.1A).

Table 3.1 Dysregulated genes in SCA1, SCA7 and SCA14 mouse models.

GENE	OFFICIAL FULL NAME	SCA1*	SCA7*	SCA14
Inpp5a	Inositol polyphosphate-5-phosphatase A	Decreased	Decreased	Increased
Rgs8	Regulator of G protein signaling 8	Decreased	Decreased	Increased
Stk17b	Serine/threonine kinase 17b	Decreased	Decreased	Increased

*Data of SCA1 and SCA7 from the published microarray data sets (Gatchel et al., 2008)

Inpp5a has already been shown to play a crucial role for the survival of Purkinje cells (Liu et al., 2020; Yang et al., 2015). Stk17b, also known as Drak2, is strongly expressed in lymphoid organs and known to transmit non-apoptotic signals during thymocyte differentiation (Friedrich et al., 2005). We further compared the key molecules to the top 50 changed transcripts in the SCA2 mouse model (Dansithong et al., 2015) and found that RGS8 is the unique dysregulated gene in the 4 different

SCA mouse models (Figure 3.1B), with a reduced expression on SCA1, 2 and 7, but an increased expression in SCA14. In order to confirm the upregulation in the SCA14 mouse model, we performed qPCR which confirmed *Rgs8* upregulation at mRNA level (Figure 3.1C). These results demonstrate that RGS8 is unique in being a dysregulated molecule in at least 4 SCA mouse models.

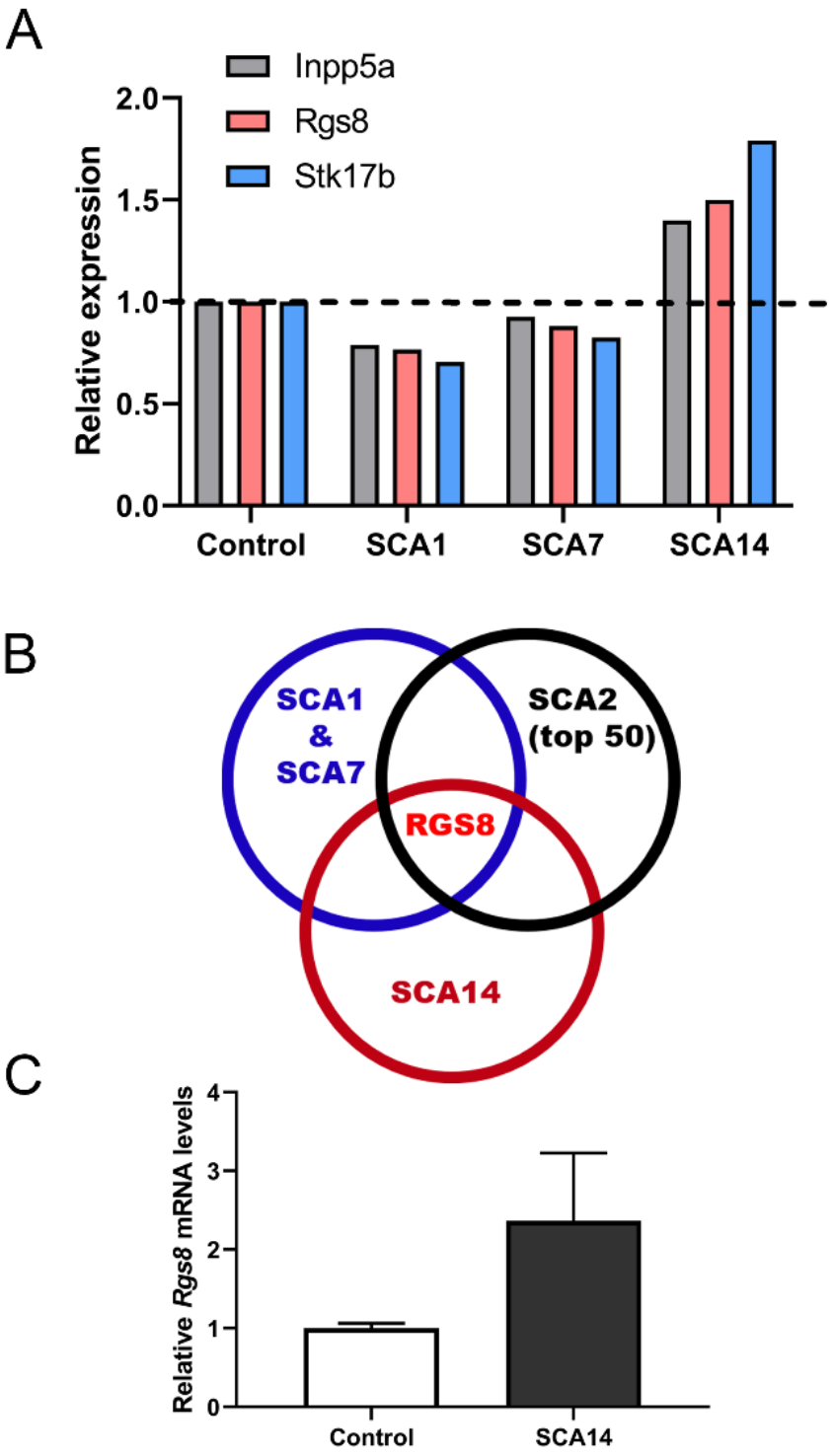

Figure 3.1 Identification RGS8 as a molecule with dysregulated expression in different SCA mouse models.

(A) The relative transcriptional levels of Inpp5a, Rgs8 and Stk17b in SCA1, SCA7 and SCA14 were evaluated by microarrays. The relative changes of Inpp5a are 0.787, 0.926 and 1.399, respectively; The relative changes of Rgs8 are 0.766, 0.88 and 1.499, respectively; The relative changes of Stk17b are 0.704, 0.825 and 1.791, respectively; The data of SCA1 and SCA7 were obtained from the published microarray data sets (Gatchel et al., 2008). **(B)** Comparison of the common dysregulated genes in SCA1, SCA7 and SCA14 with the top 50 altered genes in SCA2 mice. The data of SCA2 and the common genes of SCA1 and SCA7 were obtained from published studies (Dansithong et al., 2015; Gatchel et al., 2008). RGS8 is the only dysregulated gene in all 4 SCA mouse models. **(C)** Relative expression of Rgs8 in SCA14 evaluated by real-time qPCR. GAPDH was used as a housekeeping gene. The mean value of control is 1.000 ± 0.0659; the mean of SCA14 is 2.364 ± 0.8633. Two biological replicates were done in triplicate. Data are expressed as mean ± SD.

3.4.2 RGS8 is expressed in Purkinje cells starting at early postnatal development

The temporal expression profile of RGS8 was investigated in the developing cerebellum of the mouse from postnatal day 1 (P1) to adult by Western blot. No signal on Western blots of P1 to P7 suggested that RGS8 is not or only weakly expressed in cerebellar cells during the first postnatal week. It was mainly detectable in mouse cerebellum after P7 and remained expressed through adulthood (Figure 3.2A). In order to confirm that RGS8 was expressed in Purkinje cells, sagittal cerebellar sections were collected from the mouse cerebellum at P10 and P12. Purkinje cells, which were identified by labelling with the Purkinje cell marker Calbindin, were nicely stained by the RGS8 antibody. RGS8 staining extended from the Purkinje cell layer to the Molecular layer of the cerebellum, and RGS8 immunoreactivity was present in the cell body and the dendrites of Purkinje cells (Figure 3.2B and C). These data confirm that RGS8 is expressed in Purkinje cells from the second postnatal week on,

suggesting that it plays a role during postnatal Purkinje cell differentiation and maturation.

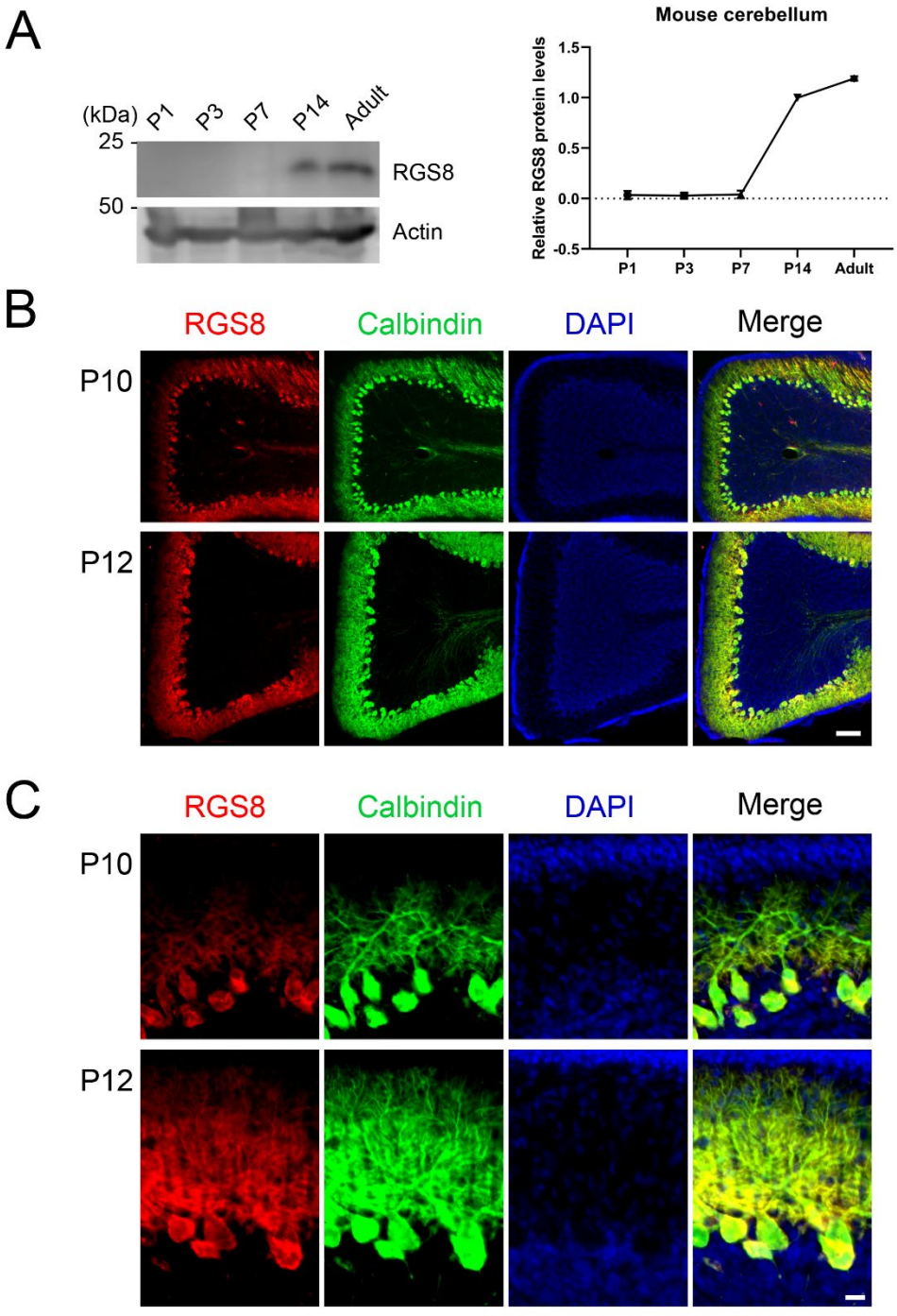

Figure 3.2 Expression of RGS8 protein in the postnatal mouse cerebellum.

(A) Western blots from mouse cerebellum at different postnatal stages. Left side: RGS expression is first evident at P14. Actin used as loading control shown in bottom panel. Right side: Quantification of protein levels from Western blots. Data are expressed as mean ± SD, with three independent biological samples for P1 (three or four pups for one sample), P3 (three or four pups for one sample) and P7, and two independent biological samples for P14 and Adult. The mean value of RGS8 protein level at P14 was set as 1, and values for the other stages were expressed relatives of this value. The mean values of P1, P3, P7 and adult were 0.034 ± 0.0410, 0.029 ± 0.0179, 0.041 ± 0.0386 and 1.191 ± 0.0217. **(B)** RGS8 immunoreactivity (red signal) is present in cerebellar Purkinje cells (identified by anti-Calbindin, green) at P10 and P12. Scale bar is 100 µm. **(C)** Viewed at higher magnification, RGS8 is present in dendrites and the soma of Purkinje cells at P10 and P12. Scale bar is 20 µm.

3.4.3 Increased RGS8 protein expression in Purkinje cells of the PKCγ(S361G) transgenic SCA14 mouse model

The gene array had indicated an increased expression of RGS8 mRNA and we now confirmed an increased expression on the protein level. We further found that RGS8 protein expression was increased in Western blots of organotypic cerebellar cultures from SCA14 PKCγ(S361G) mice (Figure 3.3A and B). In mixed dissociated cultures from S361G transgenic and control mouse pups the transgenic Purkinje cells were identified by endogenous GFP expression. We then quantified RGS8 immunoreactivity on GFP-positive Purkinje cells from S361G-transgenic mice versus GFP-negative Purkinje cells from control mice present in the same culture well (Figure 3.3C). Purkinje cells from S361G-trangenic mice have an altered morphology with reduced and thickened dendrites as previously reported (Ji et al., 2014; Shimobayashi et al., 2016). RGS8 immunoreactivity was increased to a 1.68 ± 0.53 fold higher expression of RGS8 in Purkinje cells from S361G-transgenic mice versus GFP-

negative Purkinje cells from control mice (Figure 3.3C) present in the same culture well.

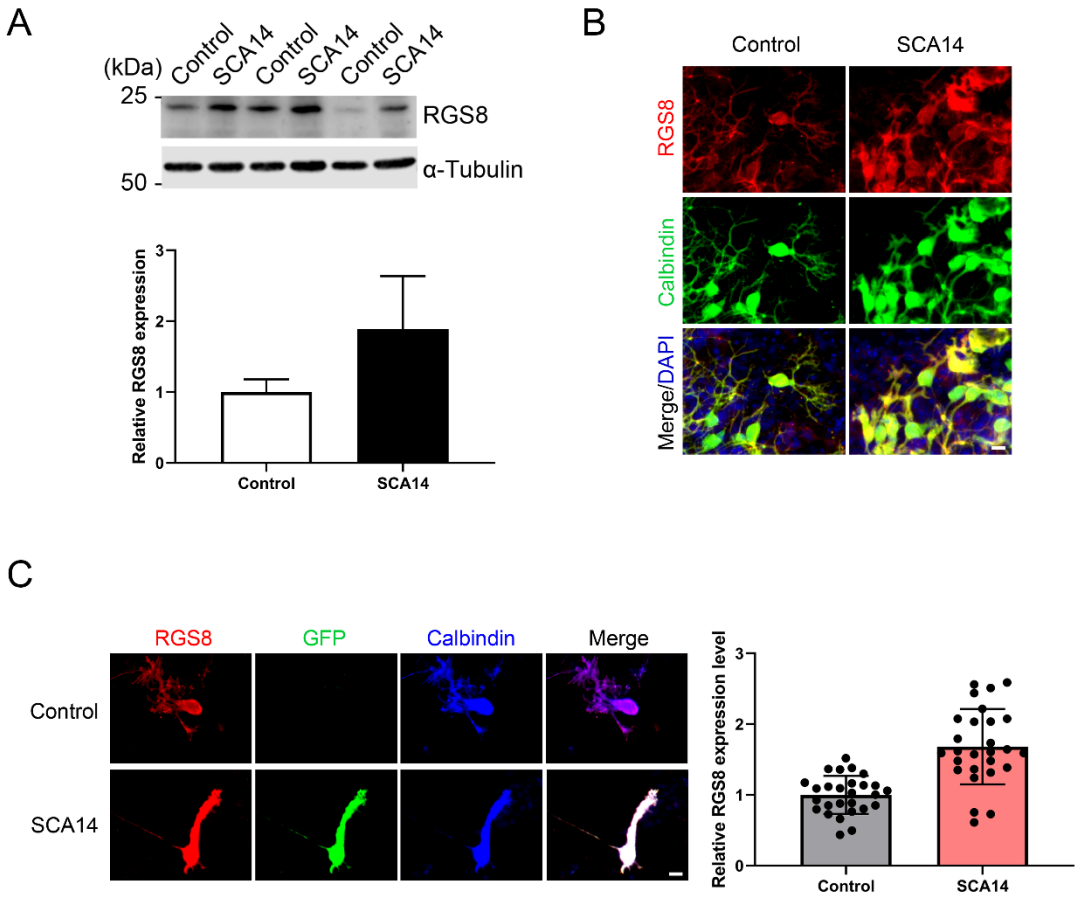

Figure 3.3 Increased RGS8 expression in Purkinje cells of the SCA14 S361G mouse model

(A) Western blots of protein extracts from at least three different experiments with organotypic cerebellar slice cultures from SCA14 PKCγ(S361G) and control mice. The quantification of the Western blots showed a 1.89 ± 0.749-fold increased expression in slice cultures from SCA14 PKCγ(S361G) transgenic mice. Data from at least 3 independent biological replicates. **(B)** RGS8 immunoreactivity was increased in Purkinje cells in cerebellar slice cultures from SCA14 PKCγ(S361G) mice versus

littermate controls. Scale bar is 20 µm. **(C)** RGS8 immunoreactivity was increased in in Purkinje cells from SCA14 PKCγ(S361G) transgenic mice in mixed dissociated cultures containing Purkinje cells derived from transgenic and control mice. Purkinje cells were identified by anti-calbindin staining (blue), and PKCγ(S361G)-transgenic cells by anti-GFP staining (green). The fluorescence of anti-RGS8 staining was quantified using ImageJ. The mean value of RGS8 expression for SCA14 PKCγ(S361G) is increased 1.68 ± 0.533-fold compared to control cells. The n was 27, and the difference in expression was significant with $P < 0.0001$ in the two-tailed Mann-Whitney test. Data are expressed as mean ± SD. Scale bar is 20 µm. Please note that PKCγ(S361G) transgenic Purkinje cells have a changed morphology as reported earlier.

3.4.4 Increased RGS8 expression in the PKCγ(S361G) cerebellum is associated with elevated mGluR1 signaling

In S361G mice there is a constitutive activation of PKCγ signaling. We verified the increased phosphorylation of PKCγ target proteins by antibodies that recognize phosphorylation of PKC substrates. In extracts from cerebellar slice cultures from SCA14 PKCγ(S361G) mice there was a strong increase of target phosphorylation. The mean value was increased to 1.67 ± 0.388-fold in S361G derived organotypic slice cultures compared to cultures from littermate controls (Figure 3.4A).

RGS8 belongs to the R4 subfamily of RGS proteins, all of which accept Gαq/11 subunit as substrates, and the structure of RGS8-Gαq complex has been reported recently (Squires et al., 2018; Taylor et al., 2016). RGS8 can interact with Gαq/11 in brain membranes of rat (O. Saitoh et al., 1997). The metabotropic glutamate receptor 1 (mGluR1) is coupled to the Gαq pathway and strongly expressed in cerebellar Purkinje cells (Tanaka et al., 2000), and it has been suggested that RGS8 is associated with activation of the mGluR1-Gαq pathway in an ataxin-2 mouse model (Dansithong et al., 2015). As mGluR1 signaling is supposed to be upstream of PKCγ signaling, we

wondered whether it would be synergistically increased or as a compensation decreased in slice cultures from S361G mice. We found by immunohistochemistry that mGluR1 was as expected expressed in Purkinje cells in organotypic culture of SCA14 mice (Figure 3.4B). In Western blots, two immunoreactive bands of mGluR1 were present representing monomeric and dimeric forms. mGluR1 monomer expression was strongly increased to 2.89 ± 1.345-fold of control. mGluR1 dimer expression was increased to 2.19 ± 0.546-fold of control. The associated increase of Gαq/11 was 1.78 ± 0.441-fold of control (Figure 3.4C). These results show that in the SCA14 PKCγ(S361G) mouse model there is a complete activation of the mGluR1-PKCγ signaling pathway.

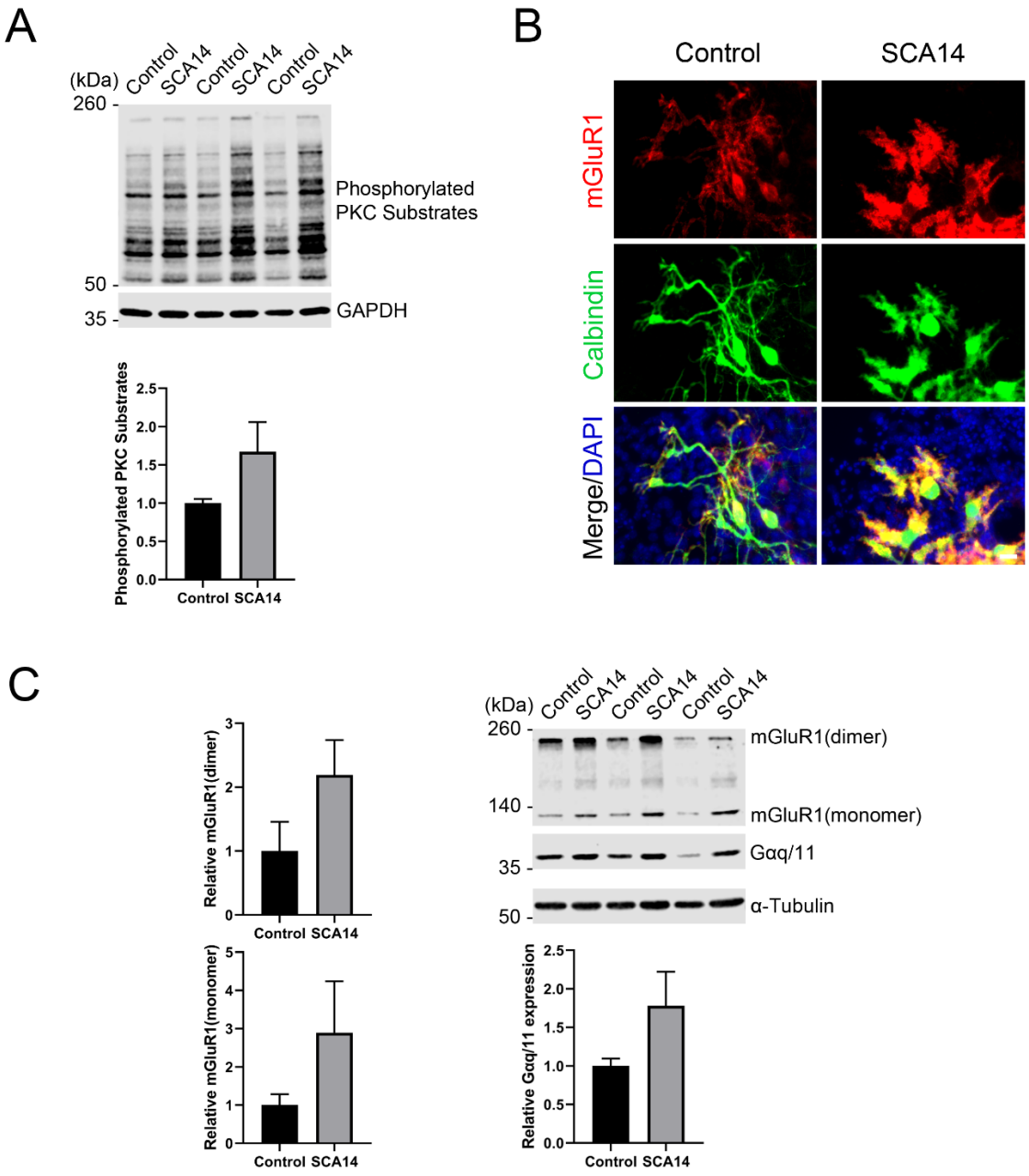

Figure 3.4 mGluR1-PKCγ signaling is elevated in SCA14 mouse model.

(A) Western blot of cerebellar slice cultures of PKCγ(S361G) and control mice stained for phosphorylated PKC substrates. Quantification of protein levels from Western blots. The mean value of the phosphorylated PKC substrates for control is 1.00 ± 0.053; the mean value of the phosphorylated PKC substrates for SCA14 PKCγ(S361G) is 1.67 ±

0.388, three biological replicates. Data are expressed as mean ± SD. **(B)** Staining of cerebellar slice cultures from PKCγ(S361G) and littermate control mice with anti-mGluR1 antibodies. mGluR is specifically expressed in Purkinje cells, and staining is more intense in Purkinje cells from PKCγ(S361G) mice. Scale bar is 20 μm. **(C)** mGluR1 and Gαq/11 expression in protein extracts from cerebellar slice cultures of PKCγ(S361G) and control mice, α-Tubulin is shown as loading control. The mean value of mGluR1 dimer in S361G-derived slice cultures is increased 2.19 ± 0.546 fold compared to control. The mean value of mGluR1 monomer in PKCγ(S361G) -derived slice cultures is increased 2.89 ± 1.345 fold compared to control, the mean value of Gαq/11 in PKCγ(S361G)-derived slice cultures is increased 1.78 ± 0.441 fold compared to control. Three biological replicates.

3.4.5 mGluR1 interacts with mutant PKCγ(S361G)

Activated PKCγ phosphorylates target proteins involved in diverse cellular signaling pathways and has been shown to phosphorylate mGluR1 mediating signaling in cerebellar Purkinje cells (Kato et al., 2012; Mao et al., 2008). We tested whether the mutated PKCγ protein from the PKCγ(S361G) mutant mouse can interact with mGluR1. Immunoprecipitation studies with proteins from transfected HEK293T cells confirmed that PKCγ(S361G) interacts with mGluR1 (Figure 3.5A). Colocalization of mGluR1 and wildtype PKCγ was confirmed in Purkinje cells (Figure 3.5B).

Because wildtype PKCγ is co-expressed together with mutated PKCγ(S361G) in the transgenic mice, we used PKCγ knockout mice in order to confirm the interaction of mutated PKCγ protein and mGluR1 in Purkinje cells. When PKCγ(S361G) was transfected into Purkinje cells from PKCγ knockout mice we still observed the colocalization of PKCγ(S361G) and mGluR1 (Figure 3.5C). Our results indicate that the mutant PKCγ(S361G) with constitutively catalytic activity interacts with mGluR1 and is likely to induce increased mGluR1 signaling.

A

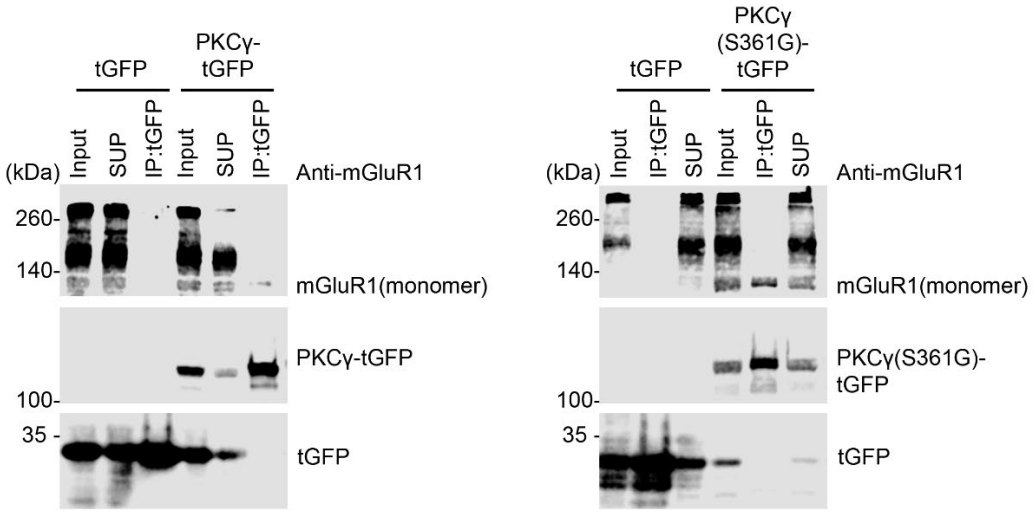
tGFP
PKCγ-tGFP
Input
SUP
IP:tGFP
(kDa)
Anti-mGluR1
260-
140-
mGluR1(monomer)
PKCγ-tGFP
100-
35 -
tGFP
PKCγ (S361G)-tGFP
PKCγ(S361G)-tGFP

B

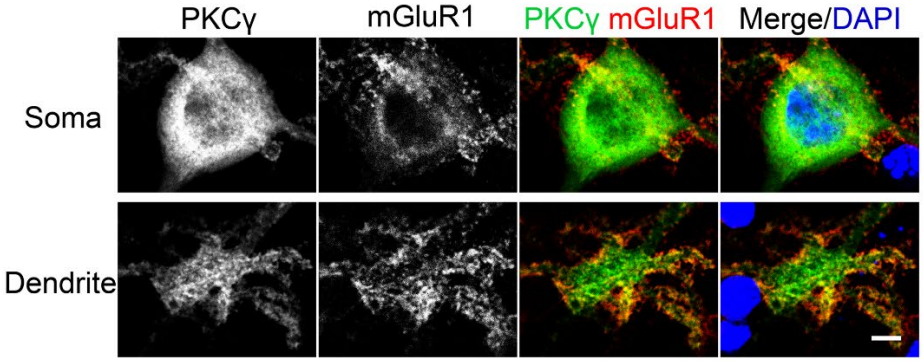
PKCγ
mGluR1
PKCγ mGluR1
Merge/DAPI
Soma
Dendrite

C

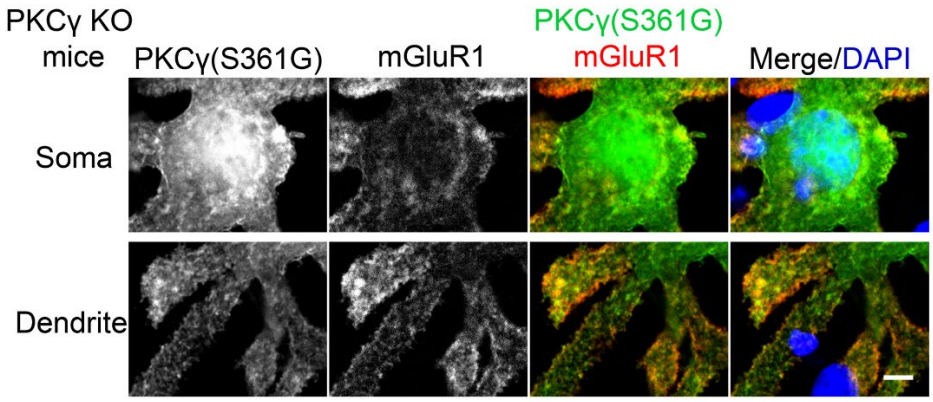
PKCγ KO mice
PKCγ(S361G)
mGluR1
PKCγ(S361G) mGluR1
Merge/DAPI
Soma
Dendrite

Figure 3.5 Interaction of mGluR1 and mutated PKCγ(S361G).

(A) HEK293T cells expressing mGluR1 were transiently transfected with either PKCγ(S361G)-tGFP or tGFP alone. Anti-tGFP immunoprecipitates (IPs), inputs, and supernatants (SUP) were analyzed by Western blot with anti-mGluR1 and Anti-tGFP antibodies. **(B)** Colocalization of mGluR1 and PKCγ in Purkinje cells from wildtype mice. **(C)** Colocalization of mGluR1 and PKCγ(S361G) in Purkinje cells from PKCγ knockout mice transfected with mutated PKCγ(S361G). Scale bar in B and C is 5 μm.

3.4.6 RGS8 upregulation counteracts elevated mGluR1 signaling in Purkinje cells

To explore the function of RGS8 in Purkinje cells, we transfected a RGS8-GFP fusion protein in Purkinje cells using a vector with the Purkinje cell specific L7 promoter (Shimobayashi et al., 2016; Wagner, McCroskery, et al., 2011). The dendritic expansion of Purkinje cells transfected with RGS8-GFP showed a trend towards decreasing dendritic tree size compared to non-transfected Purkinje cells in same culture well or Purkinje cells transfected with GFP tag alone, but the reduction did not reach statistical significance. Transfection of the GFP tag protein alone did not affect morphology of Purkinje cells compared to non-transfected Purkinje cells in the same culture well (Figure 3.6A and B). We then tested the effect of RGS8 overexpression on the mGluR1 signaling pathway. Treatment with the selective mGluR1 agonist, (S)-3,5-Dihydroxyphenylglycine (DHPG), strongly decreased the dendritic area of Purkinje cells compared to control in dissociated cultures (Figure 3.6A and B) in agreement with previous studies (Gugger and Kapfhammer, 2010; Sirzen-Zelenskaya et al., 2006). When Purkinje cells in dissociated cultures overexpressed RGS8-GFP, treatment with DHPG did not significantly change the dendritic area of overexpressing Purkinje cells showing that RGS8-GFP expression rescued the morphology of Purkinje cells after DHPG treatment and increased the size of the dendritic tree compared to control Purkinje cells treated with DHPG (Figure 3.6A and B). These results indicate

that RGS8 overexpression in Purkinje cells could protect the dendrites from the effects of mGluR1 activation. Our findings indicate that RGS8 has an inhibitory role for the mGluR1 signaling pathway in Purkinje cells.

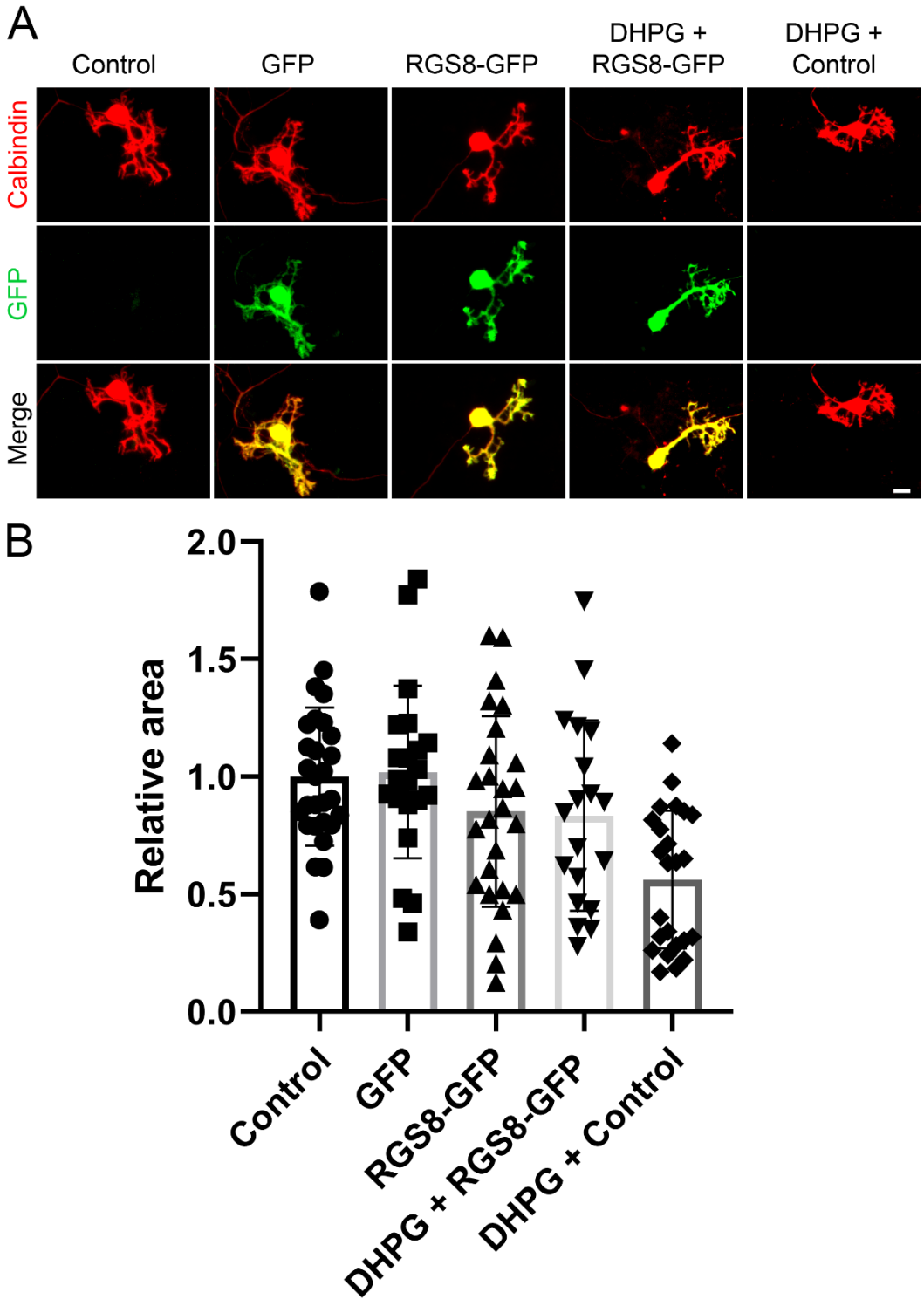

Figure 3.6 RGS8 protects the Purkinje cell dendritic tree from overshooting mGluR1 signaling.

(A) Representative images of Purkinje cells transfected with the indicated plasmids or treated with the indicated condition. **(B)** The mean values of the Purkinje cell dendritic area were measured in at least three independent culture wells, controls were the non-transfected cells from the same culture well. Control: 1.00 ± 0.29, n = 28 cells; GFP transfection: 1.02 ± 0.37, n = 21 cells; RGS8-GFP transfection: 0.85 ± 0.41, n = 26 cells; RGS8-GFP with DHPG treatment: 0.83 ± 0.40, n = 19 cells; Control cells with DHPG treatment: 0.56 ± 0.29, n = 24 cells. Control vs GFP, P = 0.8020; Control vs RGS8-GFP, P = 0.1455; GFP vs RGS8-GFP, P = 0.1101; RGS8-GFP vs DHPG + RGS8-GFP, P = 0.8547; DHPG + RGS8-GFP vs DHPG + Control, P = 0.0184; DHPG + Control vs Control, P < 0.0001 in one-way ANOVA with Kruskal–Wallis test. RGS8 transfection rescues the Purkinje cell dendritic tree from reduction by 2.5 µM DHPG treatment. Data are expressed as mean ± SD. Scale bars are 20 µm.

3.5 Discussion

Based on its transcriptional dysregulation in 4 different types of SCA we have identified RGS8 as a potential molecule involved in the pathology of SCAs. RGS8 is specifically expressed in Purkinje cells from early postnatal development. In the SCA14 PKCγ(S361G) mouse model studied in our laboratory, RGS8 expression was strongly increased in organotypic slice cultures in parallel with a reduction of dendritic tree size of the Purkinje cells. While in this mouse model the mutation produces a constitutively active form of PKCγ, we have shown that mutated PKCγ binds to mGluR1 and that there is also a strong elevation of mGluR1 signaling linking SCA14 to changes in mGluR1 signaling. RGS8 is thought to negatively regulate G-protein mediated signaling. We could show that RGS8 overexpression can indeed protect Purkinje cells from the negative effects of mGluR1 activation on dendritic growth suggesting that RGS8 upregulation in the SCA14 mouse model may have a protective role for Purkinje

cells. In other SCAs the decreased expression of RGS8 may contribute to increased mGluR1 signaling. Our findings support a critical role of mGluR1 signaling and its regulation by RGS8 in different types of SCAs.

3.5.1 RGS8 expression in the cerebellum

We show that in the cerebellum RGS8 is specifically expressed in Purkinje cells starting after P7, and that Purkinje cells at P10 already express substantial amounts of RGS8 protein. This time sequence is in agreement with an earlier report about the developmental expression of RGS8 studied by in situ-hybridization. In this study, RGS8 mRNA was not detectable at P7, but substantial hybridization signal was found at P9 and later (Osamu Saitoh and Odagiri, 2003). The beginning of the expression goes together with the expansion and maturation of Purkinje cell dendrites and the maturation of Purkinje cell electrophysiological properties (Armengol and Sotelo, 1991; McKay and Turner, 2005) and is also correlated with the maturation of mGluR1 expression and function in Purkinje cell dendrites (Ryo et al., 1993). This developmental expression profile is well compatible with a modulating role of RGS8 in mGluR1 signaling.

3.5.2 Increase of RGS8 and mGluR1 expression in the SCA14 PKCγ(S361G) mouse model

We show that RGS8 protein expression is increased in Purkinje cells with reduced dendritic expansion in organotypic slice cultures or dissociated cerebellar cultures from SCA14 PKCγ(S361G) mice. This increase is in contrast to the situation in SCA1, SCA2 and SCA7 where expression is decreased. The major change in PKCγ(S361G) Purkinje cells is a constitutive active kinase domain of PKCγ as reflected by the increased phosphorylation of PKC substrates in organotypic slice cultures from these mice (Figure 3.4A). Interestingly, this constitutive activation of PKCγ(S361G) also results in an increased expression of mGluR1 and Gαq/11 indicating elevated mGluR1 signaling in Purkinje cells. An mGluR1-PKCγ signaling cascade including mGluR1, Gαq, PLC, and PKCγ, has been shown to be important in cerebellar Purkinje cells.

Genetic mouse models lacking either mGluR1, Gαq, PLC, or PKCγ all show similar phenotypes. Gαq regulates PLC which is activated and produces two intracellular messengers (inositol 1,4,5 trisphosphate) IP3 and diacylglycerol (DAG). IP3 binds to the IP3 receptor and induces the release of calcium. DAG together with increased calcium activates PKCγ (Kano et al., 1995, 1997; Offermanns, Hashimoto, et al., 1997). We have confirmed that the mutated PKCγ(S361G) can still bind to and interact with mGluR1 and does colocalize with mGluR1 in Purkinje cells. In the moment, we do not know whether the increase in mGluR1 signaling is the result of this direct interaction. While the role of mGluR1 phosphorylation for LTD is well studied (for review see Kano et al., 2008), little is known about the effects of PKCγ-mediated phosphorylation of mGluR1 on its expression and long-term signaling. From our experiments, we cannot tell whether the increase of mGluR1 expression is a direct effect of increased mGluR1 phosphorylation by PKCγ(S361G) or is an indirect consequence of the chronically increased PKC activity present in the PKCγ(S361G) Purkinje cells. On the other hand, it seems very likely that the increased expression of RGS8 is due to the increase in mGluR1 signaling. This view is nicely compatible with the known function of RGS8 as a negative regulator of mGluR1 signaling. This model of RGS8 function in the SCA14 PKCγ(S361G) mouse is illustrated in Figure 3.7.

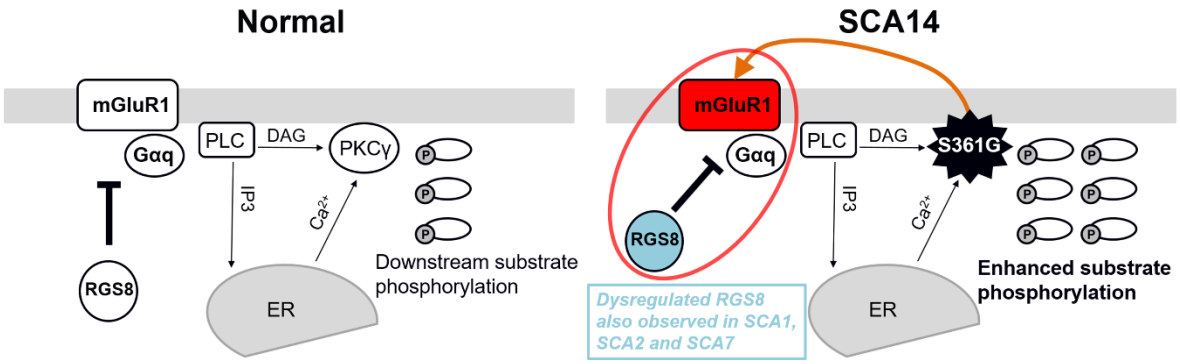

Figure 3.7 Model of the functional effect of RGS8 in SCA14.

(Left panel), mGluR1-PKCγ signaling pathway in the normal situation. mGluR1 activation via Gαq activates Phospholipase C (PLC) to produce inositol 1,4,5 trisphosphate (IP3) and diacylglycerol (DAG). IP3 binds to the IP3 receptor and calcium ions (Ca^{2+}) are released from the endoplasmic reticulum (ER). The combination of DAG and Ca^{2+} activates PKCγ and induces the phosphorylation of downstream substrates. RGS8 is involved in the regulation of mGluR1 signaling. (Right panel), In the SCA14 PKCγ(S361G) mutant with constitutively active kinase domain, the phosphorylation of PKC substrates is enhanced. PKCγ(S361G) can directly interact with mGluR1 (orange arrow) which may further promote mGluR1-PKCγ signaling. Increased expression of RGS8 inhibits overshooting mGluR1 signaling (red circle) and limits the mGluR1-PKCγ pathway activation in SCA14 PKCγ(S361G). Dysregulated RGS8 has been reported in several SCAs implicating dysregulation of the mGluR1 pathway with in the pathogenesis of SCAs.

3.5.3 RGS8 may function as a protective modifier of increased mGluR1 signaling in Purkinje cells of SCA14 PKCγ(S361G) transgenic mice

RGS8 is a member of the R4 subfamily of the regulator of G protein signaling (RGS) gene family and was shown to interact with Gαq/11. After binding, RGS8 is thought to accelerate the hydrolysis of GTP thereby limiting G protein activation (De Vries et al., 2000). Overshooting mGluR1 activation in Purkinje cells by DHPG is well known to cause a marked reduction of Purkinje cell dendritic tree development (Sirzen-Zelenskaya et al., 2006) similar to that found in PKCγ(S361G) Purkinje cells. We have now shown that overexpression of RGS8 in Purkinje cells does indeed protect the dendritic tree from DHPG induced reduction confirming the modulating role of RGS8 on mGluR1 signaling in Purkinje cells. The increased expression of RGS8 found in Purkinje cells of SCA14 PKCγ(S361G) transgenic mice is thus likely to be a consequence of increased mGluR1 signaling and to counteract dendritic reduction due to increased mGluR1 signaling in these cells. The increased expression of RGS8 is therefore likely to be one of the molecular adjustments that does allow many Purkinje

cells in SCA14 PKCγ(S361G) transgenic mice to develop a rather normal dendritic tree *in vivo* (Ji et al., 2014; Trzesniewski et al., 2019) despite constitutively increased PKC activity and elevated mGluR1 signaling.

3.5.4 RGS8 and disturbed mGluR1 signaling play important roles in the development of spinocerebellar ataxias

RGS8 is the only molecule with a known transcriptional dysregulation in 4 different mouse models of SCA, i.e. SCA1, SCA2, SCA7 and SCA14. Interestingly, the type of regulation appears to be different in the different disease types. In SCA1, RGS8 is downregulated (Gatchel et al., 2008; Ingram et al., 2016) and there is also evidence for a reduced activity of mGluR1 signaling (Notartomaso et al., 2013; Shuvaev et al., 2017) although in another study an increase in mGluR1 signaling was found (Power et al., 2016). The reduction of RGS8 expression in SCA1 has been attributed to regulation by microRNA (Rodriguez-Lebron et al., 2013). In contrast, in SCA2 there is evidence that RGS8 downregulation and the concomitant increase in mGluR1 signaling are critical for disease development and progression (Dansithong et al., 2015; Meera et al., 2016). In this model, the reduced expression of RGS8 directly leads to increased mGluR1 signaling which is causing Ca^{2+} -dysregulation and cerebellar dysfunction. In SCA7, the contribution of mGluR1 signaling to disease development is less clear (Niewiadomska-Cimicka and Trottier, 2019), but the disruption of calcium homeostasis appears to be a critical aspect for Purkinje cell dysfunction and loss in the SCA7 mouse model. RGS8 was identified as one of the calcium regulatory genes with an altered expression in the SCA7 mouse model although its role for the observed disturbance in calcium regulation was not further explored in this study (Stoyas et al., 2020). Mutations in the mGluR1 gene itself also cause spinocerebellar ataxia, irrespective of whether these mutations are gain or loss of function mutations (Watson et al., 2017) and autoantibodies against mGluR1 are a common cause of autoimmune or paraneoplastic cerebellar ataxia (Joubert and Honnorat, 2019). In the SCA14 PKCγ(S361G) mice used in this study we have identified an increased mGluR1 signaling which goes together with increased expression of RGS8. This suggests that the increase of RGS8 expression might be secondary to the elevation of mGluR1

signaling as RGS8 is known to be a negative regulator of G-protein mediated signaling. We have shown that overexpression of RGS8 does indeed protect the Purkinje cell dendritic tree from DHPG induced mGluR1 stimulation. It is well known that mGluR1 stimulation is one of the major sources for a rise in intracellular calcium either by stimulating the IP3 receptor pathway or by Ca^{2+} entering through mGluR1-gated TRPC3 channels (Jana Hartmann et al., 2008). Both ways of calcium rise upon mGluR1 stimulation require G-protein activation mediated by RGS8, pinpointing the crucial role of RGS8 for intracellular calcium regulation in Purkinje cells. As increasing evidence points towards a crucial role of Purkinje cell calcium regulation, in particular via the IP3 receptor pathway for the development of SCAs (Schorge et al., 2010; Brown and Loew, 2015; Shimobayashi and Kapfhammer, 2018), RGS8 emerges now as a major regulator of this pathway and the Purkinje cell calcium equilibrium making it an important determinant of pathogenesis of diverse spinocerebellar ataxias.

3.6 Conclusions

We have identified RGS8 as a gene being dysregulated in different mouse models of SCA and being specifically expressed in mouse cerebellar Purkinje cells. RGS8 upregulation in the SCA14 mouse model was related to increased mGluR1-PKCγ signaling and we show that RGS8 overexpression protects Purkinje cell dendrites from the negative effects of mGluR1 activation. Our findings support a critical role of mGluR1 signaling and its regulation by RGS8 in the pathogenesis of different types of SCAs.

Chapter 4: Exploration of STK17B associated with SCAs

4.1 STK17B is most strongly expressed in the nucleus of Purkinje cells

As seen in the previous chapter, STK17B is another key molecule with dysregulation in different SCA mouse models. We first investigated the temporal expression profile of STK17B in the developing cerebellum of the mouse from postnatal day 1 (P1) to adult by Western blot. There was no or only a very weak signal present at P1, but a clear signal present at P3, suggesting that STK17B is not or only weakly expressed in cerebellar cells before P3. Expression became stronger at P7 to a plateau around P14 and continued to be expressed through adulthood (Figure 4.1A). In order to confirm that STK17B was expressed in Purkinje cells, sagittal cerebellar sections from P10 and P12 were examined by immunohistochemistry. STK17B expression was detected in the Purkinje cell layer and there was only weak expression in other cells of cerebellum (Figure 4.1B). Although STK17B was present in the cell body and dendrites of Purkinje cells, the strongest expression was found in the nucleus of Purkinje cells (Figure 4.1C). Immunostainings of primary cerebellar dissociated cultures confirmed that STK17B had strongest expression in the nucleus of Purkinje cells but was also present in other cerebellar cells (Figure 4.1D).

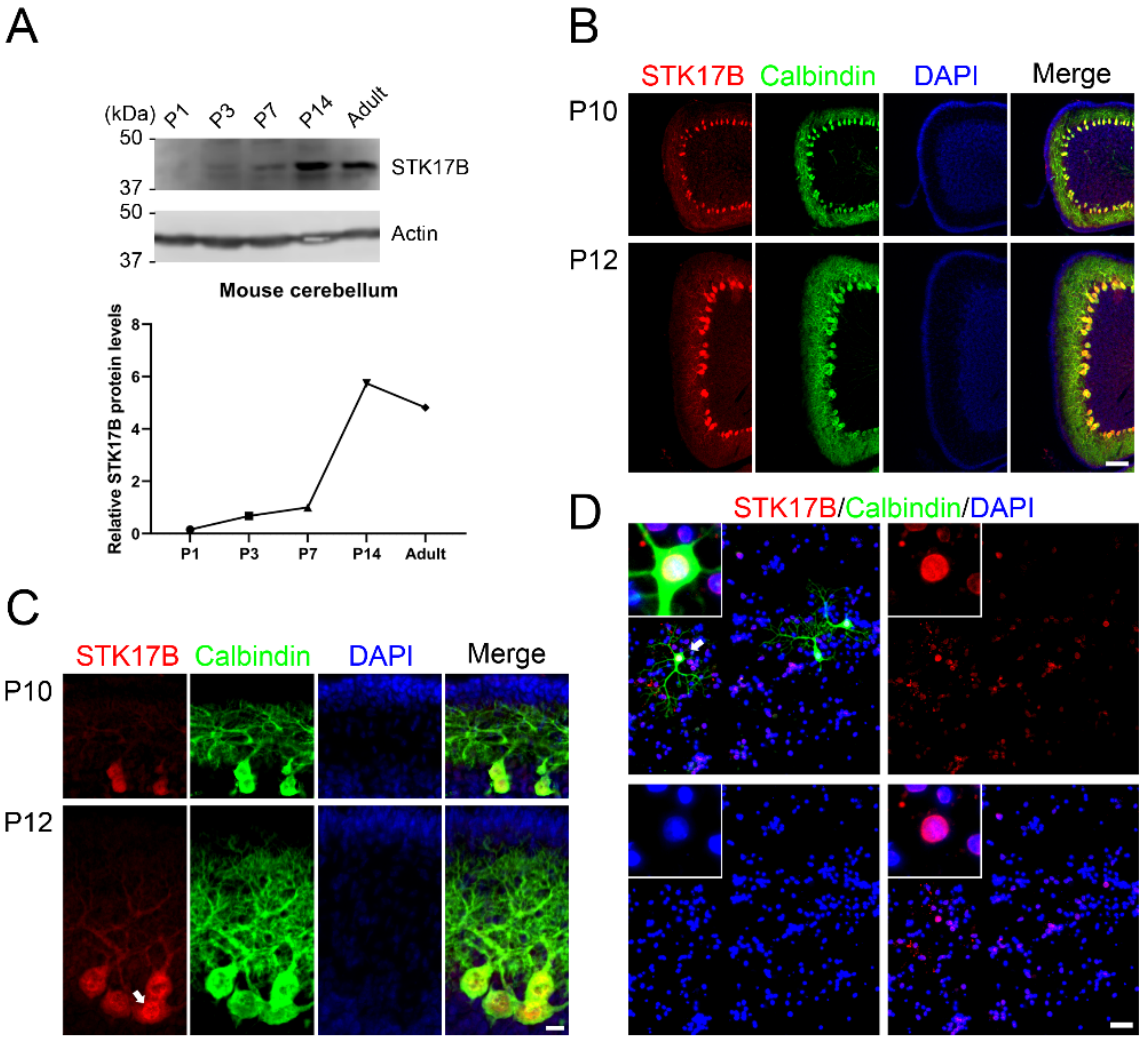

Figure 4.1 Immunostining of STK17B protein in the postnatal mouse cerebellum.

(A) Western blots from mouse cerebellum at different postnatal stages. Top panel: STK17B expression is first evident at P3. Actin was used as loading control shown in bottom panel. Bottom panel: Quantification of protein levels from Western blots. Data are expressed as mean ± SD, with three independent biological samples for P1 (three or four pups for one sample), P3 (three or four pups for one sample) and P7, and two independent biological samples for P14 and Adult. The mean value of STK17B protein level at P7 was set as 1, and values for the other stages were expressed as relatives of this value. The mean values of P1, P3, P14 and adult were 0.1570 ± 0.1276, 0.6769 ± 0.3392, 5.745 ± 1.875 and 4.817 ± 1.722. **(B)** STK17B

immunoreactivity (red signal) is present in cerebellar Purkinje cells (identified by anti-Calbindin, green) at P10 and P12. Scale bar is 100 μm. **(C)** Viewed at higher magnification, STK17B is mainly present in the soma of Purkinje cells at P10 and P12. Arrow indicates the strong expression of STK17B in the cell nucleus of Purkinje cells. Scale bar is 20 μm. **(D)** STK17B is expressed in Purkinje cells and other cells in cerebellar dissociated culture at DIV14. Insert shows that the STK17B is typically distributed in the cell nucleus of Purkinje cells. Scale bar is 50 μm.

4.2 Downregulation of STK17B is associated with Purkinje cell dendritic abnormality in SCA14(S361G) mouse model and increasing PKCγ activity in Purkinje cells

In order to look at the expression of STK17B in a SCA mouse model, we used the PKCγ(S361G) mutant mice present in the laboratory (Ji et al., 2014; Shimobayashi and Kapfhammer, 2017). In mixed dissociated cerebellar cultures from these mice and control mice, the transgenic Purkinje cells were identified by GFP staining and STK17B protein expression was compared between GFP-positive Purkinje cells from S361G-transgenic mice versus GFP-negative Purkinje cells from control mice present in the same culture well. STK17B immunoreactivity was decreased to 0.83 ± 0.21-fold lower expression in Purkinje cells from S361G-transgenic mice versus GFP-negative Purkinje cells from control mice present in the same culture well (Figure 4.2A).

In the PKCγ(S361G) mice, there is a constitutive activation of PKCγ. We tested whether the decreased expression of STK17B was linked to PKCγ activity in Purkinje cells. We treated Purkinje cells in DIV7 dissociated culture with PMA, an activator of PKC. The mean value of STK17B was decreased to 0.64 ± 0.13-fold lower expression in the Purkinje cells treated with PMA versus control Purkinje cells treated with DMSO (Figure 4.2B).

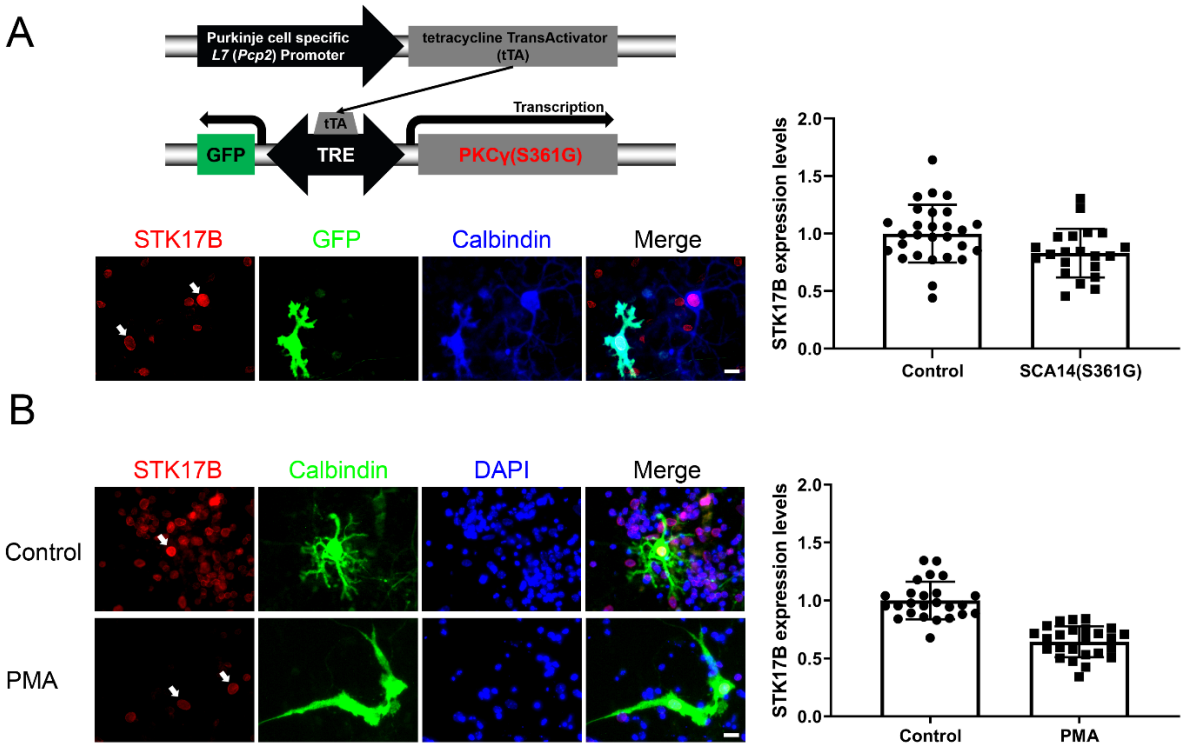

Figure 4.2 Decreased STK17B expression in Purkinje cells of the SCA14 S361G mouse model and in Purkinje cells with PMA treatment

(A) In the transgenic PKCγ(S361G) mouse line, Purkinje cell specific expression of the transgene is achieved by a bidirectional CMV promoter which expresses both GFP and mutant PKCγ. This expression is under the control of a Tetracycline response element (TRE) which will only will start transcription in the presence of the tet TransActivator (tTA), Tet-off system. The tTA protein is expressed in a second transgenic locus under the control of the L7 promoter which only will be active in Purkinje cells. Only in mice which are double transgenic for GFP-TRE-PKCγ(S361G) and L7-tTA, Purkinje cells will show expression of GFP and mutant PKCγ. Purkinje cells were identified by anti-calbindin staining (blue), and PKCγ(S361G)-transgenic cells by anti-GFP staining (green). The arrows indicate expression of STK17B in the nucleus of Purkinje cells. The fluorescence of anti-STK17B immunostaining was quantified using ImageJ. The mean value of STK17B expression in PKCγ(S361G) Purkinje cells was decreased to 0.8303 ± 0.2117-fold compared to control cells. The

n was 28 for control and 21 for SCA14, and the difference in expression was significant with P = 0.0124 in the two-tailed Mann-Whitney test. Data are expressed as mean ± SD. Scale bar is 20 μm. Please note that PKCγ(S361G) transgenic Purkinje cells have a changed morphology as reported earlier. **(B)** STK17B immunoreactivity was decreased in Purkinje cells treated with 25 nM PMA at DIV7 in dissociated cultures. Purkinje cells were identified by anti-calbindin staining (green), and cell nuclei were stained by DAPI (blue). Arrows indicate the expression of STK17B in the nucleus of Purkinje cells. The fluorescence of anti-STK17B staining was quantified using ImageJ. The mean value of STK17B expression for PMA treatment is decreased to 0.6437 ± 0.1331-fold compared to control cells. The n was 25, and the difference in expression was significant with P < 0.0001 in the two-tailed Mann-Whitney test. Data are expressed as mean ± SD. Scale bar is 20 μm.

4.3 STK17B overexpression aggravates the reduction of denritic tree size of Purkinje cells after PKC activation

As shown above, STK17B expression in Purkinje cells is reduced with increased PKC activity. As a next step, we wanted to see whether overexpression of STK17B could protect the morphology Purkinje cells after treatment with PMA. Purkinje cells were transfected with GFP-STK17B and exposed to a treatment of 0.75-1.25 nM. We found that overexpression of STK17B didn't have a rescuing effect for the dendritic tree with treatment of this low concentration of PMA. Conversely, Purkinje cells with STK17B overexpression showed a severely reduced morphology compared to control Purkinje cells with the same PMA treatment in the same culture wells (Figure 4.3A) while overexpression of STK17B in the absence of PMA had no effect on the morphology of the Purkinje cell dendritic tree (Figure 4.3B).

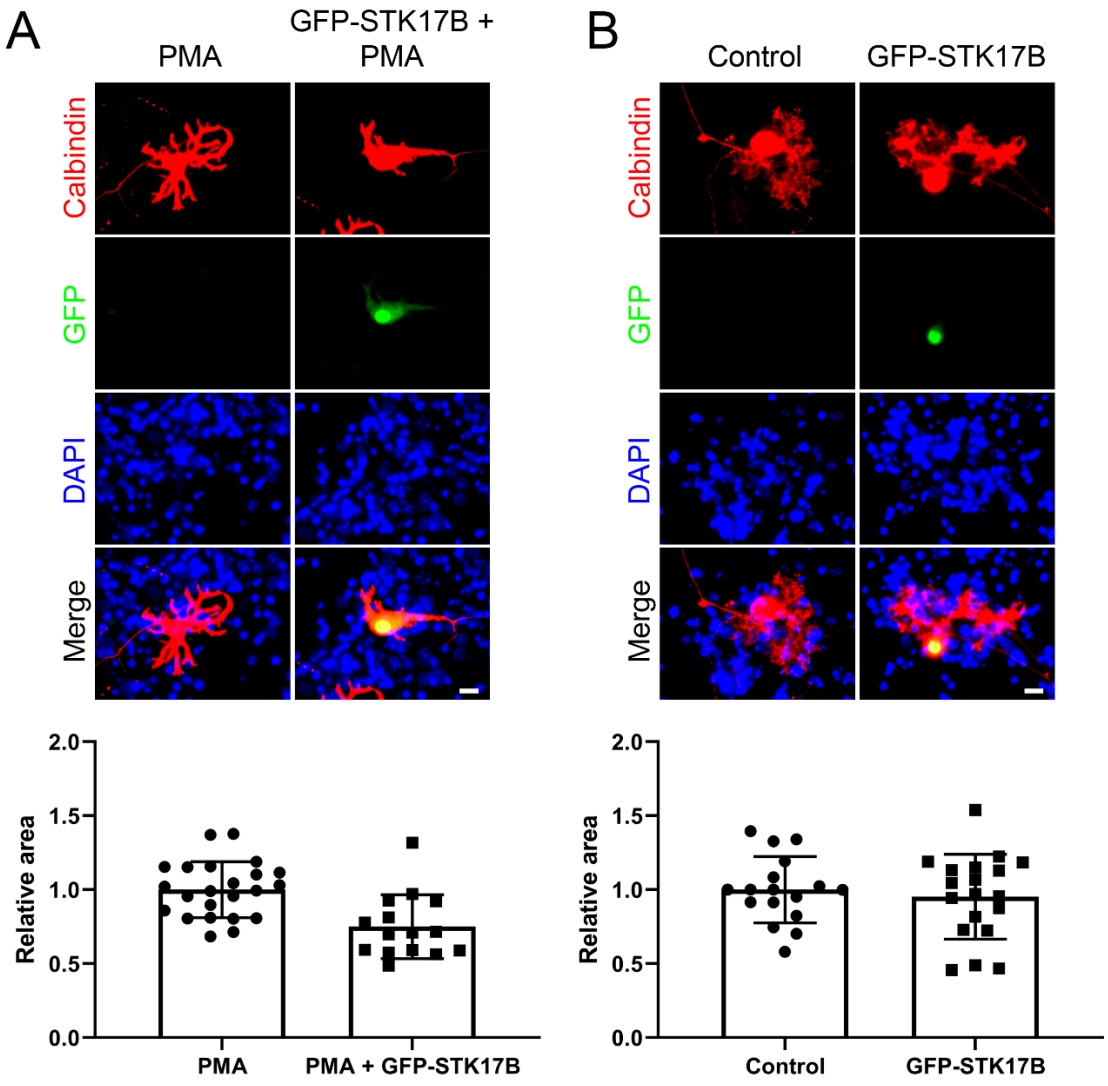

Figure 4.3 Overexpression of STK17B in Purkinje cells enhances the PMA effect.

(A) STK17B transfection enhances the reduction of the Purkinje cell dendritic tree by treatment with the PKC activator PMA. Top panel: representative images of control and STK17B-transfected Purkinje cells with 0.75-1.25 nM PMA treatment. Bottom panel: the mean values of the Purkinje cell dendritic area with PMA treatment of non-transfected cells was 1.000 ± 0.1884, and was reduced to 0.7505 ± 0.2156 in STK17B-transfected cells. The n of control was 23 cells, the n of STK17B transfected cells was 15 cells, P = 0.0004 in the two-tailed Mann-Whitney test. **(B)**

Purkinje cell morphology is not or only mildly affected after STK17B transfection. Top panel: representative images of Purkinje cells after control or STK17B transfection. Bottom panel: the mean values of the Purkinje cell dendritic area was measured, controls were the non-transfected cells from the same culture well: Control 1.000 ± 0.2237 vs GFP-STK17B 0.9524 ± 0.2862. The n for control = 17 cells and for GFP-STK17B = 19 cells from two independent transfection experiments, P = 0.7482 in the two-tailed Mann-Whitney test. Data are expressed as mean ± SD. Scale bars are 20 μm.

4.4 Serine 351 phosphorylation of STK17B mediates its localization and function in Purkinje cells

STK17B has been shown to be a PKCγ phosphorylation substrate in NIH3T3 cells and PKCγ mediated S350 phosphorylation of rat STK17B has been reported and was shown to affect its localization in these cells (Kuwahara et al., 2008). By comparison of the sequence of mouse and rat, we found the same sequence and the corresponding residue Serine 351 in mouse STK17B. We use two forms, the phosphorylation mimetic form S351D and the non-phosphorylatable S351A form. After transfection of the respective constructs we can study their effects and the impact of phosphorylation in Purkinje cells. We found that S351D strongly affect Purkinje cell dendritic development with a strong reduction of dendritic tree size (Figure 4.4A). In contrast, STK17B(S351A) did not affect Purkinje cell dendritic development (Figure 4.4B). Both STK17B(S351D) and STK17B(S351A) showed nuclear and cytoplasm localization not similar to the distribution of wild-type GFP-STK17B after overexpression and to the endogenous STK17B expression in Purkinje cells. The findings show that phosphorylation strongly affects the function of STK17B in Purkinje cells.

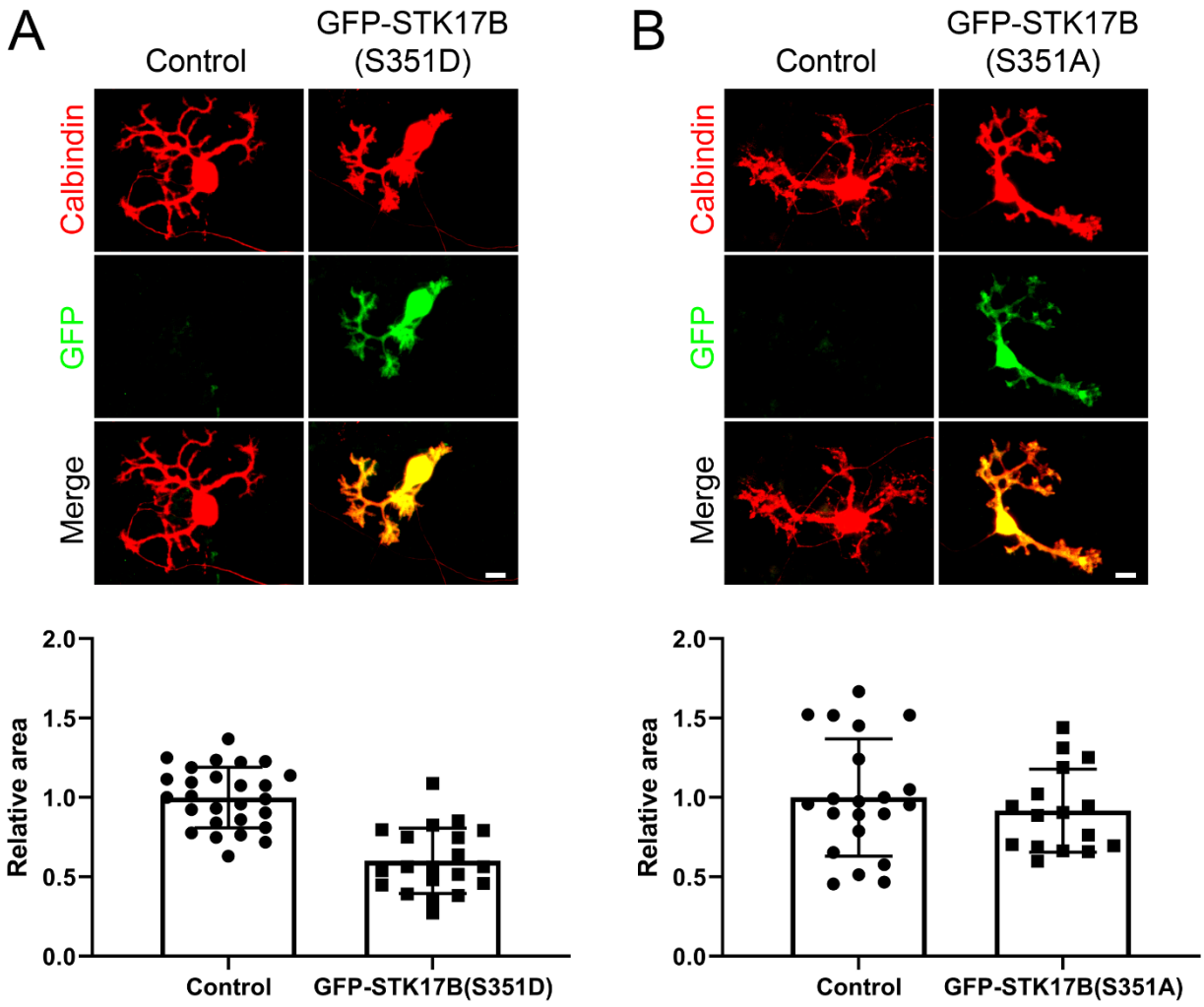

Figure 4.4 Phosphomimetic STK17B(S351D) inhibits Purkinje cell dendritic development.

(A) Purkinje cell dendritic morphology is negatively affected after transfection of STK17B(S351D). Top panel: representative images of Purkinje cells after control or STK17B(S351D) transfection. Bottom panel: The mean values of the Purkinje cell dendritic area were measured, controls were the non-transfected cells from the same culture well: Control 1.000 ± 0.1908 vs GFP-STK17B(S351D) 0.6017 ± 0.2059. The n of control = 27 cells and the n of GFP-STK17B(S351D) = 20 cells from at least three independent transfection experiments, $P < 0.0001$ in the two-tailed Mann-Whitney test. **(B)** Purkinje cell dendritic morphology is not or only mildly affected after

STK17B(S351A) transfection. Top panel: representative images of Purkinje cells after control or STK17B(S351A) transfection. Bottom panel: The mean values of the Purkinje cell dendritic area were measured, controls were the non-transfected cells from the same culture well: Control 1.000 ± 0.3688 vs GFP-STK17B(S351A) 0.9174 ± 0.2623 The n of control = 21 cells and the n of GFP-STK17B(S351A) = 16 cells from two independent transfection experiments, P = 0.4759 in the two-tailed Mann-Whitney test. Data are expressed as mean ± SD. Scale bars are 20 μm.

4.5 Inhibiting STK17B activity with a novel inhibitor of STK17B, Cpd41, does not affect Purkinje cell dendritic growth

A novel inhibitor of STK17B has been published recently with an IC50 of 0.25 μM (S. Wang et al., 2017). The inhibitor Cpd41 has been synthesized based on the reported structure (Figure 4.5A). Purkinje cells treated with 10 μM or 20 μM Cpd41 did not show any changes of dendritic development (Figure 4.5B and C). Increasing the concentration to 50 μM of Cpd41 treatment still did not affect the size of the Purkinje cell dendritic tree, however, with the compound became toxic when used at a concentration of 286 μM of Cpd41 (Figure 4.5C).

.

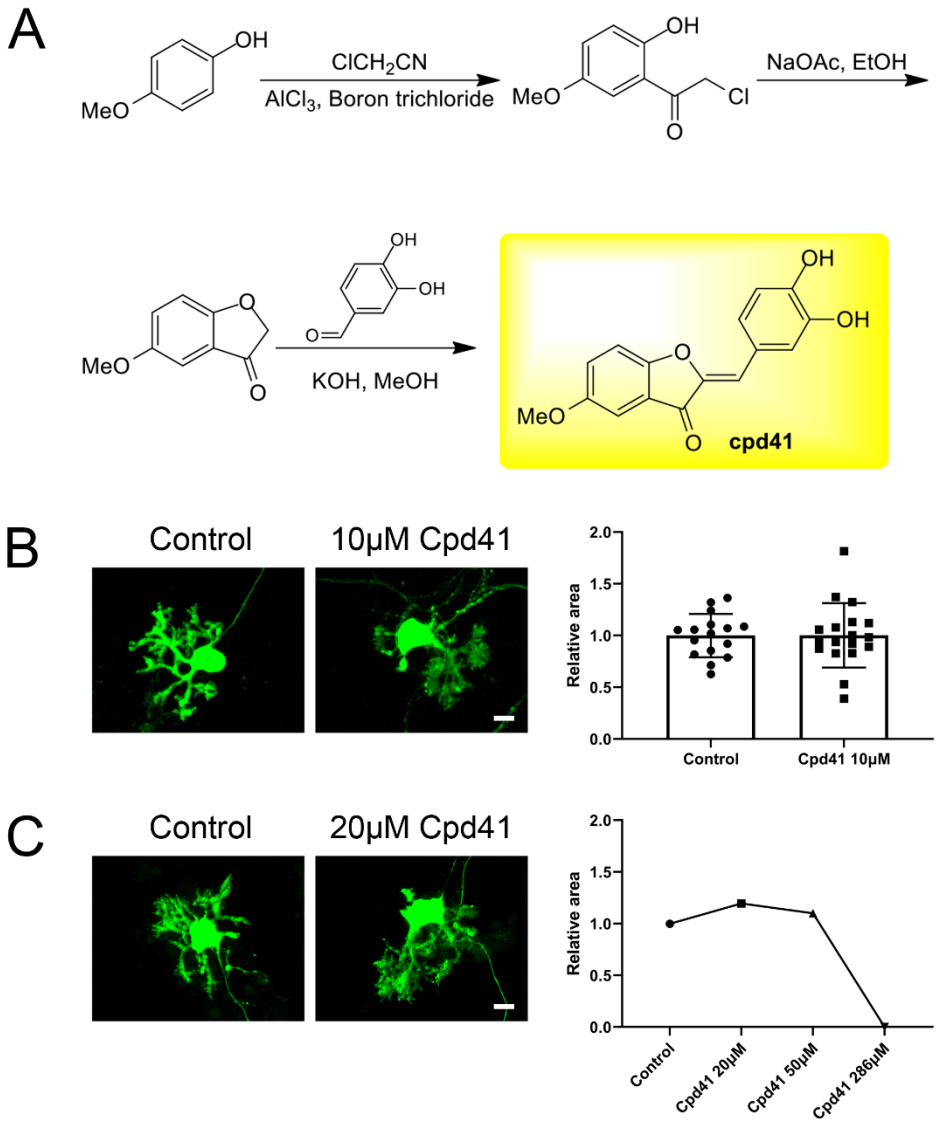

Figure 4.5 Purkinje cell morphology is not affected by treatment with the STK17B inhibitor Cpd41

(A) Synthetic scheme and structure of STK17B inhibitor Cpd41. **(B)** 10 μM Cpd41 treatment does not affect the size of the Purkinje cell dendritic tree. Left panel: representative images of Purkinje cells after control or STK17B inhibitor Cpd41 treatment. Right panel: The mean values of the Purkinje cell dendritic area were: 1.000 ± 0.2084 for control vs 1.002 ± 0.3110 for treatment with 10 μM Cpd41. The n for control = 16 cells and the n for 10 μM Cpd41 = 18 cells from two independent experiments, P > 0.9999 in the two-tailed Mann-Whitney test. **(C)** A 20-50 μM

concentration of Cpd41 treatment does not affect the size of the Purkinje cell dendritic tree, but death of Purkinje cells is observed at 286 μM high concentration of Cpd41.

4.6 Inhibiting STK17B activity enhances the inhibition of dendritic growth seen in Purkinje cells from SCA14 PKCγ(S361G) mice

To know whether inhibition of STK17B might rescue the Purkinje cell dendritic morphology in SCA14 PKCγ(S361G) Purkinje cells, dissociated cultures from PKCγ(S361G) mice were treated with 10 μM Cpd41. We found that this treatment did not rescue the dendrites from PKCγ(S361G) cells but in contrast significantly further reduced the dendritic development of PKCγ(S361G) Purkinje cells (Figure 4.6A). These results were further confirmed by treatment with 20 μM Cpd41 which had a similar inhibitory effect on dendritic growth (Figure 4.6B).

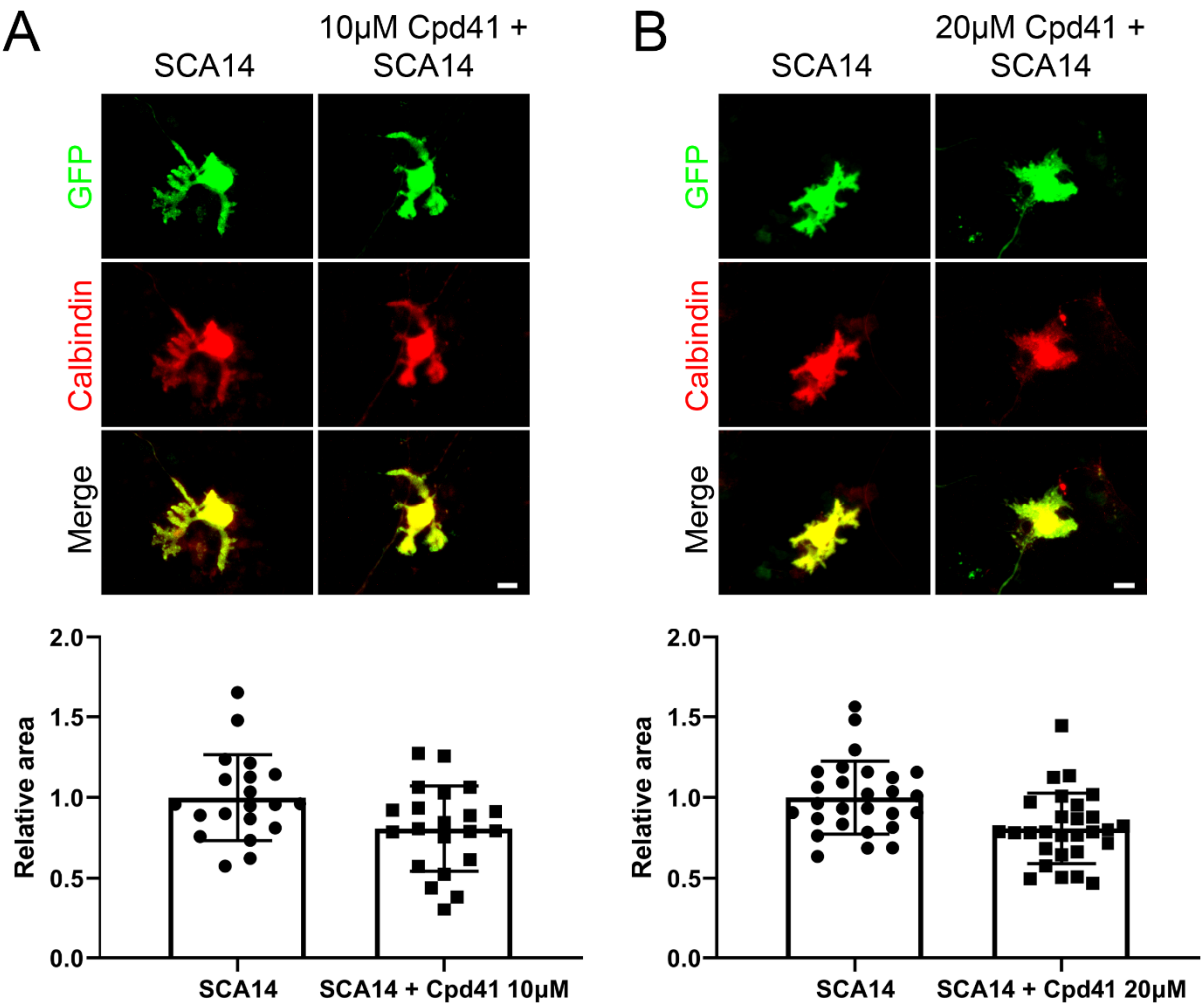

Figure 4.6 Cpd41 treatment enhances the reduction of Purkinje cell dendritic morphology from the SCA14 mouse model.

(A) 10 μM Cpd41 treatment reduces the Purkinje cell dendritic tree in the SCA14 mouse model. Top panel: representative images of Purkinje cells from SCA14 PKCγ(S361G) mouse model with or without 10 μM Cpd41 treatment. Bottom panel: The mean values of the Purkinje cell dendritic area were: non-treated Purkinje cells from SCA14 mouse model 1.000 ± 0.2662 vs 10 μM Cpd41-treated Purkinje cells from SCA14 mouse model 0.8082 ± 0.2638, the n of SCA14 was 20 cells, the n of 10 μM Cpd41-treated SCA14 was 21 cells, P = 0.0347 in the two-tailed Mann-Whitney test. **(B)** The Purkinje cell morphology of SCA14 mouse model is negatively affected after 20 μM Cpd41 treatment. Top panel: representative images of Purkinje cells

from SCA14 mouse model with or without 20 μM Cpd41 treatment. Bottom panel: The mean values of the Purkinje cell dendritic area were: non-treated Purkinje cells from SCA14 mouse model 1.000 ± 0.2261 vs 20 μM Cpd41-treated Purkinje cells from SCA14 mouse model 0.8089 ± 0.2181, the n of SCA14 was 27 cells, the n of 20 μM Cpd41-treated SCA14 was 28 cells, P = 0.0014 in the two-tailed Mann-Whitney test. Data are expressed as mean ± SD. Scale bars are 20 μm.

Chapter 5: Additional Data: The CRISPR-Cas13a system interferes with Purkinje cell dendritic development

The section 5.6 of this chapter is based on the work published in **Biochimica et Biophysica Acta (BBA) - Molecular Cell Research**, 2020, Volume 1867, Issue 7. Some text, figures, the numbering of the figure legend and the title numbering have been adapted to this thesis**.**

5.1 Preface

Gene knockdown in cerebellar Purkinje neurons is a major challenge because Purkinje cells only make up a small percentage of the cerebellum. The CRISPR-Cas13 system has been explored as a powerful new method for knockdown of transcripts in cell lines with high specificity. Little is known about the application of the knockdown efficiency and the resulting protein expression levels of the CRISPR-Cas13 method in developing postmitotic neurons. In this chapter, we adapted the Cas13a-based conditional knockdown system for cerebellar Purkinje neurons and found that this system can achieve a suppression of the target proteins in the mixed cerebellar cultures for two weeks almost exclusively restricted to Purkinje cells. This could greatly facilitate the study of gene function in Purkinje cells. No classical collateral activity was observed but a cytotoxic phenotype that does not depend on trans-RNA cleavage. Our results demonstrate the feasibility of Cas13-based conditional knockdown in developing postmitotic neurons and establish CRISPR-Cas13 as an example for a cell- or tissue-specific knockdown method.

Purkinje cells are key players in the cerebellar circuitry, providing a unique output from the cerebellar cortex (Hansel et al., 2001). Specific gene silencing for functional studies in Purkinje cells is a huge challenge because Purkinje cells represent only a small percentage of the cerebellar cells, the majority of the cells are granule cells, glia and interneurons (Wagner, McCroskery, et al., 2011). An alternative strategy of target gene silencing is through RNA interference of short hairpin RNA (shRNA) (Brummelkamp et al., 2002), however, the mere expression of shRNA within Purkinje cells is difficult to specify. The uniform expression of shRNA across all cell types is present in dense heterogeneous cultures, which may induce unwanted knockdown in other cell types such as granule cells, which are critical for survival and development of Purkinje cells (Wagner, McCroskery, et al., 2011). Furthermore, complex neuronal cell types are highly sensitive to off-target effects, as off-target effects of shRNA have been shown to severely disrupt neuronal structure and function (Alvarez et al., 2006) and shRNA-mediated knockdown may induce endogenous microRNA

dysregulation associated with changes of neurodevelopment and survival (Baek et al., 2014).

The CRISPR-associated (Cas) effector, Cas13a, previously designated as Class II candidate 2 (C2c2), has been found in bacteria (Abudayyeh et al., 2016; Gootenberg et al., 2017a). Cas13 contains two nucleotide-binding domains (HEPN) for higher eukaryotes and prokaryotes exclusively associated with RNase activity (Abudayyeh et al., 2016; O'Connell, 2019). Cas13 can be viewed as a programmable RNA-directed single-stranded RNA ribonuclease, forming Cas13-CRISPR RNA (crRNA) complex. Binding of target RNA by the Cas13-crRNA complexes activates the RNase activity. The Cas13-crRNA complex is capable of cleaving target RNA, referred to as cis-RNA cleavage. There also may be non-specific RNA cleavage called trans-RNA cleavage or collateral cleavage (Abudayyeh et al., 2016; Meeske and Marraffini, 2018; O'Connell, 2019). Trans-RNA cleavage can induce collateral effects such as inhibition of cell proliferation in bacteria, and this collateral effect is used to establish a Cas13a-based molecular detection platform for diagnostic use (Gootenberg et al., 2017a). Interestingly, unexpected collateral cleavage by the activated Cas13a-crRNA complexes was not observed in eukaryotic cells, so Cas13a guided by a crRNA with a 28-nt spacer sequence that cleaves target transcripts can be expressed in mammalian cells and plant cells for targeted gene silencing at knockdown levels comparable to small hairpin RNA (shRNA) with improved specificity (Abudayyeh et al., 2017). Due to the significantly reduced off-target effects, the Cas13a-based system has been suggested as a therapeutic tool for mutant KRAS for the treatment of pancreatic cancer (Zhao et al., 2018). More recently, the CRISPR-Cas13 system has been employed to achieve inhibition and detection of RNA viruses (Freije et al., 2019).

In this chapter, we have developed a Purkinje cell-specific Cas13a-based system (PCSC13) and this system can be engineered for conditional knockdown of specific target proteins. The utility of PCSC13 was demonstrated for the *prkcg* gene encoding protein kinase C gamma (PKCγ), which is mainly expressed in cerebellar Purkinje neurons and has been served as a candidate Purkinje cell marker (Yang et

al., 2018). No detectable collateral effect of trans-RNA cleavage after knockdown of PKCγ was observed in Purkinje cells, but the use of this system was limited by cytotoxicity in Purkinje cells.

5.2 Engineering of a Purkinje cell-specific Cas13a-based system (PCSC13)

To engineer a Purkinje cell-specific Cas13a-based system (PCSC13), we cloned a mammalian codon-optimized Cas13a from *Leptotrichia wadei* with a C terminal monomeric GFP sequence into a vector with the Purkinje cell-specific L7 (Pcp2) promoter for selective expression in cerebellar Purkinje cells. Cas13a shows programmable RNA cleavage with a CRISPR RNA (crRNA) encoding a 28-nucleotide (nt) spacer (Abudayyeh et al., 2017). Protein kinase C gamma (PKCγ), encoded by *prkcg* gene, is prominently expressed in cerebellar Purkinje cells and was used as target protein to facilitate the assessment of the gene silencing in Purkinje cells. We designed and constructed two PKCγ guide crRNAs (guide 1 and guide 2) complementary to sequences of two different regions of *prkcg* transcripts under the U6 promoter, as previously described (Figure 5.1A and B). The pL7-Cas13a-mGFP and the guide crRNAs were co-transfected into Purkinje cells at the setup of the culture and gene knockdown was analyzed after a two week culture period (Figure 5.1B). Target-RNA (also known as activator-RNA) combines with the Cas13-crRNA complex to activate RNase activity (Figure 5.1C). In bacteria, the HEPN-nuclease becomes active and is able to cleave not only the target-RNA in cis but also any other RNAs present (collateral cleavage). Surprisingly, this collateral cleavage (also known as trans-RNA cleavage) effect has only been observed in bacteria but not in eukaryotic cells, so Cas13a-based methods could target gene silencing of either reporter or endogenous transcripts in mammalian cells high specificity (Abudayyeh et al., 2016, 2017; Gootenberg et al., 2017a; Meeske and Marraffini, 2018; O'Connell, 2019).

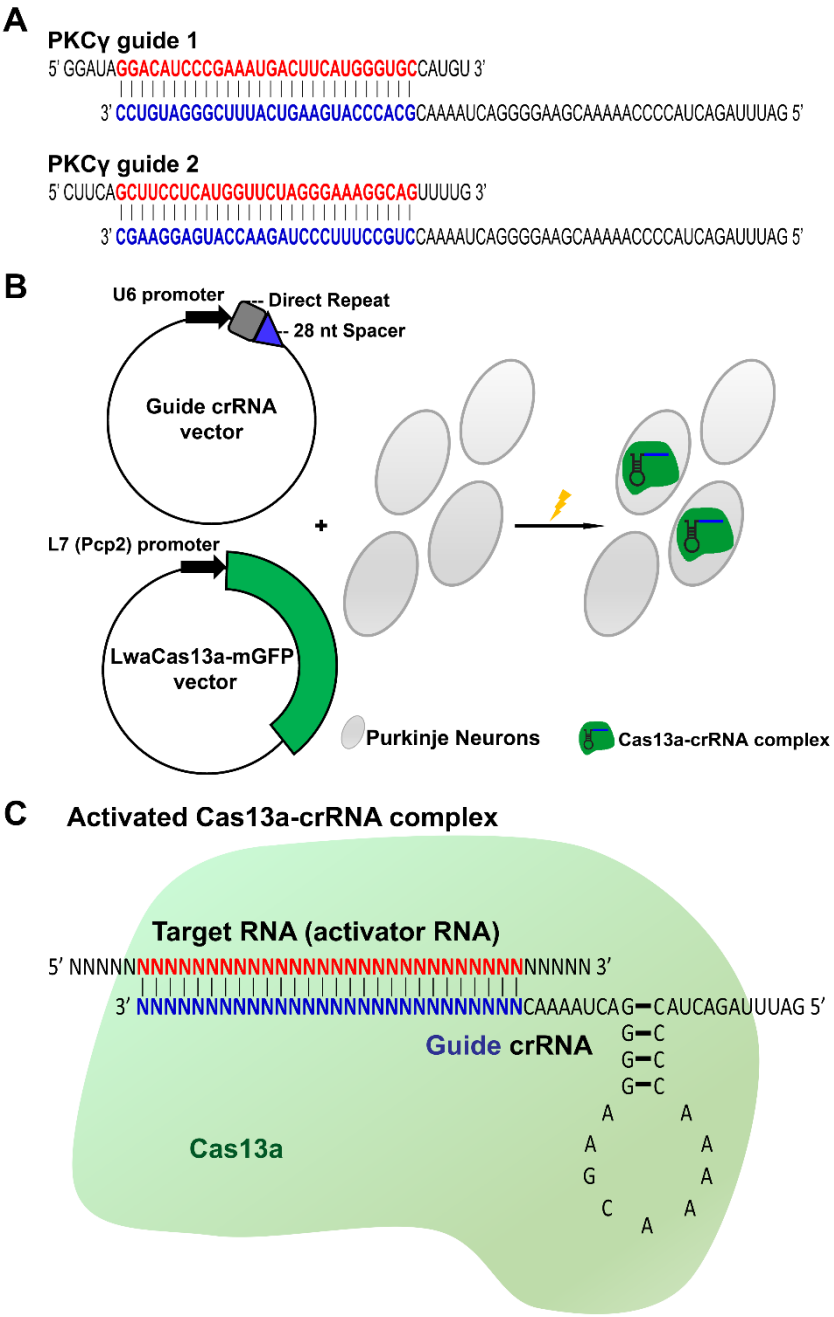

Figure 5.1 Construction of the programable CRISPR-Cas13a system in Purkinje cells.

(A) Target RNA sequences paired with PKCγ guide 1 and PKCγ guide 2 crRNAs which contain 28-nt spacers and 36-nt direct repeats. **(B)** Schematic illustration of the construction and function of CRISPR-Cas13a in Purkinje cells. Purkinje cells

were transfected with Cas13a and crRNA at the setup of the culture. **(C)** Diagrammatic representation of the activated Cas13a–crRNA complex. Target RNA serves as activator RNA. Once the Cas13a–crRNA complex binds to target RNA, Cas13a-crRNA complex is activated and produce RNase activity to cleave target transcripts.

5.3 PCSC13 is capable of conditional gene silencing

To test whether the CRISPR-Cas13a system could knockdown PKCγ in Purkinje cells, we transfected the pL7-Cas13a-mGFP vector and guide vectors into cerebellar Purkinje cells and performed triple immunofluorescence staining two weeks after transfection. The complete CRISPR-Cas13a system was visualized by anti-GFP staining, which identifies the activated Cas13a-crRNA complex. The Purkinje cells were distinguished by anti-Calbindin staining. We observed that the Cas13a-guide 1 complex resulted in a high level of knockdown. The mean level of PKCγ signal was significantly reduced to 27% in the cell body of Purkinje cells ($P < 0.0001$), 25.8% in the primary dendrites of Purkinje cells ($P < 0.0001$), to 24.1% in the secondary dendrites of Purkinje cells ($P < 0.0001$) and to 25% in the terminal dendrites of Purkinje cells ($P < 0.0001$), compared to non-transfected neighboring GFP-negative Purkinje cells in the same culture well (Figure 5.2A and B). Cas13a-guide 1 mediated better knockdown compared to guide 2. A detectable reduction in the PKCγ signal was also observed with guide 2, A mean reduction to 54.9% in the level of PKCγ signal in the cell body of Purkinje cells ($P = 0.0001$), to 44.2% in the primary dendrites of Purkinje cells ($P = 0.0004$) , to 64.7% in the secondary dendrites ($P = 0.0532$) and to 69% in the terminal dendrites of Purkinje cells ($P = 0.0595$) was achieved with Cas13a guide 1 (Figure 5.2A and C). We also performed Cas13a-guide N (nontargeting) complex experiments. The mean level of PKCγ signal was not significantly changed in the cell body, the primary dendrites, the secondary dendrites and the terminal dendrites of Purkinje cells, compared to non-transfected neighboring GFP-negative Purkinje cells in the same culture well (Figure 5.3A and

D). These results show the ability of the CRISPR-Cas13a for endogenous gene silencing in cerebellar Purkinje cells.

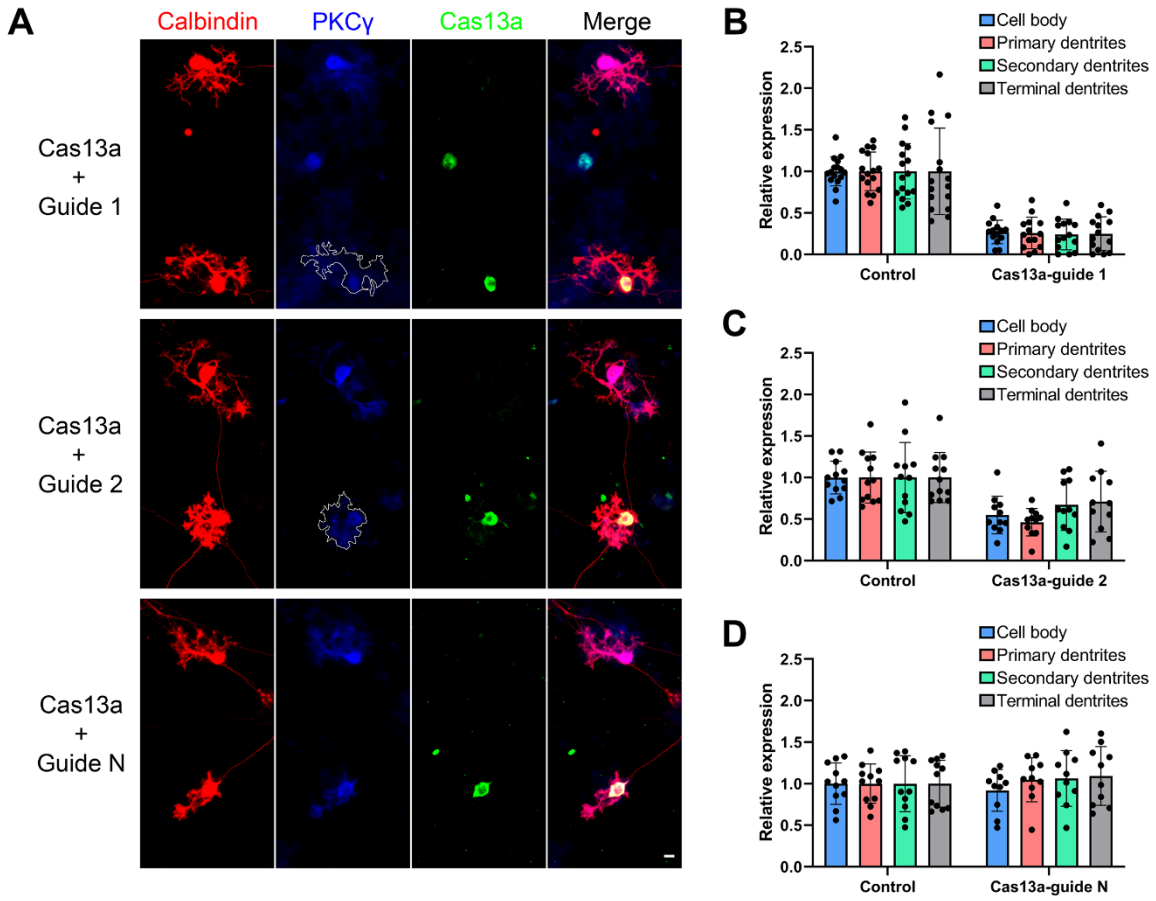

Figure 5.2 A Cas13a-based system is capable of conditional gene knockdown in Purkinje cells.

(A) Triple immunofluorescence staining with anti-GFP (green), anti-PKCγ (blue) in Purkinje cells labelled by anti-Calbindin (red). Knockdown of PKCγ with guide crRNAs with Cas13a-mGFP. Purkinje cells expressing nontargeting guide RNA (lower panel) have PKCγ expression comparable to control cells. The outlines indicate cells targeted by the CRISPR-Cas13a knockdown system stained by GFP. Scale bar, 20 μm. **(B)** Comparison of Cas13a-guide 1 complex relative knockdown efficiencies in Purkinje cells. In the control group, the mean value of PKCγ signal in the cell body of Purkinje cells is 1.000 ± 0.1749; the mean value of PKCγ signal in

primary dendrites of Purkinje cells is 1.000 ± 0.2330; the mean value of PKCγ signal in the secondary dendrites is 1.000 ± 0.3327; the mean value of PKCγ signal in the terminal dendrites 1.000 ± 0.5194; n represents 16 cells from two independent transfection experiments. In the Cas13a-guide 1 complex group, the mean value of PKCγ signal in the cell body of Purkinje cells is 0.2700 ± 0.1423; the mean value of PKCγ signal in the primary dendrites of Purkinje cells is 0.2583 ± 0.1879; the mean value of PKCγ signal in the secondary dendrites is 0.2406 ± 0.1848; the mean value of PKCγ signal in the terminal dendrites is 0.2497 ± 0.2027; n represents 14 cells from two independent transfection experiments. The results were significant with the P values < 0.0001 respectively compared with the corresponding controls. Data are shown as the mean ± SD. The P values are according to the two-tailed Mann-Whitney test. **(C)** Comparison of Cas13a-guide 2 complex relative knockdown efficiencies in Purkinje cells. In the control group, the mean value of PKCγ signal in the cell body of Purkinje cells is 1.000 ± 0.1965; the mean value of PKCγ signal in primary dendrites of Purkinje cells is 1.000 ± 0.3068; the mean value of PKCγ signal in the secondary dendrites is 1.000 ± 0.4220; the mean value of PKCγ signal in the terminal dendrites is 1.000 ± 0.3008; n represents 12 cells from two independent transfection experiments. In Cas13a-guide 2 complex group, the mean value of PKCγ signal in the cell body of Purkinje cells is 0.5492 ± 0.2266; the mean value of PKCγ signal in the primary dendrites of Purkinje cells is 0.4616 ± 0.1651; the results were significant in with the cell body and the primary dendrites with the P values of 0.0001 and < 0.0001 respectively compared with the corresponding controls. The mean value of PKCγ signal in the secondary dendrites is 0.6716 ± 0.3084; The results were not significant in the secondary dendrites with the P value of 0.0530 compared with the corresponding controls; The mean value of PKCγ signal in the terminal dendrites is 0.7099 ± 0.3657; The results were significant in the terminal dendrites with the P value of 0.0317 compared with the corresponding controls. n represents 11 cells from two independent transfection experiments. Data are shown as the mean ± SD. The P values are according to the two-tailed Mann-Whitney test. **(D)** Comparison of Cas13a-guide N complex relative knockdown efficiencies in Purkinje cells. In the control group, the mean value of PKCγ signal in the cell body of Purkinje cells is 1.000 ± 0.2496; the mean value of PKCγ signal in primary dendrites

of Purkinje cells is 1.000 ± 0.2370; the mean value of PKCγ signal in the secondary dendrites is 1.000 ± 0.3358; the mean value of PKCγ signal in the terminal dendrites is 1.000 ± 0.2824; n represents 11 cells from two independent transfection experiments. In the Cas13a-guide N complex group, the mean value of PKCγ signal in the cell body of Purkinje cells is 0.9183 ± 0.2506; the mean value of PKCγ signal in the primary dendrites of Purkinje cells is 1.047 ± 0.2645; the mean value of PKCγ signal in the secondary dendrites is 1.063 ± 0.3351; the mean value of PKCγ signal in the terminal dendrites is 1.094 ± 0.3542; n represents 10 cells from two independent transfection experiments. The results were not significant with the P values 0.5116, 0.6539, 0.7564 and 0.4262 respectively compared with the corresponding controls. Data are shown as the mean ± SD. The P values are according to the two-tailed Mann-Whitney test.

5.4 Reduced dendritic growth of Purkinje cells occur after gene silencing by use of PCSC13

Previous studies have shown that PKCγ activity is a negative regulator of dendritic growth and an increase of Purkinje cell dendritic development occurs in PKCγ-deficient mice compared to wild-type mice (Schrenk et al., 2002). PKC inhibitors also can induce an increase of development of Purkinje cells in the wild type mice (Kapfhammer, 2004). The dendritic area from GFP-positive Cas13a-guide 1 complex transfected Purkinje cells was compared to non-transfected neighboring GFP-negative Purkinje cells in the same culture well and showed no significant change (P = 0.1265) (Figure 5.2A and 3A). However, we noticed a reduction of dendritic growth two weeks after of co-transfection of guide 2 and Cas13a into Purkinje cells compared to non-transfected Cas13a neighboring GFP-negative Purkinje cells in the same culture well. We further confirmed this inhibition of dendritic growth by measuring the area of dendrites after PKCγ knockdown by use of guide 2. The size of the dendritic tree was reduced to 79% of control Purkinje cells (P = 0.0093)

(Figure 5.3A and B). Expression of crRNAs alone did not affect Purkinje cell development compared to control Purkinje cells (Figure 5.3C).

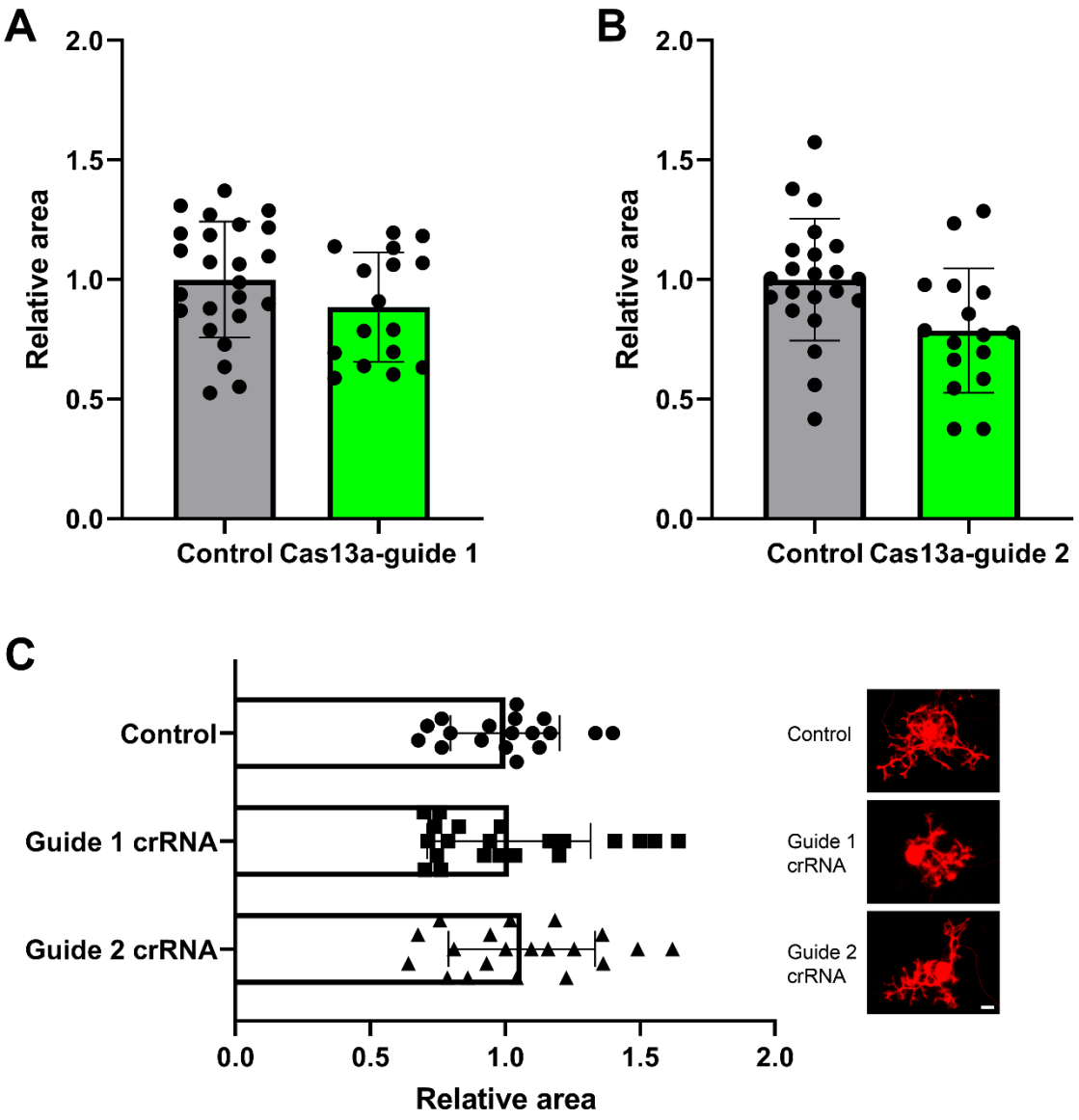

Figure 5.3 Cas13a-guide 2 complex suppresses dendritic growth in cerebellar Purkinje cells.

(A) Purkinje cells expressing the Cas13a-guide 1 complex (right side) have no significant affection of dendritic trees compared to control cells (left side). The mean value of the dendritic area for control is 1.000 ± 0.2420, n represents 24 cells from

two independent transfection experiments. The mean value for Cas13a-guide 1 complex is 0.8848 ± 0.2284. n represents 16 cells from two independent transfection experiments. P = 0.1265 in the two-tailed Mann-Whitney test. **(B)** Purkinje cells expressing the Cas13a-guide 2 complex (right side) have reduced dendritic trees compared to control cells (left side). The mean value of the dendritic area for control is 1.000 ± 0.2551, n represents 22 cells from two independent transfection experiments. The mean value for Cas13a-guide 2 complex is 0.7868 ± 0.2603. n represents 16 cells from two independent transfection experiments. The results were significant with P = 0.0093 in the two-tailed Mann-Whitney test. **(C)** Purkinje cells expressing the guide alone have no affection of dendritic growth compared to control cells treated in the same transfection condition. The mean value of the dendritic area for control is 1.000 ± 0.2031, n represents 18 cells from two independent transfection experiments. The mean value for guide 1 is 1.014 ± 0.3035, n represents 21 cells from two independent transfection experiments. The mean value for guide 2 is 1.062 ± 0.2715. n represents 20 cells from two independent transfection experiments. The P value is 0.6937 according to the non-parametric one-way ANOVA Kruskal-Wallis test. All Data are shown as the mean ± SD. Scale bar, 20 μm.

5.5 The inhibition of Purkinje cell dendritic growth by the Cas13a-crRNA complex is not caused by collateral activity, i.e. unspecific RNA cleavage

It is conceivable that the inhibition of dendritic growth of Purkinje cells observed in our experiments might be due to collateral activity of the Cas13-based system although such collateral activity was only shown in bacteria and was absent in mammalian cells (Abudayyeh et al., 2016; Meeske and Marraffini, 2018)

(Abudayyeh et al., 2016, 2017). In order to exclude the presence of collateral RNA cleavage we used a monoclonal anti-rRNA antibody (White et al., 2019) to test rRNA levels in Purkinje cells. We stained and measured the level of rRNA in Purkinje cells expressing the Cas13a-guide 1 complex, which showed the high RNase activity with the strong knockdown efficiency, and found no significant change of rRNA level compared with control cells (Figure 5.4A).

To further investigate if collateral activity might contribute to the inhibition of Purkinje cell dendritic growth, we used the same PKCγ guide crRNAs in PKCγ knockout (KO) mice, in which no target RNA is present to activate the Cas13a-crRNA complex. No PKCγ staining in Purkinje cells could be detect in PKCγ knockout (KO) mice (Figure 5.4B and C). Again, we observed a significant growth inhibition ($P = 0.0139$) of dendrites in Purkinje cells expressing the non-activated Cas13a-guide 1 complex (Figure 5.4B). Consistent with the observed inhibitory action of the Cas13a-guide 1, expression of Cas13a-guide 2 complex also demonstrates a significant reduction ($P = 0.0010$) of dendrites in Purkinje cells (Figure 5.4C). These data show that the inhibition of Purkinje cell dendritic growth by the Cas13 system cannot be due to the classical collateral activity, i.e. unspecific RNA cleavage, but rather must reflect an adverse or toxic effect of one of the components.

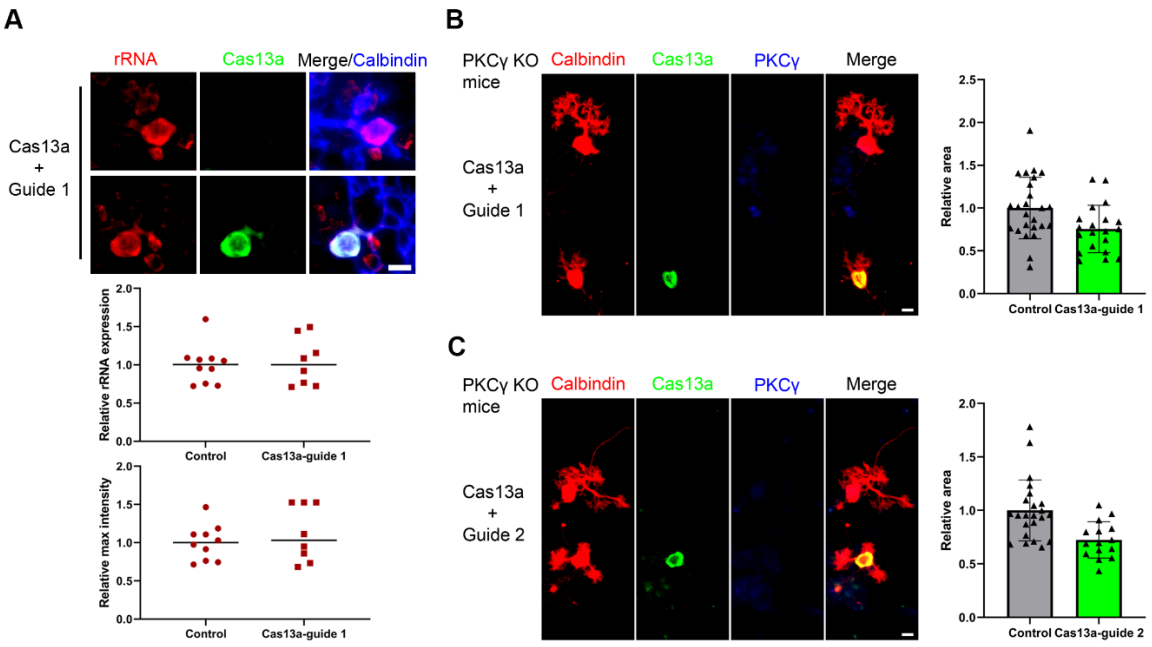

Figure 5.4 Inhibition of Purkinje cell dendritic growth is not related to collateral activity of the Cas13a-based method

(A) Triple immunofluorescence staining with anti-GFP (green), anti-rRNA (red) in Purkinje cells labelled by anti-Calbindin (blue). No changes of rRNA expression are found in the Purkinje cells after gene silencing (lower panel) compared to control cells (upper panel). Quantification of relative average expression of rRNA in cells. In control Purkinje cells, the median value is 1.004 and the mean ± SD is 1.000 ± 0.2574, n = 10 cells; in the Purkinje cells with expression of the CRISPR-Cas13a knockdown system, the median value is 1.003 and the mean ± SD is 1.038 ± 0.3128, n = 8 cells. Quantification of relative maximum intensity of rRNA in cells, in the control Purkinje cells, the median value is 1.001 and the mean ± SD is 1.000 ± 0.2325, n = 10 cells; In the Purkinje cells with expression of CRISPR-Cas13a knockdown system, the median value is 1.031 and the mean ± SD is 1.114 ± 0.3646, n = 8 cells. Scatter dot plots show the line at median. Scale bar, 20 μm. **(B)** Purkinje cells from PKCγ KO mice expressing the Cas13a-guide 1 complex (downside) have a significant reduction of dendritic trees compared to control cells (upside). The mean value of the dendritic area for control is 1.000 ± 0.3596, n represents 25 cells from two independent transfection experiments. The mean value for the Cas13a-

guide 1 complex is 0.7541 ± 0.2778. n represents 20 cells from two independent transfection experiments. P = 0.0139 in the two-tailed Mann-Whitney test. (**C)** Purkinje cells from PKCγ KO mice expressing the Cas13a-guide 2 complex (downside) have a significant reduction of dendritic trees compared to control cells (upside). The mean value of the dendritic area for control is 1.000 ± 0.2847, n represents 23 cells from two independent transfection experiments. The mean value for Cas13a-guide 2 complex is 0.7243 ± 0.1699. n represents 15 cells from two independent transfection experiments. P = 0.0010 in the two-tailed Mann-Whitney test.

5.6 The CRISPR-Cas13a system interferes with Purkinje cell dendritic development

CRISPR-Cas-based methods are now widely used for gene targeting (Pickar-Oliver and Gersbach, 2019). More recently, a variation of this method has been used for the knockdown of genes in mammalian cells based on CRISPR-Cas13a (Abudayyeh et al., 2017). The CRISPR-associated (Cas) enzyme, Cas13a, initially named C2c2, was found in bacteria, contains two higher eukaryote and prokaryote nucleotide-binding domains associated with ribonucleases (Abudayyeh et al., 2017; Gootenberg et al., 2017b). Cas13a can be utilized as an RNA-guided RNA-targeting CRISPR-Cas effector. Cas13a can be heterologously expressed in mammalian and plants cells and achieve knockdown of reporter or endogenous transcripts with levels of knockdown efficiency similar to RNAi but with substantially reduced off-target effects, making the CRISPR-Cas13a platform also suitable for therapeutic applications (Abudayyeh et al., 2017). Recent studies have already pioneered the use of the CRISPR-Cas13a system in the field of therapeutic agents. The CRISPR-Cas13a system recently have been engineered for the specific knockdown of mutant KRAS-G12D mRNA in pancreatic cancer cells (Zhao et al., 2018) and the CRISPR-Cas13a system has also shown to have a strong tumor-eliminating potential in glioma cells (Wang et al., 2019). CRISPR-Cas13a system also have been explored for antiviral

drug development in infectious diseases (Freije et al., 2019). For using the system as a method for RNA knockdown, it is essential that no collateral activities or trans RNA cleavage occur. No such effects on cellular health and differentiation by using the CRISPR-Cas13a system for gene knockdown have been found in HEK293FT cells (Abudayyeh et al., 2017). However, in a recent study, it was reported that the CRISPR-Cas13a system induced collateral ribosomal RNA cleavage after knockdown of eGFP expression and induced cell death after targeting EGFRvIII mRNA in U87 glioblastoma cells (Wang et al., 2019).

While two reports have studied the CRISPR-Cas13a system for different cancer cells, little is known about the potential effect of CRISPR-Cas13a system in normal mammalian cells. Considering the rapid advance of the CRISPR-Cas13a platform in therapeutic development (Freije et al., 2019; Zhao et al., 2018), we determined if the CRISPR-Cas13a system affects the development and health of primary mammalian neurons. We used cerebellar Purkinje neurons as a complex mammalian cell type and present findings suggesting an evident inhibitory effect of the CRISPR-Cas13a system during development of Purkinje neurons. Interestingly, the observed suppression of dendritic development of Purkinje neurons did not depend on collateral effect or trans RNA cleavage during target gene knockdown, but was caused by Cas13a itself.

We used the mammalian codon-optimized Cas13a vector consisting of LwaCas13a with C terminal monomeric GFP together with a guide CRISPR RNA (crRNA) encoding a 28-nucleotide (nt) spacer sequence originally described by the published research (Abudayyeh et al., 2017). The Cas13a vector (Plasmid #91902) and the crRNA were obtained from Addgene (Cambridge, MA, USA). Cerebellar Purkinje cells were maintained in cerebellar dissociated culture and transfected by electroporation with the pL7 vector, an expression vector containing the L7 (Pcp2) promoter directing Purkinje cell specific expression of the insert (Shimobayashi and Kapfhammer, 2017; Wagner, Brenowitz, et al., 2011; Wagner, McCroskery, et al., 2011). We have cloned the engineered GFP fusion LwaCas13a sequence from the

Addgene Plasmid #91902 into the pL7 vector. With this vector, we achieved Purkinje cell-specific expression of the engineered Cas13a.

Primary cerebellar cell cultures were prepared from neonatal FVB/N mice as described previously (Shimobayashi and Kapfhammer, 2017). We co-transfected Purkinje cells with 5 µg of pL7-LwaCas13a-mGFP plasmid and 7.5 - 10 µg of the 28-nucleotide (nt) non-targeting crRNA at the setup of the culture (DIV 0) and analyzed dendritic development after 14 days *in vitro* (DIV14). We found well developed dendritic trees in control Purkinje cells. In contrast, Purkinje cells transfected with the CRISPR-Cas13a system identified by anti-GFP and anti-Calbindin (a marker for Purkinje neurons) co-immunostaining had smaller dendritic trees (Figure 5.5A). We quantified the Purkinje cell dendritic area from GFP-positive CRISPR-Cas13a system transfected Purkinje cells and compared it to the dendritic area of non-transfected Cas13a neighboring GFP-negative Purkinje cells in the same culture well. The mean for the dendritic area was reduced to 79% of control for Purkinje cells expressing the non-targeting CRISPR-Cas13a system (Figure 5.5A) demonstrating a clear inhibition of dendritic growth by the CRISPR-Cas13a system and non-targeting crRNA-Cas13a complex display an impairment on the Purkinje cell development.

The crRNA-Cas13a complex retains catalytic activity and binds to targeting transcripts to cleave targeted single-stranded RNAs with spacer lengths as short as 20 nt, but loses RNA cleavage activity with spacer lengths less than 20 nt, while RNA binding still appears to be intact under these conditions (Abudayyeh et al., 2017). Since it is possible that the 28 nt non-targeting crRNA-Cas13a complex may coincidentally bind to targeting transcripts and cleave endogenous transcripts involved in dendritic development of Purkinje cells, a shorter spacer with 18 nt was used which does not support catalytic activity of the crRNA-Cas13a complex (Abudayyeh et al., 2017). After co-transfection of 5 µg pL7-LwaCas13a-mGFP and 7.5 µg the 18 nt crRNA into Purkinje cells, the size of the dendritic tree was reduced to 75% compared to non-transfected control Purkinje cells (Figure 5.5B), demonstrating that the reduction of dendritic development is not depending on the

collateral RNA cleavage activity of the system. These results suggest that the inhibition of Purkinje cell dendritic growth may be directly related to Cas13a.

After transfection of 5 µg pL7-LwaCas13a-mGFP alone into Purkinje cells, the size of the dendritic tree was again reduced to 83% of control Purkinje cells (Figure 5.5C). These results demonstrate that LwaCas13a-mGFP was responsible for reducing Purkinje cell dendritic growth. The observed reduction of Purkinje cell dendritic development was not related to the pL7 vector or GFP expression as transfection with 5 µg or 10 µg pL7 expressing GFP did not significantly affect dendritic development of Purkinje cells (Figure 5.5D).

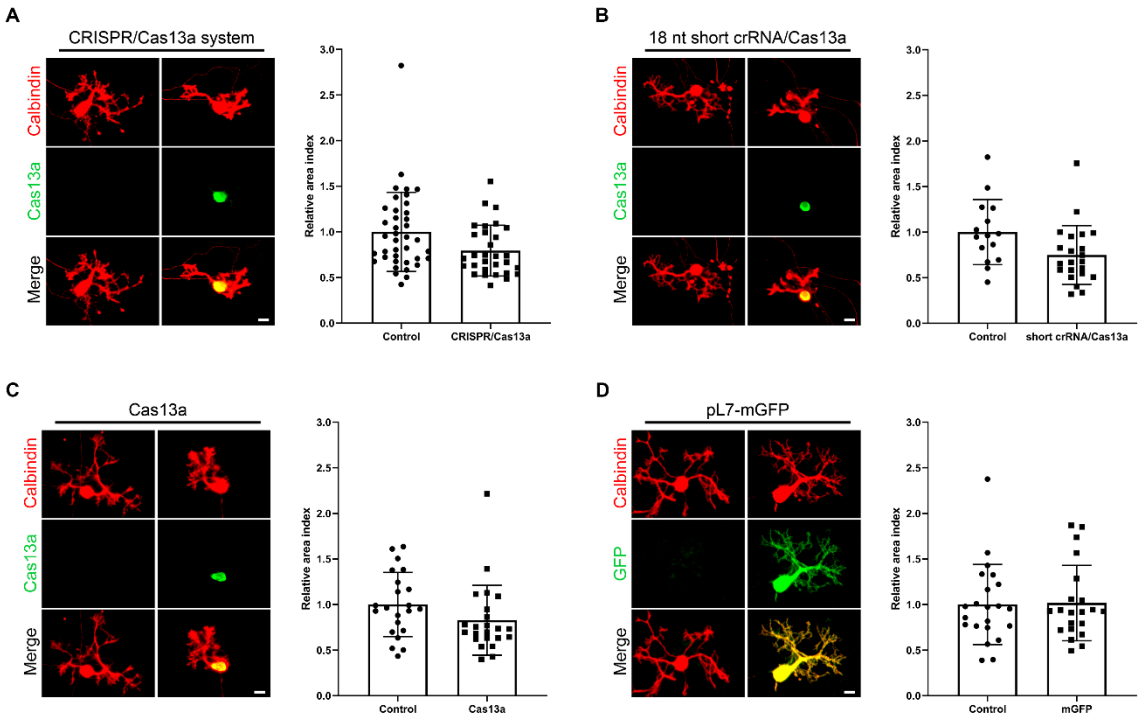

Figure 5.5 The CRISPR-Cas13a system suppresses dendritic growth in cerebellar Purkinje cells.

(A) Purkinje cells expressing the CRISPR-Cas13a system (right side) have dendritic trees with reduced size compared to control cells (left side). The mean value of the dendritic area for control is 1.000 ± 0.4338, n = 39 cells from three independent

transfection experiments. The mean value of CRISPR-Cas13a system is 0.7946 ± 0.2782. n = 30 cells from three independent transfection experiments. The results were significant with p = 0.0204 in the two-tailed Mann-Whitney test. **(B)** Purkinje cells expressing the LwaCas13a-mGFP together with an 18 nt short crRNA (right side) also have dendritic trees with reduced size compared to control cells (left side). The mean value of control is 1.000 ± 0.3568, n = 15 cells from two independent transfection experiments. The mean value of Cas13a with an 18 nt short crRNA is 0.7488 ± 0.3230, n = 22 cells from two independent transfection experiments. The results were significant with p = 0.0166 in the two-tailed Mann-Whitney test. **(C)** Purkinje cells expressing LwaCas13a-mGFP alone (right side) also have dendritic trees with reduced size compared to control cells (left side). The mean value of control is 1.000 ± 0.3519, n = 22 cells from two independent transfection experiments. The mean value of Cas13a is 0.8275 ± 0.3841, n = 23 cells from two independent transfection experiments. The results were significant with p = 0.0369 in the two-tailed Mann-Whitney test. **(D)** Purkinje cells expressing monomeric GFP only using the same pL7 expression plasmid as above develop normal dendritic trees. There is no difference in the size of the dendritic trees: 1.000 ± 0.4395, n = 22 cells from two independent transfection experiments for control and 1.016 ± 0.4133, n = 21 cells from two independent transfection experiments for pL7 vector expressing GFP. Data are shown as the mean ± SD. The P values are according to the two-tailed Mann-Whitney test. Scale bar = 20 μm.

Together, our findings demonstrate that expressing the CRISPR-Cas13a system in Purkinje cells results in reduced dendritic growth and development and that this inhibitory effect is not depending on the collateral effect or trans RNA cleavage during gene silencing by use of the CRISPR-Cas13 system but rather due to the LwaCas13a construct itself.

Abudayyeh et al. have reported that knockdown of target gene by use of CRISPR-Cas13 system had no collateral effects in HEK293FT cells. There is great potential

for using this system as platform for programmable gene knockdown because the Cas13a system is not native to eukaryotes and the probability for crosstalk with endogenous pathways is reduced (Abudayyeh et al., 2017). The system has also been explored for therapeutic use in pancreatic cancer cells using the Cas13a system for targeting mutant KRAS mRNA expression (Zhao et al., 2018). No collateral effects of the CRISPR-Cas13a system were reported in this study. Our experiments differ from previous studies using mammalian cell lines and cancer cells, in that we worked with a complex neuronal cell type in primary culture. Collateral effects have been previously reported for the use of Cas13a with targeting crRNA to knockdown target genes in U87 glioblastoma cells. This effect was not induced in Cas13a with non-targeting crRNA and was due to unwanted RNA cleavage activity of the system (Wang et al., 2019). In contrast, in the Purkinje neurons, the inhibitory effect of CRISPR-Cas13a system for dendritic development was not depending on collateral effect or trans RNA cleavage and was present after transfection of Cas13a by itself. It is not clear in the moment, if the observed negative effects for dendritic growth are due to the RNA-binding activity of Cas13a and RNA degradation or due to protein-protein interactions in endogenous developmental pathways in this complex mammalian cell type. Nevertheless, our findings send a warning that the potential neurotoxic effect of Cas13a might be present for more complex neuronal cell types in particular during development. The development of CRISPR-Cas13a for therapeutic applications deserves special attention for safety.

Chapter 6: General Discussion

6.1 Key molecule RGS8

In the chapter 3.5, we have discussed the important roles of RGS8 and mGluR1 signaling in the pathogenesis of SCAs. Our experiments show that RGS8 expressing Purkinje cell can better resist the affection induced by a mGluR1 selective agonist, supporting the functional concept that RGS8 is reducing the activity of the Gαq subunit to inhibit mGluR1 signaling. From this perspective, a loss of function of RGS8 is expected to show a phenotype similar to increased mGluR1 signaling. Interestingly, in the RGS8 null mutant mouse model with a loss of RGS8 there is a relatively normal development of Purkinje cells without apparent ataxia (Kuwata et al., 2007). Considering that many RGS8 family members are expressed in brain (Squires et al., 2018), a possible explanation is that the loss of function caused by deficient RGS8 might be compensated by other RGS family members. Such a compensation may also be happened in the testis in which RGS8 is also expressed but RGS8 deficient mice are fertile (Kuwata et al., 2007; Osamu Saitoh et al., 1999). RGS22, which was shown to interact with Gαq/11, is specifically expressed in mouse testis (Hu et al., 2008) and may be a candidate RGS member to compensate for the loss of RGS8 in testis. RGS4, which is expressed in brain and cerebellum, is closely related to RGS8 and belongs to the R4 sub-family. The highest level of RGS4 mRNA expression is in the Purkinje cell layer with lower expression in the granule cell layer (Ingi and Aoki, 2002; Squires et al., 2018). Importantly, RGS4 can inhibit the coupling of mGluR1 and mGluR5 to the Gq pathways in these brain regions (Saugstad et al., 1998), indicating that RGS4 may be able to compensate for the loss of RGS8 function in Purkinje cells.

RGS proteins are exciting new candidates for therapeutic interventions and drug development (Hollinger and Hepler, 2002; Squires et al., 2018; Zhang and Mende, 2011). RGS10, a microglia-enriched RGS family protein expressed in dopaminergic neurons, provided neuroprotection against inflammation-related degeneration in

Parkinson's disease (Lee et al., 2011, 2012). Our findings suggested that RGS8, a Purkinje cells-enriched RGS protein, can act as neuroprotective modifier. Serum levels of Neurofilament light polypeptide (NF-L) are increased in patients with SCAs suggesting they have the potential for being a progression marker of SCA (Wilke et al., 2018). However, NF-L is a nonspecific marker of neuronal damage and there is an urgent need for SCA-specific biomarkers (Klockgether et al., 2019). RGS8 expression was shown to be increased in mouse models of different SCA types. RGS8 is expected to be a candidate biomarker for SCA disease and may be further developed for the generation of therapeutic agents.

6.2 Key molecule STK17B

STK17B is strongly expressed in Purkinje cells and only relatively weakly expressed in other cells in the cerebellum. Cerebellar tissue at P3 and Purkinje cells at P10 already express substantial amounts of STK17B protein. This developmental expression profile might support a function of STK17B in development of cerebellum and Purkinje cells beyond the regulation of apoptosis as in the immune system.

We show that STK17B transcription is increased in cerebellar tissue of organotypic slice cultures from SCA14 PKCγ(S361G) mice. This overall increase is in contrast to the situation in Purkinje cells where expression is decreased. STK17B is also expressed in other cells and the fraction of Purkinje cell is only very small in cerebellar tissue (Figure 4.1), therefore the decrease in Purkinje cells of STK17B expression is masked in the microarray data by the increased expression in other cell types. STK17B has been shown to be one of the substrates of PKCγ. The constitutive active kinase domain of PKCγ(S361G) is expected to lead to increased phosphorylation of PKC substrates and it results in a reduced expression of STK17B in Purkinje cells. Interestingly, we have confirmed that the activation of PKC can reduce the expression of STK17B in Purkinje cells. In the moment, we do not know whether the reduction of STK17B is the result of increased phosphorylation. Little is known about the effects of phosphorylation of STK17B in Purkinje cells. From our experiments, we confirmed that

the transfection of the phosphomimetic form of STK17B(S351D) produced a direct negative effect on the morphology of Purkinje cells.

It seems very likely that the reduced expression of STK17B is one of the molecular adjustments in Purkinje cells due to PKCγ-mediated increased phosphorylation of STK17B. Increased PKC activation in Purkinje cells by PMA is well known to cause a marked reduction of Purkinje cell dendritic tree development similar to that found in PKCγ(S361G) Purkinje cells. We have now shown that overexpression of STK17B in Purkinje cells does indeed further reduce the development of the dendritic tree under treatment with low concentrations of PMA confirming the inhibitory effect of activation of PKCγ-mediated phosphorylation of STK17B in Purkinje cells.

In summary, STK17B is a key molecule with a known transcriptional dysregulation in the mouse models of SCA1 and SCA7, and it is downregulated on the protein level in Purkinje cells of the SCA14 mouse model. In SCA1 and SCA7, the downregulation of STK17B is based on the analysis of a sample comprising a piece of cerebellum (Gatchel et al., 2008; Ingram et al., 2016) and it is not known that if STK17B expression is actually reduced in Purkinje cells. In chapter 3, we have suggested that mGluR1-PKCγ signaling appears to be a critical shared pathway for SCAs pathogenesis. STK17B was identified as one of substrates of PKCγ, indicating that STK17B is downstream of mGluR1-PKCγ signaling. Although its role in the nervous system hasn't been elucidated, the function of STK17B on calcium regulation has been studied in T cells. It is well known that mGluR1 activation is linked to changes of intracellular calcium either by stimulating the IP3 receptor pathway or by Ca^{2+} entering through mGluR1-gated TRPC3 channels (Jana Hartmann et al., 2008). Many of the genes causing SCA are related to ion channels and these may indicate the possible role of STK17B for intracellular calcium regulation in Purkinje cells. As increasing evidence points towards a crucial role of Purkinje cell calcium regulation, in particular via the PKCγ-mediated pathway, for the development of SCAs (Schorge et al., 2010; Brown and Loew, 2015; Shimobayashi and Kapfhammer, 2018), STK17B emerges now as a new molecule mediating this pathway controlling the Purkinje cell calcium equilibrium.

STK17B could thus be an important determinant of pathogenesis of diverse spinocerebellar ataxias.

Although treatment with of the new STK17B-inhibitor Cpd41 did not or have only minor effects on Purkinje cell morphology in cultures from wildtype mice, low concentrations of Cpd41 enhanced the phenotype of Purkinje cells from SCA14 mice. These findings suggest that Purkinje cells from SCA14 are more vulnerable to inhibition of STK17B activity. We have found that high concentrations of Cpd41 are toxic and induce the death of Purkinje cells. This might be explained by an inhibition of Aurora kinase by Cpd41 with high concentrations (IC50 = 1.05 ± 0.20 µM) for Aurora kinase A (Wang et al., 2017). Aurora kinase A is highly expressed in cell bodies and dendrites of Purkinje cells and play an important role in the cerebellar long-term depression (McEvoy et al., 2007). Strong inhibition of Aurora kinase A may affect the survival of Purkinje cells, but we could not exclude other unspecific effects of Cpd41.

6.3 Cas13a-based method for gene silencing in Purkinje cells

The Cas13a-based method can be effectively reprogrammed with guide RNAs to specifically knockdown gene expression in Purkinje cells and our study provides a basis for the use of CRISPR-Cas13-based strategies in conditional gene silencing. The specificity of the Cas13a-based method for transcriptional knockdown is much higher than shRNA and Cas13a is highly sensitive to mismatches in the guide-target duplex, with no detectable off-targets (Abudayyeh et al., 2017). Our studies support the high specificity by the use of Cas13a-based method for the endogenous *Prkcg* gene silencing and a high efficiency knockdown at the protein level is shown in postmitotic Purkinje neurons with long-term culture.

Cas13a targeting in bacteria has been associated with a proliferation phenotype, potentially due to collateral activity which has been observed *in vitro*, but no evidence for collateral activity of Cas13a in mammalian cells was found (Abudayyeh et al., 2016, 2017). In our studies we observed a significant inhibition of Purkinje cell

dendritic growth but we did not find evidence for collateral activity in Purkinje cells. The inhibition of dendritic growth seen with the construct is not probably not related to collateral activity. The definition of “collateral activity” is that once Cas13a-crRNA was activated by binding to its target RNA (also called activator RNA), it cleaves the target RNA as well as other RNAs unspecifically (Abudayyeh et al., 2016; O’Connell, 2019). Guide 1 and guide 2 crRNAs for the *Prkcg* gene were shown to be specific targets in wild-type mouse Purkinje cells. By using PKCγ knockout mice, in which the target PKCγ RNA is not present and cannot activate the Cas13a-crRNA complex, we found that both Cas13a-crRNA complexes still inhibited Purkinje cell dendritic growth. We did not see a significant change of 5.8S ribosomal RNA by use of Cas13a-based knockdown making unspecific RNA degradation very unlikely. In other studies, lipofectamine-based transfection reagents were used to express the Cas13a-based gene knockdown constructs (Abudayyeh et al., 2017; Zhao et al., 2018) while in our experiments we used electroporation. However, in a recent study a collateral effect was reported in eukaryotes, and the transduction with lentivirus was used to express the Cas13a-based gene knockdown in human glioblastoma cancer cells. In this study collateral ribosomal RNA cleavage was found after knockdown of the target gene in EGFP-expressing cells (Wang et al., 2019). The CRISPR systems and the Cas proteins associated with have the original function of defending their prokaryotic hosts against the invasion of virus (Barrangou et al., 2007) and whether virus transduction may trigger the collateral activity of Cas13a in mammalian cells needs further investigation.

Although virus-based transduction has become a powerful tool for gene or shRNA delivery *in vitro* and *in vivo*, viruses have evolved to infect cells and express their genetic material to induce immunogenicity and cytotoxicity (Kim and Eberwine, 2010). Virus transduction can cause an inflammatory response and insertional mutations, as the genetic material of viruses integrates randomly into the host genome, which may lead to a disruption of tumor suppressor genes, activation of oncogenes or disruption of key genes (Woods et al., 2003). shRNA-based non-viral approaches need introduce foreign reagents by transfection or other delivery methods which might produce adverse effects, e.g. liposomes affect neuronal

morphology, growth or viability by lipofection; accelerated gold particles from biolistic particle delivery system may cause cell damage (Karra and Dahm, 2010). An ideal RNA interference method should be able to transfect neurons with high specificity and interference highly specific only with the target RNA in order to clarify the loss of function of the target gene. However, an unspecific knockdown of genes by the use of shRNA, known as off-target effect, has been shown in complex neuronal cell types (Alvarez et al., 2006; Baek et al., 2014). Differential expression analysis showed hundreds of significant off-targets in the shRNA conditions but none in Cas13a-based knockdown conditions (Abudayyeh et al., 2017), suggesting that Cas13a-based system could be a suitable tool for studying gene function in complex neuronal cell types. In cerebellar Purkinje neurons, a common problem is that most vector systems transcribe the shRNA constructs under the control of pol III promoters (Brummelkamp et al., 2002), which are constitutively expressed in all cell types. In that case, it is difficult to express the shRNA specifically in Purkinje cells, which make up only a very small fraction of cerebellar cells (Wagner, McCroskery, et al., 2011). Although our study shows that a Cas13-based approach to perform gene silencing in Purkinje cells produced unwanted effects on dendritic outgrowth, there is no evidence that this effect is due to unspecific RNA degradation. Low cytotoxicity but high specificity with acceptable adverse effect on dendritic growth in Purkinje neurons might make it still an alternative for gene function studies. Our study provides a reference for conditional gene silencing to investigate gene function in specific cell types or tissues based on the CRISPR-Cas13 system.

Chapter 7: Conclusion and Outlook

7.1 Key molecules RGS8 and STK17B

We have identified three key molecules RGS8, STK17B and INPP5A being dysregulated in different mouse models of SCA. During our studies, INPP5A has been reported recently to contribute to pathology in a mouse model of SCA17 (Liu et al., 2020) supporting our hypothesis that key molecules are involved in the pathology of diverse forms of SCA. INPP5A appears to be involved in the pathology of at least four types of SCAs, SCA1, 7, 14 and 17.

RGS8 is now known to be dysregulated also in at least four types of SCAs, SCA1, 2, 7 and 14. RGS8 is specifically expressed in mouse cerebellar Purkinje cells. Increased RGS8 expression in Purkinje cells is found with increased activity of the mGluR1 pathway. Functional experiments suggest that RGS8 mitigates overshooting mGluR-PKCγ signaling. Therefore, RGS8 is involved in the regulation of mGluR1 activity placing it upstream of PKCγ signaling. Our findings uncover and support a critical role of shared mGluR1-PKCγ signaling in the pathogenesis of different types of SCAs.

STK17B is one of the substrates of PKCγ and thus downstream of mGluR1-PKCγ signaling. STK17B is expressed in Purkinje cells from early postnatal development. In the SCA14 PKCγ(S361G) mouse model studied in our laboratory, STK17B protein expression was reduced in cerebellar dissociated cultures in parallel with a reduction of dendritic tree size of the Purkinje cells. In this mouse model the mutation produces a constitutively active form of PKCγ and we have shown that treatment with PMA, a PKC activator, also induces a strong decrease of STK17B in Purkinje cells. STK17B is thought to be phosphorylated by PKCγ. We could show that expression of a phosphorylation mimetic form, STK17B(S351D), does indeed inhibit dendritic growth of Purkinje cells. The downregulation of STK17B in the SCA14 mouse model may thus be a protective adaptation in the Purkinje cells with increased PKC activity.

7.2 Further studies

As it is known that STK17B is involved in the calcium mobilization in immune cells, it is important to see whether STK17B may have a similar role for the calcium response in Purkinje cells. Loss-of-function experiments and overexpression of STK17B will be necessary to test the effect on the calcium regulation in Purkinje cells. We would expect to find a novel connection between the mGluR1-PKCγ-STK17B signaling system to the molecules that are known to mediate or regulate intracellular calcium signaling in Purkinje cells, such as ITPR1, TRPC3, CACNA1G and CACNA1A, all of which are also known to be causative genes of SCA5, 15, 16, 29 and 42 respectively.

STK17B deficient mouse models have been used for studies of the immune system (McGargill et al., 2004; Ramos et al., 2008). Using these or similar mouse models will be useful to study the effect of a deficiency of STK17B in the cerebellum *in vivo* and use the different culture models (slice culture or dissociated culture) to further study STK17B function in cerebellar Purkinje cells. Although the inhibition of STK17B with Cpd41 did not show a strong effect on Purkinje cells, the knockdown of STK17B expression in Purkinje cells is an alternative method for studying a loss of function of STK17B. As the Cas13-based knockdown method provides high specificity and fewer off-target effects, the further study and optimization of this conditional gene silencing technology in Purkinje cells is also an important future project. It would also provide an alternative method to study how the knockdown of RGS8 will affect Purkinje cell dendritic development.

Chapter 8: Detailed Methods

8.1 Animals

All experiments were conducted in accordance with the EU Directive 2010/63/EU for the care and use of laboratory animals, approved by the Veterinary Office of the Canton of Basel and authorized by the Swiss authorities.

8.1.1 PKCγ(S361G) mice

The conditional transgenic mice of SCA14 are on a FVB background and they were produced and reported in our earlier publication (Ji et al., 2014). The SCA14-associated human PKCγ(S361G) mutation is expressed under Tetracycline Response Element (TRE) and together with GFP reporter in the transgenic mouse line. The transgenic mouse lines were crossed with Pcp2-tTA transgenic mice expressing the Tet-Transactivator under a Purkinje cell specific promoter to achieve expression of the SCA14-associated human PKCγ(S361G) mutation in Purkinje cells.

8.1.2 PKCγ knockout (KO) mice and wild type mice

PKCγ knockout (KO) mice were constructed and generated using CRISPR/Cas9-mediated gene editing technology at the Centre for Transgenic Models of University of Basel. The wild type mice used in our laboratory were FVB mice or CB6 mice.

8.2 Cerebellar organotypic slice cultures

8.2.1 Culture Media

Ingredients for 200 ml preparation medium. All ingredients were sterile and were mixed in a biological safety cabinet. Laboratory water used were sterile and distilled.

- 100 ml minimal essential medium (MEM) (Gibco, Catalog Number 11012), in two-fold concentration
- 98 ml sterile water
- 1 ml Glutamax (Gibco, Catalog Number 35050)
- 1N NaOH or 1N HCl to adjust pH to 7.2-7.4

Ingredients for 100 ml incubation medium:

- 25 ml MEM (Gibco, Catalog Number 11012), in two-fold concentration
- 23.5 ml sterile water
- 25 ml Basal Medium Eagle, with Earl's salt, without glutamine (Gibco, Catalog Number 21400)
- 25 ml horse serum, heat-inactivated (Gibco, Catalog Number 26050)
- 1 ml Glutamax (Gibco, Catalog Number 35050)
- 700 µl of a 10% glucose solution
- 1N NaOH or 1N HCl to adjust pH to 7.2-7.4

8.2.2 Procedure

Equipment

- 6 well plates (BD Falcon, Catalog Number 353046)
- 35 mm dishes (Greiner bio-one, Catalog Number 627102)
- Tissue chopper (McIllwain)
- Dissection stereomicroscope (Carl Zeiss Stemi 2000)
- Millicell-CM Organotypic tissue culture plate inserts (Millipore, Catalog Number PICM 03050)

Preparation

- A tissue chopper was cleaned by wiping the surface with 70% ethanol.
- A razor-blade was sterilized by immersion in 99.8% ethanol.
- The sterilized razor-blade was installed on the pre-wiped tissue chopper.
- Petri dishes were filled with 5 ml ice-cold preparation medium and stored at 4°C to be used. 2 or 3 dishes were required per mouse.
- 750µl of incubation medium was pipetted in each well of a 6 well plate. The plate was placed in an incubator. Culture conditions were maintained at 37°C providing a humidified atmosphere with 5% CO_2.
- Appropriate surgical instruments were prepared and sterilized.

Experimental procedure

- A P8 mouse pup was decapitated using the large scissor and the head was sprayed with 70% ethanol.
- The skull was carefully opened in the sterile work area of the laminar flow workbench.
- The cerebellum was found and located at the back of the brain. The cerebellum together with surrounding brain structures were then removed and placed immediately in a Petri dish filled with ice-cold preparation medium.

- The next steps of operation were carried out with a dissection stereomicroscope. By cutting the cerebellar peduncles and removing most of the meninges, the cerebellum was isolated from the surface.
- The cerebellar tissue was placed on the platform of the tissue chopper on which the vernier calipers was adjusted to 350 µm in thickness. Cerebellar sagittal slices were cut on the platform.
- The freshly dissected cerebellum was transferred and rapidly sliced in a fresh Petri dish containing ice-cold preparation medium. The sliced were carefully separated with each other slices and one cerebellum usually yielded 15-18 slices.
- Two tissue culture plate well inserts were moistened with the preparation medium that was added into the bottom membranes of tissue culture inserts.
- The slices were carefully laid on the membrane and the culture inserts were placed in the medium-containing well and incubated immediately.
- The incubation medium was changed every 2-3 days during the course of the experiments. Fresh incubation medium (ensure pH is between 7.2-7.4, if required) was pre-warmed to 37°C.
- Drugs were added at each culture medium change so that the original drug concentration were maintained.

8.3 Immunohistochemistry

- Organotypic slice cultures were fixed after 7 days *in vitro* in 4% paraformaldehyde in 100 mM phosphate buffer (PB) for 6-24 h at 4°C.
- The slices were washed with PB 3 times for 10 min. The plastic feet at the culture inserts were cut off to limit the required amount of antibody solution to 800µl.
- The primary antibody solution was prepared in PB as follows: 0.3-0.5 % Triton X-100, in order to permeabilize the tissue and 3 % normal goat serum, in order to block non-specific antigen binding.

- The following primary antibodies were used:
  rabbit anti-Calbindin D-28K (1:500, Swant, Marly, Switzerland,);
  mouse anti-Calbindin D-28K (1:500, Swant, Marly, Switzerland);
  sheep anti-RGS8 (1:100, R&D Systems).
- The slices were incubated in primary antibody solution at 4°C overnight.
- The slices were washed with PB 3 times for 10 min.
- The secondary antibody solution was prepared in PB as follows: 0.1 % Triton X-100, in order to prevent non-specific antigen binding.
- The following secondary antibodies were used:
  goat anti-mouse Alexa 488 (1:500, Molecular Probes, Invitrogen);
  goat anti-rabbit Alexa 488 (1:500, Molecular Probes, Invitrogen);
  donkey anti-sheep Alexa 568 (1:500, Molecular Probes, Invitrogen).
- The slices were incubated in corresponding fluorescence-conjugated secondary antibody solution in the dark at room temperature for 2 hours.
- The slices were washed in the dark with PB 3 times for 10 min.
  Stained slices were mounted on glass slides (Thermo Scientific Menzel-Gläser Superfrost Plus, Art. No. J1800AMNZ) and coverslipped with Mowiol.
- The images were captured on an Olympus AX-70 microscope equipped with a Spot Insight digital camera.

8.4 SDS-PAGE and Western blot

8.4.1 Materials

- Tris base (AppliChem, Catalog Number A1086)
- Glycine (SIGMA, Catalog Number G7126)
- SDS (BIORAD, Catalog Number 161-0301)
- Tween 20 (Sigma, Catalog Number 93773)
- Mini-PROTEAN Tetra Vertical Electrophoresis Cell (BIORAD)
- Trans-Blot Electrophoretic Transfer Cell (BIORAD)

- PhosSTOP phosphatase inhibitor (Roche, Catalog Number 04906845001)
- Complete protease inhibitor (Roche, Catalog Number 11697498001)
- Ammonium persulfate (APS) (BIORAD, Catalog Number 161-0700)
- TEMED (AppliChem, Catalog Number A1148)

10 × RIPA buffer

- 0.5 M Tris-HCl, pH 7.4
- 1.5 M NaCl
- 2.5% Sodium Deoxycholate
- 10% NP-40
- 10 mM EDTA

5 × Running Buffer

- 15.0 g Tris base
- 72.0 g Glycine
- 5.0 g SDS
- 1000 ml H_2O

1 × Transfer Buffer

- 3.03 g Tris base
- 14.4 g Glycine
- 200 ml methanol
- 800 ml H_2O

1 × Tris-buffered saline (TBS) solution

- 10 mM Tris-Cl, pH 7.4-7.6
- 150 mM NaCl

To prepare, dissolve 1.21 g Tris and 8.76 g NaCl in 800 mL of H_2O. Adjust pH to 7.4-7.6 with 1 M HCl and make volume up to 100 mL with H_2O.

Blocking buffer

- 5% BSA (GIBCO) in 1 × TBS

TBST

- 950 ml 1 × TBS Solution
- 50 ml 10% Tween 20

8.4.2 Procedure

- The culture media was aspirated and plates were kept on ice for all steps.
- The cerebellar slices were washed in ice cold PBS. Using a cell scraper, the cerebellar slices were collected and transferred into a tube.
- 750ul RIPA buffer with protease inhibitor and phosphatase inhibitor were added to each tube.

- The lysate was sonicated five times for five seconds. Sonication would be repeated if lysate was still viscous.
- The lysate was incubated on ice for 15-30 minutes.
- The cell lysate was centrifuged at 14000-15000x g for 15min at 4°C.
- Purified protein analysis and concentrations were measured with NanoDrop.
- The cell lysates were boiled in sample buffer at 95°C for 5 min.
- Protein samples were loaded in the vertical SDS-PAGE gel along with molecular weight marker.
- The gel was run for 1.5-2 hours at 120V.
- The membrane of nitrocellulose was rinsed with transfer buffer before preparing the stack.
- The stack was prepared from negative to positive voltage as follows: sponge, filter paper, gel, membrane, filter paper, sponge.
- The membrane was blocked for 1 hour at room temperature or overnight at 4°C using 5% BSA in TBS.
- The membrane was incubated with appropriate dilutions of primary antibody in blocking buffer overnight at 4°C.
- The membrane was washed in three washes of TBST, 5 min each.
- The membrane was incubated with the recommended dilution of conjugated secondary antibody in blocking buffer at room temperature for 1 h.
- The membrane was washed in three washes of TBST, 5 min each.
- For signal development, proteins were visualized by ECL (Pierce, Thermo Scientific, Reinach, Switzerland) and quantified using C-Digit Western Blot software, if membranes were incubated with HRP-labeled secondary antibodies.
- Alternatively, the proteins were directly quantified using C-Digit Western Blot software if membranes were incubated with IRDye® Secondary Antibodies (LI-COR Biosciences, Bad Homburg, Germany).

The following primary antibodies were used in this study:

- sheep anti-RGS8 (1:1000, R&D Systems)

- mouse anti-actin (1:2000, Millipore)
- rabbit anti-alpha Tubulin (1:1000, Proteintech)
- rabbit anti-phospho-PKC substrate (1:1000, Cell Signaling)
- mouse anti-GAPDH (1:4000, Proteintech)
- rabbit anti-mGluR1 (1:1000, Cell Signaling)
- mouse anti-Gαq/11 (1:300, Santa Cruz)
- mouse anti-turboGFP (1:1000, Origene)
- rabbit anti-turboGFP (1:1000, Invitrogen)
- mouse anti-Myc (1:1000, Origene)

The following secondary antibodies were used in this study:

- anti-sheep HRP conjugate antibody (1:1000, R&D Systems)
- anti-mouse HRP conjugate antibody (1:10000, Promega)
- anti-rabbit HRP conjugate antibody (1:10000, Promega)
- IRDye® 680LT Goat anti-Rabbit IgG Secondary Antibody (1:10000, LICOR)
- IRDye® 800CW Goat anti-Mouse IgG Secondary Antibody (1:10000, LICOR)

8.5 Plasmid construction

Materials

- Primers were generated by Microsynth
- CloneAmp HiFi PCR Premix (Clontech, Catalog Number 638500)
- In-Fusion HD EcoDry Cloning Kit (Clontech, Catalog Number 639678)
- In-Fusion HD Cloning Kit (Clontech, Catalog Number 638912)
- HiFi DNA Assembly Master Mix (NEB, Catalog Number E2621S)
- GENEART Site-Directed Mutagenesis System (Invitrogen, Catalog Number A13282)

- QIAquick Gel Extraction Kit (Qiagen, Catalog Number 28704)
- QIAprep Spin Miniprep Kit (Qiagen, Catalog Number 27104)
- EndoFree Plasmid Maxi prep kit (QIAGEN, Catalog Number 12362)
- Ampicillin (100 mg/ml stock)
- LB (Luria-Bertani) medium (pH 7.0)
- LB antibiotic plates
- Agarose (SIGMA, Catalog No. A9539)
- TBE buffer (89 mM Tris-borate / 2 mM EDTA)
- Ethidium bromid (MERCK)

pCMV-Rgs8, pCMV-STK17B and pCMV-mGluR1 vectors were from Origene (Rockville, MD, USA). pL7-GFP, pCMV-PKCγ-tGFP, pCMV-PKCγ(S361G)-tGFP and pL7-PKCγ(S361G)-GFP were gifts from Dr. Etsuko Shimobayashi (Shimobayashi and Kapfhammer, 2017).

Plasmids pL7-RGS8-GFP, pL7-GFP-STK17B and pL7-Cas13a-GFP were made according to the instruction manuals of In-Fusion HD Cloning Kit or HiFi DNA Assembly Master Mix. pL7-GFP-STK17B(S351D), pL7-GFP-STK17B(S351A) were made according to the instruction manuals of GENEART Site-Directed Mutagenesis System. Here, the procedure of pL7-RGS8-GFP construction were taken as example. Rgs8 fragment was amplificated by PCR according the instruction manual of In-Fusion HD EcoDry Cloning Kit.

The following primers were used for PCR:

Rgs8 forward primer 5’-CAG GAT CCA GCG GCC GCA TGG CTG CCT TAC TGA TGC CA-3’;

Rgs8 Reverse primer 5’-CCC TTG CTC ACC ATG GTG CTG AGC CTC CTC TGG CTC TG-3’.

The insert Rgs8 PCR fragment reaction was set up.

PCR mix	12.5 µl
Forward Primer of Rgs8	1ul, 5 µM
Reverse Primer of Rgs8	1ul, 5 µM
Rgs8	1ul, 100ug
RNase-Free Water	up to 25 µl

Initial Denaturation	95°C	1 min
35 Cycles	98°C 55°C 72°C	10 seconds 15 seconds 2 min
Final Extension	72°C	7 minutes
Hold	4°C	

Linearized pL7-mGFP vector was obtained according to the below reaction:

NotI-HF	1µl
NcoI-HF	1µl
pL7-mGFP vector	1ul, 1ug
CutSmart® Buffer 10x	5ul
Total Reaction Volume	RNase-Free Water up to 50ul

Incubation Time	1 hour Incubate at 37°C

The PCR product of Rgs8 was purified by using the NucleoSpin Gel and PCR Clean-Up kit.

The In-Fusion reaction was set up:

Purified PCR fragment	5ul
Linearized vector	1ul
5X In-Fusion HD Enzyme Premix	Powder
RNase-Free Water	4 ul

- The aluminum seal was peeled back from the tube. 10 µl volume of mixture was added to In-Fusion HD EcoDry pellet.
- The reaction was incubated for 15 min at 37 °C, followed by 15 min at 50°C, and placed on ice.
- Stellar competent cells were thawed on ice before use. 2.5-10 ul In-fusion production was added in 50-100 ul of the Stellar Competent Cells.
- The tube was placed on ice for 30 min.
- The cells were treated by heat shock for exactly 45 sec at 42°C. The tube was placed on ice for 1-2 min.
- SOC medium, warmed to 37°C, was added to bring the final volume to 500 µl. The tube was incubated by shaking at 160-225 rpm for 1 hr at 37°C.
- The appropriate transformation reaction was spread on a LB plate containing Ampicillin (LA).

- The next day, individual isolated colonies were picked from the LA plate and analysed by Ecoli NightSeq (Microsynth), or the plasmid DNA was isolated by miniprep and analysed by Sanger sequencing of plasmids from E. coli.

8.6 HEK293T cell transfection

8.6.1 Media Components

- DMEM, high glucose
- Heat Inactivated Fetal Bovine Serum (GIBCO)
- Trypsin-EDTA
- PBS
- Antibiotic-Antimycotic 100 ×

8.6.2 Reagents and Equipment

- 15ml/High Clarity Polypropylene Conical tubes
- 75 cm2 Tissue Culture Flasks (FALCON, Ca No. 353136)
- 6 well cell culture plate (FALCON, Ca No. 353046)
- Biological safety cabinet
- Hemacytometer
- Inverted microscope
- Lipofectamine 3000 (Life Technologies)

8.6.3 Transfection steps

- The HEK293T cells were seeded per well of a 6 well plate with 1.6 ml growth medium containing serum and antibiotics. The cells were incubated under a normal growth condition of 37°C and 5% CO_2. The cells were 70-90% confluent at the time of transfection.

- On the day of transfection, Lipofectamine 3000 reagent was diluted in Opti-MEM medium and was mixed by vortexing for 2-3 sec.
- 500-2500 ng indicated plasmids DNA was diluted in Opti-MEM medium and then P3000 reagent was added.
- The diluted DNA was added to the diluted Lipofectamine 3000 reagent according to 1:1 ratio. The mixed sample was incubated at room temperature (15-25°C) for 10-15 min to allow transfection complex formation.
- The transfection complexes were added drop-wise onto the cells in the 6-well plates. Gently swirl the dish to ensure uniform distribution of the transfection complexes.
- Incubate the cells with the transfection complexes under their normal growth conditions for 2-4 days for expression of the transfected gene.

8.7 Immunoprecipitation

8.7.1 Buffer composition

Lysis buffer

- 10 mM Tris/Cl pH 7.5
- 150 mM NaCl
- 0.5 mM EDTA
- 0.5% NP-40
- 0.09% Na-Azide

Dilution/Wash buffer

- 10 mM Tris/Cl pH 7.5
- 150 mM NaCl
- 0.5 mM EDTA

- 0.018% Na-Azide

8.7.2 Protocol

- Cells monolayer was washed gently by ice cold PBS twice.
- 200 to 250ul RIPA or Lysis buffer with inhibitors was added to each plate.
- The cells were scraped by using a cell scraper and transferred to a tube.
- The lysate was incubated on ice for 15-30 minutes with extensively pipetting every 5-10 min.
- The cell lysate was centrifuged at 15000-20000x g for 10-15min at 4°C.
- The cell lysate was added 300 µl Dilution buffer.
- TurboGFP-Trap agarose beads were resuspended and 25 µl bead slurry was pipetted into 500 µl ice-cold Dilution buffer. The tubes were centrifuged at 2500x g for 2 min at 4°C. The supernatant was discarded and the wash steps were repeated twice.
- The diluted lysate was added to equilibrated TurboGFP-Trap agarose beads. 50 µl of diluted lysate was saved. The tubes were tumbled end-over-end for 1-24 hour at 4°C.
- The tubes were centrifuged at 2500x g for 2 min at 4°C. 50 µl supernatant was saved and remaining supernatant was discarded.
- TurboGFP-Trap agarose beads were resuspended in 500 µl ice-cold Wash buffer.
- The tubes were centrifuged at 2500x g for 2 min at 4°C. Supernatant was discarded and wash steps were repeated twice.
- The agarose beads were resuspended in 80 µl 2x SDS-sample buffer.
- The agarose beads were boiled for 5 min at 95°C to dissociate immunocomplexes from beads.
- The agarose beads were spined down for 2 min at 2500x g. The supernatant was collected.
- The samples were analysed by SDS-PAGE and Western blot.

8.8 Microarray Study and Quantitative real-time PCR

The data of genes whose expression is commonly altered in SCA1 and SCA7 mouse models was used from the published study (Gatchel et al., 2008). The data of the top 50 genes in SCA2 mouse models was used from the published study (Dansithong et al., 2015). The data from organotypic cerebellar slice cultures of SCA14 PKCγ(S361G) and control mice were previously established in the laboratory (Shimobayashi et al., 2016). Organotypic cerebellar slices of SCA14 and control mice were harvested and submerged in RNAlater solution and total RNA isolated and purified according to manufacturers' protocols (Life Technologies, Zug, Switzerland). The slices were from three to four pups after 5 days *in vitro* culture. The *in vitro* transcription, cDNA synthesis, and hybridization onto the oligonucleotide arrays of Mouse Gene 1.0 ST Arrays (Affymetrix, Santa, Clara, CA, USA) were carried out and analysed by Dr. Philippe Demougin of the Life Science Training Facility (LSTF) core facility of the University of Basel. Analysis of the dysregulated genes list were calculated and the threshold was set at a fold change exceeding 1.2 with the P value less than 0.1 by Dr. Etsuko Shimobayashi. 266 up-regulated and 121 down-regulated probe sets were identified in SCA14 mouse models. Raw data were processed and analysed using Partek Genomics Suite Analysis Software of version 6.12.0907. The total RNA was extracted from organotypic cerebellar slices harvested at DIV5-7, and total cDNA was synthesized with reverse transcriptase-quantitative PCR (RT-qPCR) using oligo(dT) primers (Applied Biosystems, Foster City, CA).

Quantitative real-time PCR was performed with the manufacturer's SYBR green master mix and on a StepOne real-time PCR system (Applied Biosystems, Zug, Switzerland). The cDNA samples from organotypic cerebellar slice cultures of SCA14 PKCγ(S361G) and control mice were gifts from Dr. Etsuko Shimobayashi (Shimobayashi et al., 2016).

The Real-time PCR reaction was set up:

cDNA,100 ng/µl	1 µl
F primer, 5 µM	0.2 µl
R primer, 5 µM	0.2 µl
SYBR™ Green PCR Master Mix	5.0 µl
PCR Water	3.6 µl
Total volume	10.0 µl

Real-time PCR reactions were performed on a 48-well format with One step real-time detector (Applied Biosystems) using the following parameters.

Temperature	Duration	Number of Cycles
95°C	10 minutes	1
95°C	15 seconds	40
60°C	60 seconds	
95°C	15 seconds	1
60°C	60 seconds	
95°C	15 seconds	

The following primers were used:

Rgs8 forward primer 5’-AGG TCA ACT GCA AAG CTA GTC-3’,

Rgs8 reverse primer 5’-CAA AAC AAG TCA GGG ATG GC-3’;

GAPDH forward primer 5’-AAC TTT GGC ATT GTG GAA GG-3’,

GAPDH reverse primer 5’-ACA CAT TGG GGG TAG GAA CA-3’.

Reactions were quantified by a relative standard curve system and the cycle threshold method using the StepOne Software v2.1 (Applied Biosystems, Foster City, CA).

8.9 Primary cerebellar cell cultures

- Primary cerebellar cell cultures were prepared from neonatal mice as described previously (Shimobayashi and Kapfhammer, 2017; Wagner, McCroskery, et al., 2011).
- Heads from postnatal day 0 mice were separated.
- Cerebella was dissected from the skull and transferred into a Petri dish with pre-cooled HBSS;
- The cerebellum was isolated by cutting the cerebellar peduncles and removing most of the meninges;
- The isolated cerebellums were diced into small pieces of approximately 1 mm square using the scissors.
- 250 µl papain solution was added into the diced cerebellar tissue and incubated for 15-20 minutes at 37°C.
- 1 ml HBSS with fetal bovine serum (FBS) was added to stop the digestion and the cerebellar tissue was centrifuged at 700x g for 4 min.
- The supernatant was removed and 300 µl DNase solution was added.

- The cerebellar tissue was triturated 30-50 times with Gilson Pipetman P1000 equipped with a sterile 1000 µl tip until the suspension is homogenous.
- The triturated dices of tissue were passed through a nylon mesh and the cells were harvested by centrifugation for 4 min at 700x g.
- 1ml of HBSS was added and the cells were centrifuged for 4 mins at 700x g. This step was repeated twice.
- The cell pellet was carefully resuspended by adding DFM medium with 10% FBS, or was resuspended by Neon Resuspension Buffer if using Neon transfection system (see next section).
- The cells were transferred to Poly-D-Lysine Laminin culture slide.
- The culture was maintained in a humidified 37 °C / 5% CO_2 incubator.
- The medium was carefully replaced with fresh culture medium without serum at the second day after culture setup.
- Half of medium was replaced with fresh medium every 3-4 days.

8.10 Transfection system

- The cells were resuspended in the appropriate Neon Resuspension Buffer and were added to a sterile 1.5 mL microcentrifuge tube containing plasmid DNA and gently mix.
- Neon Tube was filled with 3 mL Electrolytic Buffer and the Tube was inserted into the Neon Pipette Station.
- The push-button on the Neon Pipette was pressed to the second stop to open the clamp and the top-head of the Neon Pipette was inserted into the Neon Tip up the mounting stem of the piston. The push-button was gently released continuing to apply a downward pressure on the pipette.
- The push-button on the Neon Pipette was pressed to the first stop and the Neon Tip was immersed into the cell-DNA mixture. The push-button on the pipette was slowly released to aspirate the cell-DNA mixture into the Neon Tip.

- The Neon Pipette with the sample vertically was inserted into the Neon Tube placed in the Neon Pipette Station.
- The button of Start was pressed with the following settings: Pulse voltage 1200 V, Pulse width 30 ms, Pulse number 1.
- The Neon Pipette was removed from the Neon Pipette Station and immediately transferred the samples from the Neon Tip by pressing the push-button on the pipette to the first stop into the prepared culture slides containing prewarm medium with serum.
- The cells were incubated in culture slides at 37°C in a humidified CO_2 incubator. The following culture steps were mentioned in previous section.

8.11 Immunocytochemistry

- Primary dissociated cerebellar Purkinje cells were fixed after two weeks *in vitro* in 4% paraformaldehyde in Phosphate Buffer (PB) for 30 min at room temperature.
- The cells were washed with Phosphate Buffered Saline (PBS) or PB 3 times for 10 min.
- The primary antibody solution was prepared in PBS or PB as follows: 0.3-0.5 % Triton X-100, in order to permeabilize the tissue and 3 % normal goat serum, in order to block non-specific antigen binding.
- The following primary antibodies were used:
  rabbit anti-Calbindin D-28K (1:4000, Swant, Marly, Switzerland)
  mouse anti-Calbindin D-28K (1:4000, Swant, Marly, Switzerland)
  rabbit anti-GFP (1:2000, Abcam, Cambridge, UK)
  chicken anti-GFP (1:2000, Abcam, Cambridge, UK)
  sheep anti-RGS8 (1:400, R&D Systems)
- The cells were incubated in primary antibody solution at room temperature for 1 hour or 4°C overnight.
- The cells were washed with PBS or PB 3 times for 10 min.

- The secondary antibody solution was prepared in PBS or PB as follows: 0.1 % Triton X-100, in order to prevent non-specific antigen binding.
- The following secondary antibodies were used:
  goat anti-mouse Alexa 568 (1:2000, Molecular Probes, Invitrogen);
  goat anti-rabbit Alexa 488 (1:2000, Molecular Probes, Invitrogen);
  goat anti-chicken Alexa 488 (1:2000, Molecular Probes, Invitrogen);
  goat anti-mouse Alexa 350 (1:2000, Molecular Probes, Invitrogen);
  donkey anti-sheep Alexa 568 (1:2000, Molecular Probes, Invitrogen).
- The cells were incubated in corresponding fluorescence-conjugated secondary antibody solution in the dark at room temperature for 2 hours.
- The cells were washed in the dark with PBS or PB 3 times for 10 min.
- Stained cells were mounted with Mowiol (Sigma-Aldrich, Buchs, Switzerland).
- The images were captured on an Olympus AX-70 fluorescence microscope or Zeiss LSM700 upright confocal microscope.

8.12 Quantification of Purkinje cell dendritic expansion and fluorescence intensity of immunostainings in dissociated cerebellar cultures

- In order to ensure a comparable growth environment, non-transfected Purkinje cells close to the Purkinje cells transfected with the indicated vectors from the same well were taken as control in this study.
- Purkinje cells were viewed with a 20x lens of microscope and photographed with a digital camera.
- The Investigators were blinded to whether the measured cells were GFP positive or not. The dendritic area of anti-Calbindin stained Purkinje cell dendritic trees was traced and measured using an image analysis program ImageJ.
- The codes were broken and the cell measurements were grouped into controls and experimental groups.

- The mean dendritic area of the control group was set as 1, and the areas of the experimental groups were expressed as ratios of the control value.
- The raw images were used for the fluorescence intensity analysis and the mean fluorescence intensity of the Purkinje cell soma was calculated by ImageJ
- The shown images were linearly adjusted in brightness and contrast.
- The data were analysed using GraphPad Prism software (San Diego, USA).
- The statistical significance of differences in parameters was assessed by the nonparametric two-tailed Mann–Whitney's test. Confidence intervals were 95%, statistical significance was assumed with $P < 0.05$.

References

Abeliovich, A., Paylor, R., Chen, C., Kim, J. J., Wehner, J. M., and Tonegawa, S. (1993). PKCγ mutant mice exhibit mild deficits in spatial and contextual learning. *Cell*. https://doi.org/10.1016/0092-8674(93)90614-V

Abudayyeh, O. O., Gootenberg, J. S., Essletzbichler, P., Han, S., Joung, J., Belanto, J. J., Verdine, V., Cox, D. B. T., Kellner, M. J., Regev, A., Lander, E. S., Voytas, D. F., Ting, A. Y., and Zhang, F. (2017). RNA targeting with CRISPR-Cas13. *Nature*, *550*(7675), 280–284. https://doi.org/10.1038/nature24049

Abudayyeh, O. O., Gootenberg, J. S., Konermann, S., Joung, J., Slaymaker, I. M., Cox, D. B. T., Shmakov, S., Makarova, K. S., Semenova, E., Minakhin, L., Severinov, K., Regev, A., Lander, E. S., Koonin, E. V., and Zhang, F. (2016). C2c2 is a single-component programmable RNA-guided RNA-targeting CRISPR effector. *Science*, *353*(6299). https://doi.org/10.1126/science.aaf5573

Adachi, N., Kobayashi, T., Takahashi, H., Kawasaki, T., Shirai, Y., Ueyama, T., Matsuda, T., Seki, T., Sakai, N., and Saito, N. (2008). Enzymological analysis of mutant protein kinase Cγ causing spinocerebellar ataxia type 14 and dysfunction in Ca2+ homeostasis. *Journal of Biological Chemistry*. https://doi.org/10.1074/jbc.M801492200

Adcock, K. H., Metzger, F., and Kapfhammer, J. P. (2004). Purkinje cell dendritic tree development in the absence of excitatory neurotransmission and of brain-derived neurotrophic factor in organotypic slice cultures. *Neuroscience*. https://doi.org/10.1016/j.neuroscience.2004.04.032

Ahlers, K. E., Chakravarti, B., and Fisher, R. A. (2016). RGS6 as a novel therapeutic target in CNS diseases and cancer. In *AAPS Journal*. https://doi.org/10.1208/s12248-016-9899-9

Aiba, A., Chen, C., Herrup, K., Rosenmund, C., Stevens, C. F., and Tonegawa, S. (1994). Reduced hippocampal long-term potentiation and context-specific deficit in associative learning in mGluR1 mutant mice. *Cell*. https://doi.org/10.1016/0092-8674(94)90204-6

Airaksinen, M. S., Eilers, J., Garaschuk, O., Thoenen, H., Konnerth, A., and Meyer, M. (1997). Ataxia and altered dendritic calcium signaling in mice carrying a targeted null mutation of the calbindin D28k gene. *Proceedings of the National Academy of Sciences of the United States of America*. https://doi.org/10.1073/pnas.94.4.1488

Al-Qahtani, A., Xu, Z., Zan, H., Walsh, C., and Casali, P. (2008). A role for DRAK2 in the germinal center reaction and the antibody response. *Autoimmunity*. https://doi.org/10.1080/08916930802170633

Alba, A., Kano, M., Chen, C., Stanton, M. E., Fox, G. D., Herrup, K., Zwingman, T. A., and Tonegawa, S. (1994). Deficient cerebellar long-term depression and impaired motor learning in mGluR1 mutant mice. *Cell*. https://doi.org/10.1016/0092-8674(94)90205-4

Alonso, I., Jardim, L. B., Artigalas, O., Saraiva-Pereira, M. L., Matsuura, T., Ashizawa, T., Sequeiros, J., and Silveira, I. (2006). Reduced penetrance of intermediate size alleles in spinocerebellar ataxia type 10. *Neurology*. https://doi.org/10.1212/01.wnl.0000216266.30177.bb

Alonso, Isabel, Barros, J., Tuna, A., Coelho, J., Sequeiros, J., Silveira, I., and Coutinho, P. (2003). Phenotypes of spinocerebellar ataxia type 6 and familial hemiplegic migraine caused by a unique CACNA1A missense mutation in patients from a large family. *Archives of Neurology*. https://doi.org/10.1001/archneur.60.4.610

Alshbool, F. Z., Karim, Z. A., Vemana, H. P., Conlon, C., Lin, O. A., and Khasawneh, F. T. (2015). The regulator of G-protein signaling 18 regulates platelet

aggregation, hemostasis and thrombosis. *Biochemical and Biophysical Research Communications*. https://doi.org/10.1016/j.bbrc.2015.04.143

Altman, J. (1972). Postnatal development of the cerebellar cortex in the rat. II. Phases in the maturation of Purkinje cells and of the molecular layer. *Journal of Comparative Neurology*. https://doi.org/10.1002/cne.901450402

Alvarez, V. A., Ridenour, D. A., and Sabatini, B. L. (2006). Retraction of synapses and dendritic spines induced by off-target effects of RNA interference. *Journal of Neuroscience*, *26*(30), 7820–7825. https://doi.org/10.1523/JNEUROSCI.1957-06.2006

Amstadter, A. B., Koenen, K. C., Ruggiero, K. J., Acierno, R., Galea, S., Kilpatrick, D. G., and Gelernter, J. (2009). Variant in RGS2 moderates posttraumatic stress symptoms following potentially traumatic event exposure. *Journal of Anxiety Disorders*. https://doi.org/10.1016/j.janxdis.2008.12.005

Andressen, C., Blümcke, I., and Celio, M. R. (1993). Calcium-binding proteins: selective markers of nerve cells. In *Cell and Tissue Research*. https://doi.org/10.1007/BF00318606

Armbrust, K. R., Wang, X., Hathorn, T. J., Cramer, S. W., Chen, G., Zu, T., Kangas, T., Zink, A. N., Öz, G., Ebner, T. J., and Ranum, L. P. W. (2014). Mutant β-III spectrin causes mGluR1α mislocalization and functional deficits in a mouse model of spinocerebellar ataxia type 5. *Journal of Neuroscience*, *34*(30), 9891–9904. https://doi.org/10.1523/JNEUROSCI.0876-14.2014

Armengol, J. A., and Sotelo, C. (1991). Early dendritic development of Purkinje cells in the rat cerebellum. A light and electron microscopic study using axonal tracing in “in vitro” slices. *Developmental Brain Research*. https://doi.org/10.1016/0165-3806(91)90213-3

Atkey, M. R., Lachance, J. F. B., Walczak, M., Rebello, T., and Nilson, L. A. (2006).

Capicua regulates follicle cell fate in the Drosophila ovary through repression of mirror. *Development*. https://doi.org/10.1242/dev.02369

Azevedo, F. A. C., Carvalho, L. R. B., Grinberg, L. T., Farfel, J. M., Ferretti, R. E. L., Leite, R. E. P., Filho, W. J., Lent, R., and Herculano-Houzel, S. (2009). Equal numbers of neuronal and nonneuronal cells make the human brain an isometrically scaled-up primate brain. *Journal of Comparative Neurology*. https://doi.org/10.1002/cne.21974

Baek, S. T., Kerjan, G., Bielas, S. L., Lee, J. E., Fenstermaker, A. G., Novarino, G., and Gleeson, J. G. (2014). Off-target effect of doublecortin family shRNA on neuronal migration associated with endogenous MicroRNA dysregulation. *Neuron*, *82*(6), 1255–1262. https://doi.org/10.1016/j.neuron.2014.04.036

Barmack, N. H., Qian, Z., and Yoshimura, J. (2000). Regional and cellular distribution of protein kinase C in rat cerebellar Purkinje cells. *Journal of Comparative Neurology*. https://doi.org/10.1002/1096-9861(20001113)427:2<235::AID-CNE6>3.0.CO;2-6

Barrangou, R., Fremaux, C., Deveau, H., Richards, M., Boyaval, P., Moineau, S., Romero, D. A., and Horvath, P. (2007). CRISPR provides acquired resistance against viruses in prokaryotes. *Science*. https://doi.org/10.1126/science.1138140

Becker, E. B. E., Oliver, P. L., Glitsch, M. D., Banks, G. T., Achilli, F., Hardy, A., Nolan, P. M., Fisher, E. M. C., and Davies, K. E. (2009). A point mutation in TRPC3 causes abnormal Purkinje cell development and cerebellar ataxia in moonwalker mice. *Proceedings of the National Academy of Sciences*, *106*(16), 6706–6711. https://doi.org/10.1073/pnas.0810599106

Berman, D. M., Wilkie, T. M., and Gilman, A. G. (1996). GAIP and RGS4 are GTPase-activating proteins for the G(i) subfamily of G protein α subunits. *Cell*. https://doi.org/10.1016/S0092-8674(00)80117-8

Bihannic, L., and Ayrault, O. (2016). Insights into cerebellar development and medulloblastoma. In *Bulletin du Cancer*. https://doi.org/10.1016/j.bulcan.2015.11.002

Binda, F., Pernaci, C., and Saxena, S. (2020). Cerebellar Development and Circuit Maturation: A Common Framework for Spinocerebellar Ataxias. In *Frontiers in Neuroscience*. https://doi.org/10.3389/fnins.2020.00293

Boukhtouche, F. (2006). Retinoid-Related Orphan Receptor Controls the Early Steps of Purkinje Cell Dendritic Differentiation. *Journal of Neuroscience*, *26*(5), 1531–1538. https://doi.org/10.1523/JNEUROSCI.4636-05.2006

Boukhtouche, Fatiha, Doulazmi, M., Frederic, F., Dusart, I., Brugg, B., and Mariani, J. (2006). RORα, a pivotal nuclear receptor for Purkinje neuron survival and differentiation: From development to ageing. In *Cerebellum*. https://doi.org/10.1080/14734220600750184

Brown, S. A., and Loew, L. M. (2015). Integration of modeling with experimental and clinical findings synthesizes and refines the central role of inositol 1,4,5-trisphosphate receptor 1 in spinocerebellar ataxia. In *Frontiers in Neuroscience*. https://doi.org/10.3389/fnins.2014.00453

Brummelkamp, T. R., Bernards, R., and Agami, R. (2002). A system for stable expression of short interfering RNAs in mammalian cells. *Science*, *296*(5567), 550–553. https://doi.org/10.1126/science.1068999

Campbell, D. B., Lange, L. A., Skelly, T., Lieberman, J., Levitt, P., and Sullivan, P. F. (2008). Association of RGS2 and RGS5 variants with schizophrenia symptom severity. *Schizophrenia Research*. https://doi.org/10.1016/j.schres.2008.01.006

Cao, Y., Pahlberg, J., Sarria, I., Kamasawa, N., Sampath, A. P., and Martemyanov, K. A. (2012). Regulators of G protein signaling RGS7 and RGS11 determine the onset of the light response in on bipolar neurons. *Proceedings of the National*

Academy of Sciences of the United States of America. https://doi.org/10.1073/pnas.1202332109

Carlson, K. M., Andresen, J. M., and Orr, H. T. (2009). Emerging pathogenic pathways in the spinocerebellar ataxias. *Current Opinion in Genetics and Development*, *19*(3), 247–253. https://doi.org/10.1016/j.gde.2009.02.009

Carper, M. B., Denvir, J., Boskovic, G., Primerano, D. A., and Claudio, P. P. (2014). RGS16, a novel p53 and prb cross-talk candidate inhibits migration and invasion of pancreatic cancer cells. *Genes and Cancer*. https://doi.org/10.18632/genesandcancer.43

Catania, M. V., Bellomo, M., Di Giorgi-Gerevini, V., Seminara, G., Giuffrida, R., Romeo, R., De Blasi, A., and Nicoletti, F. (2001). Endogenous activation of group-I metabotropic glutamate receptors is required for differentiation and survival of cerebellar Purkinje cells. *Journal of Neuroscience*. https://doi.org/10.1523/jneurosci.21-19-07664.2001

Catania, M. V., Landwehrmeyer, G. B., Testa, C. M., Standaert, D. G., Penney, J. B., and Young, A. B. (1994). Metabotropic glutamate receptors are differentially regulated during development. *Neuroscience*. https://doi.org/10.1016/0306-4522(94)90428-6

Celio, M. R. (1990). Calbindin D-28k and parvalbumin in the rat nervous system. *Neuroscience*. https://doi.org/10.1016/0306-4522(90)90091-H

Cerminara, N. L., Lang, E. J., Sillitoe, R. V., and Apps, R. (2015). Redefining the cerebellar cortex as an assembly of non-uniform Purkinje cell microcircuits. In *Nature Reviews Neuroscience*. https://doi.org/10.1038/nrn3886

Chan, R. K., and Otte, C. A. (1982). Isolation and genetic analysis of Saccharomyces cerevisiae mutants supersensitive to G1 arrest by a factor and alpha factor pheromones. *Molecular and Cellular Biology*.

https://doi.org/10.1128/mcb.2.1.11

Chen, D. H., Cimino, P. J., Ranum, L. P. W., Zoghbi, H. Y., Yabe, I., Schut, L., Margolis, R. L., Lipe, H. P., Feleke, A., Matsushita, M., Wolff, J., Morgan, C., Lau, D., Fernandez, M., Sasaki, H., Raskind, W. H., and Bird, T. D. (2005). The clinical and genetic spectrum of spinocerebellar ataxia 14. *Neurology*, *64*(7), 1258–1260. https://doi.org/10.1212/01.WNL.0000156801.64549.6B

Conquet, F., Bashir, Z. I., Davies, C. H., Daniel, H., Ferraguti, F., Bordi, F., Franz-Bacon, K., Reggiani, A., Matarese, V., Condé, F., Collingridge, G. L., and Crépel, F. (1994). Motor deficit and impairment of synaptic plasticity in mice lacking mGluR1. *Nature*. https://doi.org/10.1038/372237a0

Coutelier, M., Blesneac, I., Monteil, A., Monin, M. L., Ando, K., Mundwiller, E., Brusco, A., Le Ber, I., Anheim, M., Castrioto, A., Duyckaerts, C., Brice, A., Durr, A., Lory, P., and Stevanin, G. (2015). A recurrent mutation in CACNA1G alters Cav3.1 T-type calcium-channel conduction and causes autosomal-dominant cerebellar ataxia. *American Journal of Human Genetics*. https://doi.org/10.1016/j.ajhg.2015.09.007

Croze, E., Tran, T., Paz, P., Velichko, S., Cifrese, J., Belur, P., Yamaguchi, K. D., Ku, K., Mirshahpanah, P., and Reder, A. T. (2010). Interferonβ-1b induces the expression of RGS1 a negative regulator of G-protein signaling. *International Journal of Cell Biology*. https://doi.org/10.1155/2010/529376

Cui, H., Nishiguchi, N., Ivleva, E., Yanagi, M., Fukutake, M., Nushida, H., Ueno, Y., Kitamura, N., Maeda, K., and Shirakawa, O. (2008). Association of RGS2 gene polymorphisms with suicide and increased RGS2 immunoreactivity in the postmortem brain of suicide victims. *Neuropsychopharmacology*. https://doi.org/10.1038/sj.npp.1301557

D'Angelo, E., and Casali, S. (2013). Seeking a unified framework for cerebellar function and dysfunction: From circuit operations to cognition. In *Frontiers in*

Neural Circuits.

Dansithong, W., Paul, S., Figueroa, K. P., Rinehart, M. D., Wiest, S., Pflieger, L. T., Scoles, D. R., and Pulst, S. M. (2015). Ataxin-2 Regulates RGS8 Translation in a New BAC-SCA2 Transgenic Mouse Model. *PLoS Genetics*, *11*(4), 1–29. https://doi.org/10.1371/journal.pgen.1005182

De Vries, L., Mousli, M., Wurmser, A., and Farquhar, M. G. (1995). GAIP, a protein that specifically interacts with the trimeric G protein Gαi3, is a member of a protein family with a highly conserved core domain. *Proceedings of the National Academy of Sciences of the United States of America*. https://doi.org/10.1073/pnas.92.25.11916

De Vries, L., Zheng, B., Fischer, T., Elenko, E., and Farquhar, M. G. (2000). The Regulator of G Protein Signaling Family. *Annual Review of Pharmacology and Toxicology*. https://doi.org/10.1146/annurev.pharmtox.40.1.235

Dohlman, H. G., Apaniesk, D., Chen, Y., Song, J., and Nusskern, D. (1995). Inhibition of G-protein signaling by dominant gain-of-function mutations in Sst2p, a pheromone desensitization factor in Saccharomyces cerevisiae. *Molecular and Cellular Biology*. https://doi.org/10.1128/mcb.15.7.3635

Druey, K. M., Blumer, K. J., Kang, V. H., and Kehrl, J. H. (1996). Inhibition of G-protein-mediated MAP kinase activation by a new mammalian gene family. *Nature*. https://doi.org/10.1038/379742a0

Du, X., and Gomez, C. M. (2018). Spinocerebellum ataxia type 6: Molecular mechanisms and calcium channel genetics. In *Advances in Experimental Medicine and Biology*. https://doi.org/10.1007/978-3-319-71779-1_7

Duarri, A., Jezierska, J., Fokkens, M., Meijer, M., Schelhaas, H. J., Den Dunnen, W. F. A., Van Dijk, F., Verschuuren-Bemelmans, C., Hageman, G., Van De Vlies, P., Küsters, B., Van De Warrenburg, B. P., Kremer, B., Wijmenga, C., Sinke, R.

J., Swertz, M. A., Kampinga, H. H., Boddeke, E., and Verbeek, D. S. (2012). Mutations in potassium channel KCND3 cause spinocerebellar ataxia type 19. *Annals of Neurology*. https://doi.org/10.1002/ana.23700

Durr, A. (2010). Autosomal dominant cerebellar ataxias: Polyglutamine expansions and beyond. *The Lancet Neurology*, *9*(9), 885–894. https://doi.org/10.1016/S1474-4422(10)70183-6

Emilsson, L., Saetre, P., and Jazin, E. (2006). Low mRNA levels of RGS4 splice variants in Alzheimer's disease: Association between a rare haplotype and decreased mRNA expression. *Synapse*. https://doi.org/10.1002/syn.20226

Esposito, F., Patsopoulos, N. A., Cepok, S., Kockum, I., Leppä, V., Booth, D. R., Heard, R. N., Stewart, G. J., Cox, M., Scott, R. J., Lechner-Scott, J., Goris, A., Dobosi, R., Dubois, B., Rioux, J. D., Oturai, A. B., Søndergaard, H. B., Sellebjerg, F., Sørensen, P. S., … De Jager, P. L. (2010). IL12A, MPHOSPH9/CDK2AP1 and RGS1 are novel multiple sclerosis susceptibility loci. *Genes and Immunity*. https://doi.org/10.1038/gene.2010.28

Fogel, B. L., Hanson, S. M., and Becker, E. B. E. (2015). Do mutations in the murine ataxia gene TRPC3 cause cerebellar ataxia in humans? In *Movement Disorders*. https://doi.org/10.1002/mds.26096

Freije, C. A., Myhrvold, C., Boehm, C. K., Lin, A. E., Welch, N. L., Carter, A., Metsky, H. C., Luo, C. Y., Abudayyeh, O. O., Gootenberg, J. S., Yozwiak, N. L., Zhang, F., and Sabeti, P. C. (2019). Programmable Inhibition and Detection of RNA Viruses Using Cas13. *Molecular Cell*, *76*(5), 826-837.e11. https://doi.org/10.1016/j.molcel.2019.09.013

Friedman, M. J., Shah, A. G., Fang, Z. H., Ward, E. G., Warren, S. T., Li, S., and Li, X. J. (2007). Polyglutamine domain modulates the TBP-TFIIB interaction: Implications for its normal function and neurodegeneration. *Nature Neuroscience*. https://doi.org/10.1038/nn2011

Friedman, M. J., Wang, C. E., Li, X. J., and Li, S. (2008). Polyglutamine expansion reduces the association of TATA-binding protein with DNA and induces DNA binding-independent neurotoxicity. *Journal of Biological Chemistry*. https://doi.org/10.1074/jbc.M709674200

Friedrich, M. L., Cui, M., Hernandez, J. B., Weist, B. M., Andersen, H. M., Zhang, X., Huang, L., and Walsh, C. M. (2007). Modulation of DRAK2 autophosphorylation by antigen receptor signaling in primary lymphocytes. *Journal of Biological Chemistry*, *282*(7), 4573–4584. https://doi.org/10.1074/jbc.M606675200

Friedrich, M. L., Wen, B. G., Bain, G., Kee, B. L., Katayama, C., Murre, C., Hedrick, S. M., and Walsh, C. M. (2005). DRAK2, a lymphoid-enriched DAP kinase, regulates the TCR activation threshold during thymocyte selection. *International Immunology*, *17*(11), 1379–1390. https://doi.org/10.1093/intimm/dxh315

Fryer, J. D., Yu, P., Kang, H., Mandel-Brehm, C., Carter, A. N., Crespo-Barreto, J., Gao, Y., Flora, A., Shaw, C., Orr, H. T., and Zoghbi, H. Y. (2011). Exercise and genetic rescue of SCA1 via the transcriptional repressor Capicua. *Science*. https://doi.org/10.1126/science.1212673

Gagnon, A. W., Murray, D. L., and Leadley, R. J. (2002). Cloning and characterization of a novel regulator of G protein signalling in human platelets. *Cellular Signalling*. https://doi.org/10.1016/S0898-6568(02)00012-8

Gao, Y., Perkins, E. M., Clarkson, Y. L., Tobia, S., Lyndon, A. R., Jackson, M., and Rothstein, J. D. (2011). β-III spectrin is critical for development of Purkinje cell dendritic tree and spine morphogenesis. *Journal of Neuroscience*. https://doi.org/10.1523/JNEUROSCI.3332-11.2011

Gatchel, J. R., Watase, K., Thaller, C., Carson, J. P., Jafar-Nejad, P., Shaw, C., Zu, T., Orr, H. T., and Zoghbi, H. Y. (2008). The insulin-like growth factor pathway is altered in spinocerebellar ataxia type 1 and type 7. *Proceedings of the National Academy of Sciences of the United States of America*, *105*(4), 1291–1296.

https://doi.org/10.1073/pnas.0711257105

Gatzka, M., Newton, R. H., and Walsh, C. M. (2009). Altered Thymic Selection and Increased Autoimmunity Caused by Ectopic Expression of DRAK2 during T Cell Development. *The Journal of Immunology*. https://doi.org/10.4049/jimmunol.0803530

Gatzka, M., and Walsh, C. (2008). Negative Regulation of TCR Signaling in Immunological Tolerance: Taming Good and Evil. *Current Immunology Reviews*. https://doi.org/10.2174/157339508786447968

Gold, D. A., Baek, S. H., Schork, N. J., Rose, D. W., Larsen, D. L. D., Sachs, B. D., Rosenfeld, M. G., and Hamilton, B. A. (2003). RORα coordinates reciprocal signaling in cerebellar development through sonic hedgehog and calcium-dependent pathways. *Neuron*. https://doi.org/10.1016/S0896-6273(03)00769-4

Gold, S. J., Heifets, B. D., Pudiak, C. M., Potts, B. W., and Nestler, E. J. (2002). Regulation of regulators of G protein signaling mRNA expression in rat brain by acute and chronic electroconvulsive seizures. *Journal of Neurochemistry*. https://doi.org/10.1046/j.1471-4159.2002.01002.x

Gold, S. J., Hoang, C. V., Potts, B. W., Porras, G., Pioli, E., Ki, W. K., Nadjar, A., Qin, C., LaHoste, G. J., Li, Q., Bioulac, B. H., Waugh, J. L., Gurevich, E., Neve, R. L., and Bezard, E. (2007). RGS9-2 negatively modulates L-3,4-dihydroxyphenylalanine-induced dyskinesia in experimental Parkinson's disease. *Journal of Neuroscience*. https://doi.org/10.1523/JNEUROSCI.4223-07.2007

Gold, S. J., Ni, Y. G., Dohlman, H. G., and Nestler, E. J. (1997). Regulators of G-protein signaling (RGS) proteins: Region-specific expression of nine subtypes in rat brain. *Journal of Neuroscience*. https://doi.org/10.1523/jneurosci.17-20-08024.1997

Gootenberg, J. S., Abudayyeh, O. O., Lee, J. W., Essletzbichler, P., Dy, A. J., Joung, J., Verdine, V., Donghia, N., Daringer, N. M., Freije, C. A., Myhrvold, C., Bhattacharyya, R. P., Livny, J., Regev, A., Koonin, E. V., Hung, D. T., Sabeti, P. C., Collins, J. J., and Zhang, F. (2017a). Nucleic acid detection with CRISPR-Cas13a/C2c2. *Science*, *356*(6336), 438–442. https://doi.org/10.1126/science.aam9321

Gootenberg, J. S., Abudayyeh, O. O., Lee, J. W., Essletzbichler, P., Dy, A. J., Joung, J., Verdine, V., Donghia, N., Daringer, N. M., Freije, C. A., Myhrvold, C., Bhattacharyya, R. P., Livny, J., Regev, A., Koonin, E. V., Hung, D. T., Sabeti, P. C., Collins, J. J., and Zhang, F. (2017b). Nucleic acid detection with CRISPR-Cas13a/C2c2. *Science*. https://doi.org/10.1126/science.aam9321

Göres, T. J., Penke, B., Böti, Z., Katarova, Z., and Hámori, J. (1993). Immunohistochemical visualization of a metabotropic glutamate receptor. *NeuroReport*. https://doi.org/10.1097/00001756-199303000-00014

Grafstein-Dunn, E., Young, K. H., Cockett, M. I., and Khawaja, X. Z. (2001). Regional distribution of regulators of G-protein signaling (RGS) 1, 2, 13, 14, 16, and GAIP messenger ribonucleic acids by in situ hybridization in rat brain. *Molecular Brain Research*. https://doi.org/10.1016/S0169-328X(01)00038-9

Grayson, T. H., Ohms, S. J., Brackenbury, T. D., Meaney, K. R., Peng, K., Pittelkow, Y. E., Wilson, S. R., Sandow, S. L., and Hill, C. E. (2007). Vascular microarray profiling in two models of hypertension identifies caveolin-1, Rgs2 and Rgs5 as antihypertensive targets. *BMC Genomics*. https://doi.org/10.1186/1471-2164-8-404

Guergueltcheva, V., Azmanov, D. N., Angelicheva, D., Smith, K. R., Chamova, T., Florez, L., Bynevelt, M., Nguyen, T., Cherninkova, S., Bojinova, V., Kaprelyan, A., Angelova, L., Morar, B., Chandler, D., Kaneva, R., Bahlo, M., Tournev, I., and Kalaydjieva, L. (2012). Autosomal-recessive congenital cerebellar ataxia is caused by mutations in metabotropic glutamate receptor 1. *American Journal of*

Human Genetics. https://doi.org/10.1016/j.ajhg.2012.07.019

Gugger, O. S., and Kapfhammer, J. P. (2010). Reduced size of the dendritic tree does not protect Purkinje cells from excitotoxic death. *Journal of Neuroscience Research*. https://doi.org/10.1002/jnr.22247

Häggmark, A., Mikus, M., Mohsenchian, A., Hong, M. G., Forsström, B., Gajewska, B., Barańczyk-Kuźma, A., Uhlén, M., Schwenk, J. M., Kuźma-Kozakiewicz, M., and Nilsson, P. (2014). Plasma profiling reveals three proteins associated to amyotrophic lateral sclerosis. *Annals of Clinical and Translational Neurology*. https://doi.org/10.1002/acn3.83

Haller, C., Fillatreau, S., Hoffmann, R., and Agenès, F. (2002). Structure, chromosomal localization and expression of the mouse regulator of G-protein signaling10 gene (mRGS10). *Gene*. https://doi.org/10.1016/S0378-1119(02)00883-1

Han, S. B., Moratz, C., Huang, N. N., Kelsall, B., Cho, H., Shi, C. S., Schwartz, O., and Kehrl, J. H. (2005). Rgs1 and Gnai2 regulate the entrance of B lymphocytes into lymph nodes and B cell motility within lymph node follicles. *Immunity*. https://doi.org/10.1016/j.immuni.2005.01.017

Hansel, C., Linden, D. J., and D'Angelo, E. (2001). Beyond parallel fiber LTD: The diversity of synaptic and non-synaptic plasticity in the cerebellum. In *Nature Neuroscience*. https://doi.org/10.1038/87419

Hara, K., Shiga, A., Nozaki, H., Mitsui, J., Takahashi, Y., Ishiguro, H., Yomono, H., Kurisaki, H., Goto, J., Ikeuchi, T., Tsuji, S., Nishizawa, M., and Onodera, O. (2008). Total deletion and a missense mutation of ITPR1 in Japanese SCA15 families. *Neurology*. https://doi.org/10.1212/01.wnl.0000311277.71046.a0

Hartmann, J., Blum, R., Kovalchuk, Y., Adelsberger, H., Kuner, R., Durand, G. M., Miyata, M., Kano, M., Offermanns, S., and Konnerth, A. (2004). Distinct roles of

Gαq Gα11 and Purkinje cell signaling and motor behavior. *Journal of Neuroscience*. https://doi.org/10.1523/JNEUROSCI.4193-03.2004

Hartmann, Jana, Dragicevic, E., Adelsberger, H., Henning, H. A., Sumser, M., Abramowitz, J., Blum, R., Dietrich, A., Freichel, M., Flockerzi, V., Birnbaumer, L., and Konnerth, A. (2008). TRPC3 Channels Are Required for Synaptic Transmission and Motor Coordination. *Neuron*. https://doi.org/10.1016/j.neuron.2008.06.009

Hartmann, Jana, Henning, H. A., and Konnerth, A. (2011). mGluR1/TRPC3-mediated synaptic transmission and calcium signaling in mammalian central neurons. *Cold Spring Harbor Perspectives in Biology*. https://doi.org/10.1101/cshperspect.a006726

Hashiguchi, S., Doi, H., Kunii, M., Nakamura, Y., Shimuta, M., Suzuki, E., Koyano, S., Okubo, M., Kishida, H., Shiina, M., Ogata, K., Hirashima, F., Inoue, Y., Kubota, S., Hayashi, N., Nakamura, H., Takahashi, K., Katsumoto, A., Tada, M., … Tanaka, F. (2019). Ataxic phenotype with altered CaV3.1 channel property in a mouse model for spinocerebellar ataxia 42. *Neurobiology of Disease*. https://doi.org/10.1016/j.nbd.2019.104516

Hashimoto, T., Ase, K., Sawamura, S., Kikkawa, U., Saito, N., Tanaka, C., and Nishizuka, Y. (1988). Postnatal development of a brain-specific subspecies of protein kinase C in rat. *Journal of Neuroscience*. https://doi.org/10.1523/jneurosci.08-05-01678.1988

Havel, L. S., Li, S., and Li, X. J. (2009). Nuclear accumulation of polyglutamine disease proteins and neuropathology. In *Molecular Brain*. https://doi.org/10.1186/1756-6606-2-21

Hayasaka, N., Aoki, K., Kinoshita, S., Yamaguchi, S., Wakefield, J. K., Tsuji-Kawahara, S., Horikawa, K., Ikegami, H., Wakana, S., Murakami, T., Ramabhadran, R., Miyazawa, M., and Shibata, S. (2011). Attenuated food

anticipatory activity and abnormal circadian locomotor rhythms in RGS16 knockdown mice. *PLoS ONE*. https://doi.org/10.1371/journal.pone.0017655

Hayes, M. P., and Roman, D. L. (2016). Regulator of G protein signaling 17 as a negative modulator of GPCR signaling in multiple human cancers. In *AAPS Journal*. https://doi.org/10.1208/s12248-016-9894-1

Helmlinger, D., Tora, L., and Devys, D. (2006). Transcriptional alterations and chromatin remodeling in polyglutamine diseases. In *Trends in Genetics*. https://doi.org/10.1016/j.tig.2006.07.010

Hepler, J. R., Berman, D. M., Gilman, A. G., and Kozasa, T. (1997). RGS4 and GAIP are GTPase-activating proteins for Gqα and block activation of phospholipase Cβ by γ-thio-GTP-Gqα. *Proceedings of the National Academy of Sciences of the United States of America*. https://doi.org/10.1073/pnas.94.2.428

Heuer, H., and Mason, C. A. (2003). Thyroid Hormone Induces Cerebellar Purkinje Cell Dendritic Development via the Thyroid Hormone Receptor α1. *Journal of Neuroscience*. https://doi.org/10.1523/jneurosci.23-33-10604.2003

Hirai, H. (2018). Protein Kinase C in the Cerebellum: Its Significance and Remaining Conundrums. In *Cerebellum*. https://doi.org/10.1007/s12311-017-0898-x

Hirasawa, M., Xu, X., Trask, R. B., Maddatu, T. P., Johnson, B. A., Naggert, J. K., Nishina, P. M., and Ikeda, A. (2007). Carbonic anhydrase related protein 8 mutation results in aberrant synaptic morphology and excitatory synaptic function in the cerebellum. *Molecular and Cellular Neuroscience*. https://doi.org/10.1016/j.mcn.2007.02.013

Hohoff, C., Neumann, A., Domschke, K., Jacob, C., Maier, W., Fritze, J., Bandelow, B., Krakowitzky, P., Rothermundt, M., Arolt, V., and Deckert, J. (2009). Association analysis of Rgs7 variants with panic disorder. *Journal of Neural Transmission*. https://doi.org/10.1007/s00702-008-0097-5

Hollinger, S., and Hepler, J. R. (2002). Cellular regulation of RGS proteins: Modulators and integrators of G protein signaling. *Pharmacological Reviews*, *54*(3), 527–559. https://doi.org/10.1124/pr.54.3.527

Hollinger, S., Taylor, J. B., Goldman, E. H., and Hepler, J. R. (2001). RGS14 is a bifunctional regulator of Gαi/o activity that exists in multiple populations in brain. *Journal of Neurochemistry*. https://doi.org/10.1046/j.1471-4159.2001.00629.x

Holmes, S. E., O'Hearn, E. E., McInnis, M. G., Gorelick-Feldman, D. A., Kleiderlein, J. J., Callahan, C., Kwak, N. G., Ingersoll-Ashworth, R. G., Sherr, M., Sumner, A. J., Sharp, A. H., Ananth, U., Seltzer, W. K., Boss, M. A., Vieria-Saecker, A. M., Epplen, J. T., Riess, O., Ross, C. A., and Margolis, R. L. (1999). Expansion of a novel CAG trinucleotide repeat in the 5' region of PPP2R2B is associated with SCA12. *Nature Genetics*, *23*(4), 391–392. https://doi.org/10.1038/70493

Hsiao, C. T., Fu, S. J., Liu, Y. T., Lu, Y. H., Zhong, C. Y., Tang, C. Y., Soong, B. W., and Jeng, C. J. (2019). Novel SCA19/22-associated KCND3 mutations disrupt human KV4.3 protein biosynthesis and channel gating. *Human Mutation*. https://doi.org/10.1002/humu.23865

Hu, Y., Xing, J., Chen, L., Guo, X., Du, Y., Zhao, C., Zhu, Y., Lin, M., Zhou, Z., and Sha, J. (2008). RGS22, A Novel Testis-Specific Regulator of G-protein Signaling Involved in Human and Mouse Spermiogenesis along with GNA12/13 Subunits1. *Biology of Reproduction*, *79*(6), 1021–1029. https://doi.org/10.1095/biolreprod.107.067504

Huang, F. L., Yoshida, Y., Nakabayashi, H., Young, W. S., and Huang, K. P. (1988). Immunocytochemical localization of protein kinase C isozymes in rat brain. *Journal of Neuroscience*. https://doi.org/10.1523/jneurosci.08-12-04734.1988

Huang, J., Chen, L., Yao, Y., Tang, C., Ding, J., Fu, C., Li, H., and Ma, G. (2016). Pivotal role of regulator of G-protein signaling 12 in pathological cardiac hypertrophy. *Hypertension*.

https://doi.org/10.1161/HYPERTENSIONAHA.115.06877

Huang, L., Chardon, J. W., Carter, M. T., Friend, K. L., Dudding, T. E., Schwartzentruber, J., Zou, R., Schofield, P. W., Douglas, S., Bulman, D. E., and Boycott, K. M. (2012). Missense mutations in ITPR1 cause autosomal dominant congenital nonprogressive spinocerebellar ataxia. *Orphanet Journal of Rare Diseases*. https://doi.org/10.1186/1750-1172-7-67

Huang, W. C., Young, J. S., and Glitsch, M. D. (2007). Changes in TRPC channel expression during postnatal development of cerebellar neurons. *Cell Calcium*. https://doi.org/10.1016/j.ceca.2006.11.002

Hunt, T. W., Fields, T. A., Casey, P. J., and Peralta, E. G. (1996). RGS10 is a selective activator of Gα(i) GTPase activity. *Nature*. https://doi.org/10.1038/383175a0

Hutchison, R. M., Chidiac, P., and Leung, L. S. (2009). Hippocampal long-term potentiation is enhanced in urethane-anesthetized RGS2 knockout mice. *Hippocampus*. https://doi.org/10.1002/hipo.20582

Hwang, I. Y., Hwang, K. S., Park, C., Harrison, K. A., and Kehrl, J. H. (2013). Rgs13 Constrains Early B Cell Responses and Limits Germinal Center Sizes. *PLoS ONE*. https://doi.org/10.1371/journal.pone.0060139

Ikeda, Y., Dick, K. A., Weatherspoon, M. R., Gincel, D., Armbrust, K. R., Dalton, J. C., Stevanin, G., Dürr, A., Zühlke, C., Bürk, K., Clark, H. B., Brice, A., Rothstein, J. D., Schut, L. J., Day, J. W., and Ranum, L. P. W. (2006). Spectrin mutations cause spinocerebellar ataxia type 5. *Nature Genetics*. https://doi.org/10.1038/ng1728

Ingi, T., and Aoki, Y. (2002). Expression of RGS2, RGS4 and RGS7 in the developing postnatal brain. *European Journal of Neuroscience*, *15*(5), 929–936. https://doi.org/10.1046/j.1460-9568.2002.01925.x

Ingram, M., Wozniak, E. A. L., Duvick, L., Yang, R., Bergmann, P., Carson, R., O'Callaghan, B., Zoghbi, H. Y., Henzler, C., and Orr, H. T. (2016). Cerebellar Transcriptome Profiles of ATXN1 Transgenic Mice Reveal SCA1 Disease Progression and Protection Pathways. *Neuron*. https://doi.org/10.1016/j.neuron.2016.02.011

Itoh, M., Nagatomo, K., Kubo, Y., and Saitoh, O. (2006). Alternative splicing of RGS8 gene changes the binding property to the M1 muscarinic receptor to confer receptor type-specific Gq regulation. *Journal of Neurochemistry*. https://doi.org/10.1111/j.1471-4159.2006.04220.x

Iwaki, A., Kawano, Y., Miura, S., Shibata, H., Matsuse, D., Li, W., Furuya, H., Ohyagi, Y., Taniwaki, T., Kira, J., and Fukumaki, Y. (2008). Heterozygous deletion of ITPR1, but not SUMF1, in spinocerebellar ataxia type 16. *Journal of Medical Genetics*. https://doi.org/10.1136/jmg.2007.053942

Iwaki, S., Lu, Y., Xie, Z., and Druey, K. M. (2011). p53 negatively regulates RGS13 protein expression in immune cells. *Journal of Biological Chemistry*. https://doi.org/10.1074/jbc.M111.228924

Ji, J., Hassler, M. L., Shimobayashi, E., Paka, N., Streit, R., and Kapfhammer, J. P. (2014). Increased protein kinase C gamma activity induces Purkinje cell pathology in a mouse model of spinocerebellar ataxia 14. *Neurobiology of Disease*, *70*, 1–11. https://doi.org/10.1016/j.nbd.2014.06.002

Ji, Y. R., Kim, H. J., Park, S. J., Bae, K. B., Park, S. J., Jang, W. Y., Kang, M. C., Jeong, J., Sung, Y. H., Choi, M., Lee, W., Lee, D. G., Park, S. J., Lee, S., Kim, M. O., and Ryoo, Z. Y. (2015). Critical role of Rgs19 in mouse embryonic stem cell proliferation and differentiation. *Differentiation*. https://doi.org/10.1016/j.diff.2015.01.002

Joubert, B., and Honnorat, J. (2019). Nonparaneoplastic autoimmune cerebellar ataxias. In *Current Opinion in Neurology*.

https://doi.org/10.1097/WCO.0000000000000678

Ju, H., Kokubu, H., and Lim, J. (2014). Beyond the Glutamine Expansion: Influence of Posttranslational Modifications of Ataxin-1 in the Pathogenesis of Spinocerebellar Ataxia Type 1. In *Molecular Neurobiology*. https://doi.org/10.1007/s12035-014-8703-z

Kannarkat, G. T., Lee, J. K., Ramsey, C. P., Chung, J., Chang, J., Porter, I., Oliver, D., Shepherd, K., and Tansey, M. G. (2015). Age-related changes in regulator of G-protein signaling (RGS)-10 expression in peripheral and central immune cells may influence the risk for age-related degeneration. *Neurobiology of Aging*. https://doi.org/10.1016/j.neurobiolaging.2015.02.006

Kano, M., Hashimoto, K., Chen, C., Abeliovich, A., Aiba, A., Kurihara, H., Watanabe, M., Inoue, Y., and Tonegawa, S. (1995). Impaired synapse elimination during cerebellar development in PKCγ mutant mice. *Cell*, *83*(7), 1223–1231. https://doi.org/10.1016/0092-8674(95)90147-7

Kano, M., Hashimoto, K., Kurihara, H., Watanabe, M., Inoue, Y., Aiba, A., and Tonegawa, S. (1997). Persistent multiple climbing fiber innervation of cerebellar purkinje cells in mice lacking mGluR1. *Neuron*. https://doi.org/10.1016/S0896-6273(01)80047-7

Kano, M., Hashimoto, K., and Tabata, T. (2008). Type-1 metabotropic glutamate receptor in cerebellar Purkinje cells: A key molecule responsible for long-term depression, endocannabinoid signalling and synapse elimination. In *Philosophical Transactions of the Royal Society B: Biological Sciences*. https://doi.org/10.1098/rstb.2008.2270

Kano, M., Hashimoto, K., Watanabe, M., Kurihara, H., Offermanns, S., Jiang, H., Wu, Y., Jun, K., Shin, H. S., Inoue, Y., Simon, M. I., and Wu, D. (1998). Phospholipase Cβ4 is specifically involved in climbing fiber synapse elimination in the developing cerebellum. *Proceedings of the National Academy of Sciences*

of the United States of America. https://doi.org/10.1073/pnas.95.26.15724

Kapfhammer, J. P. (2004). Cellular and molecular control of dendritic growth and development of cerebellar Purkinje cells. *Progress in Histochemistry and Cytochemistry*, *39*(3), 131–182. https://doi.org/10.1016/j.proghi.2004.07.002

Kapfhammer, J. P., and Gugger, O. S. (2012). The Analysis of Purkinje Cell Dendritic Morphology in Organotypic Slice Cultures. *Journal of Visualized Experiments*, *61*, 1–8. https://doi.org/10.3791/3637

Karra, D., and Dahm, R. (2010). Transfection techniques for neuronal cells. In *Journal of Neuroscience*. https://doi.org/10.1523/JNEUROSCI.0183-10.2010

Kasumu, A. W., Hougaard, C., Rode, F., Jacobsen, T. A., Sabatier, J. M., Eriksen, B. L., Strobæk, D., Liang, X., Egorova, P., Vorontsova, D., Christophersen, P., Ronn, L. C. B., and Bezprozvanny, I. (2012). Selective positive modulator of calcium-activated potassium channels exerts beneficial effects in a mouse model of spinocerebellar ataxia type 2. *Chemistry and Biology*. https://doi.org/10.1016/j.chembiol.2012.07.013

Kato, A. S., Knierman, M. D., Siuda, E. R., Isaac, J. T. R., Nisenbaum, E. S., and Bredt, D. S. (2012). Glutamate receptor δ2 associates with metabotropic glutamate receptor 1 (mGluR1), protein kinase Cγ, and canonical transient receptor potential 3 and regulates mGluR1-mediated synaptic transmission in cerebellar Purkinje neurons. *Journal of Neuroscience*, *32*(44), 15296–15308. https://doi.org/10.1523/JNEUROSCI.0705-12.2012

Khare, S., Galeano, K., Zhang, Y., Nick, J. A., Nick, H. S., Subramony, S. H., Sampson, J., Kaczmarek, L. K., and Waters, M. F. (2018). C-terminal proline deletions in KCNC3 cause delayed channel inactivation and an adult-onset progressive SCA13 with spasticity. *Cerebellum*. https://doi.org/10.1007/s12311-018-0950-5

Khare, S., Nick, J. A., Zhang, Y., Galeano, K., Butler, B., Khoshbouei, H., Rayaprolu, S., Hathorn, T., Ranum, L. P. W., Smithson, L., Golde, T. E., Paucar, M., Morse, R., Raff, M., Simon, J., Nordenskjold, M., Wirdefeldt, K., Rincon-Limas, D. E., Lewis, J., … Waters, M. F. (2017). A KCNC3 mutation causes a neurodevelopmental, non-progressive SCA13 subtype associated with dominant negative effects and aberrant EGFR trafficking. *PLoS ONE*. https://doi.org/10.1371/journal.pone.0173565

Kim, T. K., and Eberwine, J. H. (2010). Mammalian cell transfection: The present and the future. *Analytical and Bioanalytical Chemistry*. https://doi.org/10.1007/s00216-010-3821-6

Klein, A. P., Ulmer, J. L., Quinet, S. A., Mathews, V., and Mark, L. P. (2016). Nonmotor functions of the cerebellum: An introduction. *American Journal of Neuroradiology*. https://doi.org/10.3174/ajnr.A4720

Klockgether, T., Mariotti, C., and Paulson, H. L. (2019). Spinocerebellar ataxia. *Nature Reviews Disease Primers*, *5*(1), 1–21. https://doi.org/10.1038/s41572-019-0074-3

Ko, W. K. D., Martin-Negrier, M. L., Bezard, E., Crossman, A. R., and Ravenscroft, P. (2014). RGS4 is involved in the generation of abnormal involuntary movements in the unilateral 6-OHDA-lesioned rat model of Parkinson's disease. *Neurobiology of Disease*. https://doi.org/10.1016/j.nbd.2014.06.013

Kobayashi, Y., Takemoto, R., Yamato, S., Okada, T., Iijima, M., Uematsu, Y., Chaki, S., and Saito, Y. (2018). Depression-resistant Phenotype in Mice Overexpressing Regulator of G Protein Signaling 8 (RGS8). *Neuroscience*. https://doi.org/10.1016/j.neuroscience.2018.05.005

Koht, J., Stevanin, G., Durr, A., Mundwiller, E., Brice, A., and Tallaksen, C. M. E. (2012). SCA14 in Norway, two families with autosomal dominant cerebellar ataxia and a novel mutation in the PRKCG gene. *Acta Neurologica*

Scandinavica. https://doi.org/10.1111/j.1600-0404.2011.01504.x

Konno, A., Shuvaev, A. N., Miyake, N., Miyake, K., Iizuka, A., Matsuura, S., Huda, F., Nakamura, K., Yanagi, S., Shimada, T., and Hirai, H. (2014). Mutant ataxin-3 with an abnormally expanded polyglutamine chain disrupts dendritic development and metabotropic glutamate receptor signaling in mouse cerebellar Purkinje cells. *Cerebellum*, *13*(1), 29–41. https://doi.org/10.1007/s12311-013-0516-5

Kosaka, T., Kosaka, K., Nakayama, T., Hunziker, W., and Heizmann, C. W. (1993). Axons and axon terminals of cerebellar Purkinje cells and basket cells have higher levels of parvalbumin immunoreactivity than somata and dendrites: quantitative analysis by immunogold labeling. *Experimental Brain Research*. https://doi.org/10.1007/BF00229363

Kose, A., Saito, N., Ito, H., Kikkawa, U., Nishizuka, Y., and Tanaka, C. (1988). Electron microscopic localization of type I protein kinase C in rat Purkinje cells. *Journal of Neuroscience*. https://doi.org/10.1523/jneurosci.08-11-04262.1988

Kozasa, T., Jiang, X., Hart, M. J., Sternweis, P. M., Singer, W. D., Gilman, A. G., Bollag, G., and Sternweis, P. C. (1998). p115 RhoGEF, a GTPase activating protein for Gα12 and Gα13. In *Science*. https://doi.org/10.1126/science.280.5372.2109

Kurrasch, D. M., Huang, J., Wilkie, T. M., and Repa, J. J. (2004). Quantitative real-time polymerase chain reaction measurement of regulators of G-protein signaling mRNA levels in mouse tissues. *Methods in Enzymology*. https://doi.org/10.1016/S0076-6879(04)89001-3

Kuwahara, H., Nakamura, N., and Kanazawa, H. (2006). Nuclear localization of the serine/threonine kinase DRAK2 is involved in UV-induced apoptosis. *Biological and Pharmaceutical Bulletin*, *29*(2), 225–233. https://doi.org/10.1248/bpb.29.225

Kuwahara, H., Nishizaki, M., and Kanazawa, H. (2008). Nuclear localization signal and phosphorylation of serine350 specify intracellular localization of DRAK2. *Journal of Biochemistry*, *143*(3), 349–358. https://doi.org/10.1093/jb/mvm236

Kuwata, H., Nakao, K., Harada, T., Matsuda, I., and Aiba, A. (2007). Generation of RGS8 Null Mutant Mice by Cre / loxP System. *System*, *53*(6), 275–281.

Kveberg, L., Ryan, J. C., Rolstad, B., and Inngjerdingen, M. (2005). Expression of regulator of G protein signalling proteins in natural killer cells, and their modulation by Ly49A and Ly49D. *Immunology*. https://doi.org/10.1111/j.1365-2567.2005.02174.x

Lainé, J., and Axelrad, H. (1994). The candelabrum cell: A new interneuron in the cerebellar cortex. *Journal of Comparative Neurology*. https://doi.org/10.1002/cne.903390202

Lam, Y. C., Bowman, A. B., Jafar-Nejad, P., Lim, J., Richman, R., Fryer, J. D., Hyun, E. D., Duvick, L. A., Orr, H. T., Botas, J., and Zoghbi, H. Y. (2006). ATAXIN-1 Interacts with the Repressor Capicua in Its Native Complex to Cause SCA1 Neuropathology. *Cell*. https://doi.org/10.1016/j.cell.2006.11.038

Larminie, C., Murdock, P., Walhin, J. P., Duckworth, M., Blumer, K. J., Scheideler, M. A., and Garnier, M. (2004). Selective expression of regulators of G-protein signaling (RGS) in the human central nervous system. *Molecular Brain Research*. https://doi.org/10.1016/j.molbrainres.2003.11.014

Lee, J. K., Chung, J., Druey, K. M., and Tansey, M. G. (2012). RGS10 exerts a neuroprotective role through the PKA/c-AMP response-element (CREB) pathway in dopaminergic neuron-like cells. *Journal of Neurochemistry*, *122*(2), 333–343. https://doi.org/10.1111/j.1471-4159.2012.07780.x

Lee, J. K., Chung, J., McAlpine, F. E., and Tansey, M. G. (2011). Regulator of G-protein signaling-10 negatively regulates NF-κB in microglia and neuroprotects

dopaminergic neurons in hemiparkinsonian rats. *Journal of Neuroscience*, *31*(33), 11879–11888. https://doi.org/10.1523/JNEUROSCI.1002-11.2011

Lee, J. K., Kannarkat, G. T., Chung, J., Lee, H., Graham, K. L., and Tansey, M. G. (2016). RGS10 deficiency ameliorates the severity of disease in experimental autoimmune encephalomyelitis. *Journal of Neuroinflammation*. https://doi.org/10.1186/s12974-016-0491-0

Lee, M. S., Son, M. Y., Park, J. Il, Park, C., Lee, Y. C., Son, C. B., Kim, Y. S., Paik, S. G., Yoon, W. H., Park, S. K., Hwang, B. D., and Lim, K. (2001). Modification of octamer binding transcriptional factor is related to H2B histone gene repression during dimethyl sulfoxide-dependent differentiation of HL-60 cells. *Cancer Letters*. https://doi.org/10.1016/S0304-3835(01)00654-1

Lee, Y. C., Durr, A., Majczenko, K., Huang, Y. H., Liu, Y. C., Lien, C. C., Tsai, P. C., Ichikawa, Y., Goto, J., Monin, M. L., Li, J. Z., Chung, M. Y., Mundwiller, E., Shakkottai, V., Liu, T. T., Tesson, C., Lu, Y. C., Brice, A., Tsuji, S., … Soong, B. W. (2012). Mutations in KCND3 cause spinocerebellar ataxia type 22. *Annals of Neurology*. https://doi.org/10.1002/ana.23701

Lein, E. S., Hawrylycz, M. J., Ao, N., Ayres, M., Bensinger, A., Bernard, A., Boe, A. F., Boguski, M. S., Brockway, K. S., Byrnes, E. J., Chen, L., Chen, L., Chen, T. M., Chin, M. C., Chong, J., Crook, B. E., Czaplinska, A., Dang, C. N., Datta, S., … Jones, A. R. (2007). Genome-wide atlas of gene expression in the adult mouse brain. *Nature*. https://doi.org/10.1038/nature05453

Li, Y., Tang, X. hong, Li, X. hui, Dai, H. jiang, Miao, R. jia, Cai, J. jing, Huang, Z. jun, Chen, A. F., Xing, X. wei, Lu, Y., and Yuan, H. (2016). Regulator of G protein signalling 14 attenuates cardiac remodelling through the MEK–ERK1/2 signalling pathway. *Basic Research in Cardiology*. https://doi.org/10.1007/s00395-016-0566-1

Liang, G., Bansal, G., Xie, Z., and Druey, K. M. (2009). RGS16 inhibits breast cancer

cell growth by mitigating phosphatidylinositol 3-kinase signaling. *Journal of Biological Chemistry*. https://doi.org/10.1074/jbc.M109.028407

Lim, J., Crespo-Barreto, J., Jafar-Nejad, P., Bowman, A. B., Richman, R., Hill, D. E., Orr, H. T., and Zoghbi, H. Y. (2008). Opposing effects of polyglutamine expansion on native protein complexes contribute to SCA1. *Nature*. https://doi.org/10.1038/nature06731

Lin, X., Antalffy, B., Kang, D., Orr, H. T., and Zoghbi, H. Y. (2000). Polyglutamine expansion down-regulates specific neuronal genes before pathologic changes in SCA1. *Nature Neuroscience*. https://doi.org/10.1038/72101

Liu, J., Tang, T. S., Tu, H., Nelson, O., Herndon, E., Huynh, D. P., Pulst, S. M., and Bezprozvanny, I. (2009). Deranged calcium signaling and neurodegeneration in spinocerebellar ataxia type 2. *Journal of Neuroscience*, *29*(29), 9148–9162. https://doi.org/10.1523/JNEUROSCI.0660-09.2009

Liu, Q., Huang, S., Yin, P., Yang, S., Zhang, J., Jing, L., Cheng, S., Tang, B., Li, X. J., Pan, Y., and Li, S. (2020). Cerebellum-enriched protein INPP5A contributes to selective neuropathology in mouse model of spinocerebellar ataxias type 17. *Nature Communications*. https://doi.org/10.1038/s41467-020-14931-8

Liu, Y., Huang, H., Zhang, Y., Zhu, X. Y., Zhang, R., Guan, L. H., Tang, Q., Jiang, H., and Huang, C. (2014). Regulator of G protein signaling 3 protects against cardiac hypertrophy in mice. *Journal of Cellular Biochemistry*. https://doi.org/10.1002/jcb.24741

Manzur, M., and Ganss, R. (2009). Regulator of G Protein Signaling 5: A New Player in Vascular Remodeling. In *Trends in Cardiovascular Medicine*. https://doi.org/10.1016/j.tcm.2009.04.002

Mao, H., Zhao, Q., Daigle, M., Ghahremani, M. H., Chidiac, P., and Albert, P. R. (2004). RGS17/RGSZ2, a novel regulator of Gi/o, Gz, and Gq signaling. *Journal*

of Biological Chemistry, *279*(25), 26314–26322. https://doi.org/10.1074/jbc.M401800200

Mao, J., Luo, H., and Wu, J. (2008). Drak2 overexpression results in increased β-cell apoptosis after free fatty acid stimulation. *Journal of Cellular Biochemistry*. https://doi.org/10.1002/jcb.21910

Mao, J., Qiao, X., Luo, H., and Wu, J. (2006). Transgenic Drak2 overexpression in mice leads to increased T cell apoptosis and compromised memory T cell development. *Journal of Biological Chemistry*. https://doi.org/10.1074/jbc.M600497200

Mao, L. M., Liu, X. Y., Zhang, G. C., Chu, X. P., Fibuch, E. E., Wang, L. S., Liu, Z., and Wang, J. Q. (2008). Phosphorylation of group I metabotropic glutamate receptors (mGluR1/5) in vitro and in vivo. *Neuropharmacology*, *55*(4), 403–408. https://doi.org/10.1016/j.neuropharm.2008.05.034

Matsumoto, M., Nakagawa, T., Inoue, T., Nagata, E., Tanaka, K., Takano, H., Minowa, O., Kuno, J., Sakakibara, S., Yamada, M., Yoneshima, H., Miyawaki, A., Fukuuchi, Y., Furuichi, T., Okano, H., Mikoshiba, K., and Noda, T. (1996). Ataxia and epileptic seizures in mice lacking type 1 inositol 1,4,5-trisphosphate receptor. *Nature*. https://doi.org/10.1038/379168a0

Matsuura, T., Yamagata, T., Burgess, D. L., Rasmussen, A., Grewal, R. P., Watase, K., Khajavi, M., McCall, A. E., Davis, C. F., Zu, L., Achari, M., Pulst, S. M., Alonso, E., Noebels, J. L., Nelson, D. L., Zoghbi, H. Y., and Ashizawa, T. (2000). Large expansion of the ATTCT pentanucleotide repeat in spinocerebellar ataxia type 10. *Nature Genetics*, *26*(2), 191–194. https://doi.org/10.1038/79911

McEvoy, M., Cao, G., Llopis, P. M., Kundel, M., Jones, K., Hofler, C., Shin, C., and Wells, D. G. (2007). Cytoplasmic polyadenylation element binding protein 1-mediated mRNA translation in Purkinje neurons is required for cerebellar long-

term depression and motor coordination. *Journal of Neuroscience*. https://doi.org/10.1523/JNEUROSCI.5211-06.2007

McGargill, M. A., Choy, C., Wen, B. G., and Hedrick, S. M. (2008). Drak2 Regulates the Survival of Activated T Cells and Is Required for Organ-Specific Autoimmune Disease. *The Journal of Immunology*. https://doi.org/10.4049/jimmunol.181.11.7593

McGargill, M. A., Wen, B. G., Walsh, C. M., and Hedrick, S. M. (2004). A deficiency in Drak2 results in a T cell hypersensitivity and an unexpected resistance to autoimmunity. *Immunity*. https://doi.org/10.1016/j.immuni.2004.10.008

McKay, B. E., and Turner, R. W. (2005). Physiological and morphological development of the rat cerebellar Purkinje cell. In *Journal of Physiology*. https://doi.org/10.1113/jphysiol.2005.089383

McMahon, S. J., Pray-Grant, M. G., Schieltz, D., Yates, J. R., and Grant, P. A. (2005). Polyglutamine-expanded spinocerebellar ataxia-7 protein disrupts normal SAGA and SLIK histone acetyltransferase activity. *Proceedings of the National Academy of Sciences of the United States of America*. https://doi.org/10.1073/pnas.0503493102

Meera, P., Pulst, S. M., and Otis, T. S. (2016). Cellular and circuit mechanisms underlying spinocerebellar ataxias. *The Journal of Physiology*, *594*(16), 4653–4660. https://doi.org/10.1113/JP271897

Meeske, A. J., and Marraffini, L. A. (2018). RNA Guide Complementarity Prevents Self-Targeting in Type VI CRISPR Systems. *Molecular Cell*. https://doi.org/10.1016/j.molcel.2018.07.013

Metzger, F., and Kapfhammer, J. P. (2000). Protein kinase C activity modulates dendritic differentiation of rat Purkinje cells in cerebellar slice cultures. *European Journal of Neuroscience*. https://doi.org/10.1046/j.1460-9568.2000.00086.x

Michael, A. J., Lu, Y., Liu, Y., Haris, G. V., and You, M. (2009). RGS17, an overexpressed gene in human lung and prostate cancer, induces tumor cell proliferation through the cyclic AMP-PKA-CREB pathway. *Cancer Research*. https://doi.org/10.1158/0008-5472.CAN-08-3495

Millward, T. A., Zolnierowicz, S., and Hemmings, B. A. (1999). Regulation of protein kinase cascades by protein phosphatase 2A. In *Trends in Biochemical Sciences*. https://doi.org/10.1016/S0968-0004(99)01375-4

Min, C., Cheong, S. Y., Cheong, S. J., Kim, M., Cho, D. I., and Kim, K. M. (2012). RGS4 exerts inhibitory activities on the signaling of dopamine D 2 receptor and D 3 receptor through the N-terminal region. *Pharmacological Research*. https://doi.org/10.1016/j.phrs.2011.08.008

Mirnics, K., Middleton, F. A., Stanwood, G. D., Lewis, D. A., and Levitt, P. (2001). Disease-specific changes in regulator of G-protein signaling 4 (RGS4) expression in schizophrenia. *Molecular Psychiatry*. https://doi.org/10.1038/sj.mp.4000866

Miyamoto-Matsubara, M., Saitoh, O., Maruyama, K., Aizaki, Y., and Saito, Y. (2008). Regulation of melanin-concentrating hormone receptor 1 signaling by RGS8 with the receptor third intracellular loop. *Cellular Signalling*, *20*(11), 2084–2094. https://doi.org/10.1016/j.cellsig.2008.07.019

Miyata, M., Kim, H. T., Hashimoto, K., Lee, T. K., Cho, S. Y., Jiang, H., Wu, Y., Jun, K., Wu, D., Kano, M., and Shin, H. S. (2001). Deficient long-term synaptic depression in the rostral cerebellum correlated with impaired motor learning in phospholipase C β4 mutant mice. *European Journal of Neuroscience*. https://doi.org/10.1046/j.0953-816X.2001.01570.x

Miyoshi, N., Ishii, H., Sekimoto, M., Doki, Y., and Mori, M. (2009). RGS16 is a marker for prognosis in colorectal cancer. *Annals of Surgical Oncology*. https://doi.org/10.1245/s10434-009-0690-3

Moratz, C., Hayman, J. R., Gu, H., and Kehrl, J. H. (2004). Abnormal B-Cell Responses to Chemokines, Disturbed Plasma Cell Localization, and Distorted Immune Tissue Architecture in Rgs1−/− Mice. *Molecular and Cellular Biology*. https://doi.org/10.1128/mcb.24.13.5767-5775.2004

Moriya, M., and Tanaka, S. (1994). Prominent expression of protein kinase C (γ) mRNA in the dendrite-rich neuropil of mice cerebellum at the critical period for synaptogenesis. *NeuroReport*. https://doi.org/10.1097/00001756-199404000-00019

Napper, R. M. A., and Harvey, R. J. (1988). Number of parallel fiber synapses on an individual Purkinje cell in the cerebellum of the rat. *Journal of Comparative Neurology*. https://doi.org/10.1002/cne.902740204

Newton, A. C. (1995). Protein kinase C: Structure, function, and regulation. In *Journal of Biological Chemistry*. https://doi.org/10.1074/jbc.270.48.28495

Newton, R. H., Leverrier, S., Srikanth, S., Gwack, Y., Cahalan, M. D., and Walsh, C. M. (2011). Protein Kinase D Orchestrates the Activation of DRAK2 in Response to TCR-Induced Ca 2+ Influx and Mitochondrial Reactive Oxygen Generation . *The Journal of Immunology*. https://doi.org/10.4049/jimmunol.1000942

Niewiadomska-Cimicka, A., and Trottier, Y. (2019). Molecular Targets and Therapeutic Strategies in Spinocerebellar Ataxia Type 7. In *Neurotherapeutics*. https://doi.org/10.1007/s13311-019-00778-5

Notartomaso, S., Zappulla, C., Biagioni, F., Cannella, M., Bucci, D., Mascio, G., Scarselli, P., Fazio, F., Weisz, F., Lionetto, L., Simmaco, M., Gradini, R., Battaglia, G., Signore, M., Puliti, A., and Nicoletti, F. (2013). Pharmacological enhancement of mGlu1 metabotropic glutamate receptors causes a prolonged symptomatic benefit in a mouse model of spinocerebellar ataxia type 1. *Molecular Brain*. https://doi.org/10.1186/1756-6606-6-48

Novak, M. J. U., Sweeney, M. G., Li, A., Treacy, C., Chandrashekar, H. S., Giunti, P., Goold, R. G., Davis, M. B., Houlden, H., and Tabrizi, S. J. (2010). An ITPR1 gene deletion causes spinocerebellar ataxia 15/16: A genetic, clinical and radiological description. *Movement Disorders*. https://doi.org/10.1002/mds.23223

O'Connell, M. R. (2019). Molecular Mechanisms of RNA Targeting by Cas13-containing Type VI CRISPR–Cas Systems. *Journal of Molecular Biology*, *431*(1), 66–87. https://doi.org/10.1016/j.jmb.2018.06.029

Offermanns, S., Hashimoto, K., Watanabe, M., Sun, W., Kurihara, H., Thompson, R. F., Inoue, Y., Kano, M., and Simon, M. I. (1997). Impaired motor coordination and persistent multiple climbing fiber innervation of cerebellar Purkinje cells in mice lacking Gαq. *Proceedings of the National Academy of Sciences of the United States of America*, *94*(25), 14089–14094. https://doi.org/10.1073/pnas.94.25.14089

Offermanns, S., Toombs, C. F., Hu, Y. H., and Simon, M. I. (1997). Defective platelet activation in Gα(q)-deficient mice. *Nature*. https://doi.org/10.1038/38284

Ohara, O., Ohara, R., Yamakawa, H., Nakajima, D., and Nakayama, M. (1998). Characterization of a new β-spectrin gene which is predominantly expressed in brain. *Molecular Brain Research*. https://doi.org/10.1016/S0169-328X(98)00068-0

Opel, A., Nobles, M., Montaigne, D., Finlay, M., Anderson, N., Breckenridge, R., and Tinker, A. (2015). Absence of the regulator of G-protein Signaling, RGS4, predisposes to atrial fibrillation and is associated with abnormal calcium handling. *Journal of Biological Chemistry*. https://doi.org/10.1074/jbc.M115.666719

Ophoff, R. A., Terwindt, G. M., Vergouwe, M. N., Van Eijk, R., Oefner, P. J., Hoffman, S. M. G., Lamerdin, J. E., Mohrenweiser, H. W., Bulman, D. E.,

Ferrari, M., Haan, J., Lindhout, D., Van Ommen, G. J. B., Hofker, M. H., Ferrari, M. D., and Frants, R. R. (1996). Familial hemiplegic migraine and episodic ataxia type-2 are caused by mutations in the Ca2+ channel gene CACNL1A4. *Cell*. https://doi.org/10.1016/S0092-8674(00)81373-2

Oppenheimer, J. H., and Schwartz, H. L. (1997). Molecular basis of thyroid hormone-dependent brain development. In *Endocrine Reviews*. https://doi.org/10.1210/er.18.4.462

Ortega, Z., and Lucas, J. J. (2014). Ubiquitin-proteasome system involvement in huntington's disease. *Frontiers in Molecular Neuroscience*. https://doi.org/10.3389/fnmol.2014.00077

Pashkov, V., Huang, J., Parameswara, V. K., Kedzierski, W., Kurrasch, D. M., Tall, G. G., Esser, V., Gerard, R. D., Uyeda, K., Towle, H. C., and Wilkie, T. M. (2011). Regulator of G protein signaling (Rgs16) inhibits hepatic fatty acid oxidation in a carbohydrate response element-binding protein (ChREBP)-dependent manner. *Journal of Biological Chemistry*. https://doi.org/10.1074/jbc.M110.216234

Patten, M., Bünemann, J., Thoma, B., Krämer, E., Thoenes, M., Stübe, S., Mittmann, C., and Wieland, T. (2002). Endotoxin induces desensitization of cardiac endothelin-1 receptor signaling by increased expression of RGS4 and RGS16. *Cardiovascular Research*. https://doi.org/10.1016/S0008-6363(01)00443-6

Pentcheva-Hoang, T., Corse, E., and Allison, J. P. (2009). Negative regulators of T-cell activation: Potential targets for therapeutic intervention in cancer, autoimmune disease, and persistent infections. In *Immunological Reviews*. https://doi.org/10.1111/j.1600-065X.2009.00763.x

Perkins, E., Suminaite, D., and Jackson, M. (2016). Cerebellar ataxias: β-III spectrin's interactions suggest common pathogenic pathways. In *Journal of Physiology*. https://doi.org/10.1113/JP271195

Pickar-Oliver, A., and Gersbach, C. A. (2019). The next generation of CRISPR–Cas technologies and applications. In *Nature Reviews Molecular Cell Biology*. https://doi.org/10.1038/s41580-019-0131-5

Poulain, F. E., Chauvin, S., Wehrlé, R., Desclaux, M., Mallet, J., Vodjdani, G., Dusart, I., and Sobel, A. (2008). SCLIP is crucial for the formation and development of the Purkinje cell dendritic arbor. *Journal of Neuroscience*. https://doi.org/10.1523/JNEUROSCI.1942-08.2008

Power, E. M., Morales, A., and Empson, R. M. (2016). Prolonged type 1 metabotropic glutamate receptor dependent synaptic signaling contributes to spino-cerebellar ataxia type 1. *Journal of Neuroscience*. https://doi.org/10.1523/JNEUROSCI.3953-15.2016

Prestori, F., Moccia, F., and D'angelo, E. (2020). Disrupted calcium signaling in animal models of human spinocerebellar ataxia (SCA). In *International Journal of Molecular Sciences*. https://doi.org/10.3390/ijms21010216

Ramos, S. J., Hernandez, J. B., Gatzka, M., and Walsh, C. M. (2008). Enhanced T Cell Apoptosis within Drak2 -Deficient Mice Promotes Resistance to Autoimmunity . *The Journal of Immunology*. https://doi.org/10.4049/jimmunol.181.11.7606

Rodriguez-Lebron, E., Liu, G., Keiser, M., Behlke, M. A., and Davidson, B. L. (2013). Altered Purkinje cell miRNA expression and SCA1 pathogenesis. *Neurobiology of Disease*, *54*, 456–463. https://doi.org/10.1016/j.nbd.2013.01.019

Ross, E. M., and Wilkie, T. M. (2000). GTPase-Activating Proteins for Heterotrimeric G Proteins: Regulators of G Protein Signaling (RGS) and RGS-Like Proteins. *Annual Review of Biochemistry*. https://doi.org/10.1146/annurev.biochem.69.1.795

Rossi, P. I. A., Vaccari, C. M., Terracciano, A., Doria-Lamba, L., Facchinetti, S.,

Priolo, M., Ayuso, C., De Jorge, L., Gimelli, S., Santorelli, F. M., Ravazzolo, R., and Puliti, A. (2010). The metabotropic glutamate receptor 1, GRM1: Evaluation as a candidate gene for inherited forms of cerebellar ataxia. *Journal of Neurology*. https://doi.org/10.1007/s00415-009-5380-3

Roy, A. A., Lemberg, K. E., and Chidiac, P. (2003). Recruitment of RGS2 and RGS4 to the plasma membrane by G proteins and receptors reflects functional interactions. *Molecular Pharmacology*. https://doi.org/10.1124/mol.64.3.587

Ryo, Y., Miyawaki, A., Furuichi, T., and Mikoshiba, K. (1993). Expression of the metabotropic glutamate receptor mGluR1α and the ionotropic glutamate receptor GluR1 in the brain during the postnatal development of normal mouse and in the cerebellum from mutant mice. In *Journal of Neuroscience Research*. https://doi.org/10.1002/jnr.490360104

Ryu, J., Woo, J., Shin, J., Ryoo, H., Kim, Y., and Lee, C. (2014). Profile of differential promoter activity by nucleotide substitution at GWAS signals for multiple sclerosis. *Medicine (United States)*. https://doi.org/10.1097/MD.0000000000000281

Saito, N., and Shirai, Y. (2002). Protein kinase Cγ (PKCγ): Function of neuron specific isotype. In *Journal of Biochemistry*. https://doi.org/10.1093/oxfordjournals.jbchem.a003274

Saitoh, O., Kubo, Y., Miyatani, Y., Asano, T., and Nakata, H. (1997). RGS8 accelerates G-protein-mediated modulation of K+ currents. *Nature*, *390*(6659), 525–529. https://doi.org/10.1038/37385

Saitoh, Osamu, Kubo, Y., Odagiri, M., Ichikawa, M., Yamagata, K., and Sekine, T. (1999). RGS7 and RGS8 differentially accelerate G protein-mediated modulation of K+ currents. *Journal of Biological Chemistry*, *274*(14), 9899–9904. https://doi.org/10.1074/jbc.274.14.9899

Saitoh, Osamu, Masuho, I., Itoh, M., Abe, H., Komori, K., and Odagiri, M. (2003). Distribution of regulator of G protein signaling 8 (RGS8) protein in the cerebellum. *Cerebellum*, *2*(2), 154–160. https://doi.org/10.1080/14734220309409

Saitoh, Osamu, and Odagiri, M. (2003). RGS8 expression in developing cerebellar Purkinje cells. *Biochemical and Biophysical Research Communications*, *309*(4), 836–842. https://doi.org/10.1016/j.bbrc.2003.08.083

Sanjo, H., Kawait, T., and Akira, S. (1998). DRAKs, novel serine/threonine kinases related to death-associated protein kinase that trigger apoptosis. *Journal of Biological Chemistry*. https://doi.org/10.1074/jbc.273.44.29066

Saugstad, J. A., Marino, M. J., Folk, J. A., Hepler, J. R., and Conn, P. J. (1998). RGS4 inhibits signaling by group I metabotropic glutamate receptors. *Journal of Neuroscience*. https://doi.org/10.1523/jneurosci.18-03-00905.1998

Schaumburg, C. S., Gatzka, M., Walsh, C. M., and Lane, T. E. (2007). DRAK2 regulates memory T cell responses following murine coronavirus infection. *Autoimmunity*. https://doi.org/10.1080/08916930701651139

Schmidt, H., Arendt, O., Brown, E. B., Schwaller, B., and Eilers, J. (2007). Parvalbumin is freely mobile in axons, somata and nuclei of cerebellar Purkinje neurones. *Journal of Neurochemistry*. https://doi.org/10.1111/j.1471-4159.2006.04231.x

Schorge, S., van de Leemput, J., Singleton, A., Houlden, H., and Hardy, J. (2010). Human ataxias: a genetic dissection of inositol triphosphate receptor (ITPR1)-dependent signaling. *Trends in Neurosciences*. https://doi.org/10.1016/j.tins.2010.02.005

Schrenk, K., Kapfhammer, J. P., and Metzger, F. (2002). Altered dendritic development of cerebellar Purkinje cells in slice cultures from protein kinase Cγ-

deficient mice. *Neuroscience*, *110*(4), 675–689. https://doi.org/10.1016/S0306-4522(01)00559-0

Seidel, K., Den Dunnen, W. F. A., Schultz, C., Paulson, H., Frank, S., De Vos, R. A., Brunt, E. R., Deller, T., Kampinga, H. H., and Rüb, U. (2010). Axonal inclusions in spinocerebellar ataxia type 3. *Acta Neuropathologica*. https://doi.org/10.1007/s00401-010-0717-7

Seidel, K., Siswanto, S., Brunt, E. R. P., Den Dunnen, W., Korf, H. W., and Rüb, U. (2012). Brain pathology of spinocerebellar ataxias. *Acta Neuropathologica*, *124*(1), 1–21. https://doi.org/10.1007/s00401-012-1000-x

Sekerková, G., Kim, J. A., Nigro, M. J., Becker, E. B. E., Hartmann, J., Birnbaumer, L., Mugnaini, E., and Martina, M. (2013). Early onset of ataxia in moonwalker mice is accompanied by complete ablation of type II unipolar brush cells and purkinje cell dysfunction. *Journal of Neuroscience*. https://doi.org/10.1523/JNEUROSCI.2294-13.2013

Seki, N., Sugano, S., Suzuki, Y., Nakagawara, A., Ohira, M., Muramatsu, M. A., Saito, T., and Hori, T. A. (1998). Isolation, tissue expression, and chromosomal assignment of human RGS5, a novel G-protein signaling regulator gene. *Journal of Human Genetics*. https://doi.org/10.1007/s100380050071

Serra, H. G., Byam, C. E., Lande, J. D., Tousey, S. K., Zoghbi, H. Y., and Orr, H. T. (2004). Gene profiling links SCA1 pathophysiology to glutamate signaling in Purkinje cells of transgenic mice. *Human Molecular Genetics*. https://doi.org/10.1093/hmg/ddh268

Serra, H. G., Duvick, L., Zu, T., Carlson, K., Stevens, S., Jorgensen, N., Lysholm, A., Burright, E., Zoghbi, H. Y., Clark, H. B., Andresen, J. M., and Orr, H. T. (2006). RORα-Mediated Purkinje Cell Development Determines Disease Severity in Adult SCA1 Mice. *Cell*, *127*(4), 697–708. https://doi.org/10.1016/j.cell.2006.09.036

Sethakorn, N., and Dulin, N. O. (2013). RGS expression in cancer: Oncomining the cancer microarray data. *Journal of Receptors and Signal Transduction*. https://doi.org/10.3109/10799893.2013.773450

Shankar, S. P., Wilson, M. S., DiVietro, J. A., Mentink-Kane, M. M., Xie, Z., Wynn, T. A., and Druey, K. M. (2012). RGS16 Attenuates Pulmonary Th2/Th17 Inflammatory Responses. *The Journal of Immunology*. https://doi.org/10.4049/jimmunol.1103781

Shi, G.-X., Harrison, K., Wilson, G. L., Moratz, C., and Kehrl, J. H. (2002). RGS13 Regulates Germinal Center B Lymphocytes Responsiveness to CXC Chemokine Ligand (CXCL)12 and CXCL13. *The Journal of Immunology*. https://doi.org/10.4049/jimmunol.169.5.2507

Shigemoto, R., Nakanishi, S., and Mizuno, N. (1992). Distribution of the mRNA for a metabotropic glutamate receptor (mGluR1) in the central nervous system: An in situ hybridization study in adult and developing rat. *Journal of Comparative Neurology*. https://doi.org/10.1002/cne.903220110

Shima, Y., Copeland, N. G., Gilbert, D. J., Jenkins, N. A., Chisaka, O., Takeichi, M., and Uemura, T. (2002). Differential expression of the seven-pass transmembrane cadherin genes Celsr1-3 and distribution of the Celsr2 protein during mouse development. *Developmental Dynamics*. https://doi.org/10.1002/dvdy.10054

Shima, Y., Kengaku, M., Hirano, T., Takeichi, M., and Uemura, T. (2004). Regulation of dendritic maintenance and growth by a mammalian 7-pass transmembrane cadherin. *Developmental Cell*, *7*(2), 205–216. https://doi.org/10.1016/j.devcel.2004.07.007

Shimobayashi, E., and Kapfhammer, J. P. (2017). Increased biological activity of protein Kinase C gamma is not required in Spinocerebellar ataxia 14. *Molecular Brain*, *10*(1), 1–11. https://doi.org/10.1186/s13041-017-0313-z

Shimobayashi, E., and Kapfhammer, J. P. P. (2018). Calcium Signaling, PKC Gamma, IP3R1 and CAR8 Link Spinocerebellar Ataxias and Purkinje Cell Dendritic Development. *Current Neuropharmacology*, *16*(2). https://doi.org/10.2174/1570159x15666170529104000

Shimobayashi, E., Wagner, W., and Kapfhammer, J. P. (2016). Carbonic Anhydrase 8 Expression in Purkinje Cells Is Controlled by PKCγ Activity and Regulates Purkinje Cell Dendritic Growth. *Molecular Neurobiology*, *53*(8), 5149–5160. https://doi.org/10.1007/s12035-015-9444-3

Shirafuji, T., Shimazaki, H., Miyagi, T., Ueyama, T., Adachi, N., Tanaka, S., Hide, I., Saito, N., and Sakai, N. (2019). Spinocerebellar ataxia type 14 caused by a nonsense mutation in the PRKCG gene. *Molecular and Cellular Neuroscience*. https://doi.org/10.1016/j.mcn.2019.05.005

Shuvaev, A. N., Hosoi, N., Sato, Y., Yanagihara, D., and Hirai, H. (2017). Progressive impairment of cerebellar mGluR signalling and its therapeutic potential for cerebellar ataxia in spinocerebellar ataxia type 1 model mice. *Journal of Physiology*. https://doi.org/10.1113/JP272950

Sirzen-Zelenskaya, A., Zeyse, J., and Kapfhammer, J. P. (2006). Activation of class I metabotropic glutamate receptors limits dendritic growth of Purkinje cells in organotypic slice cultures. *European Journal of Neuroscience*. https://doi.org/10.1111/j.1460-9568.2006.05196.x

Smoller, J. W., Paulus, M. P., Fagerness, J. A., Purcell, S., Yamaki, L. H., Hirshfeld-Becker, D., Biederman, J., Rosenbaum, J. F., Gelernter, J., and Stein, M. B. (2008). Influence of RGS2 on anxiety-related temperament, personality, and brain function. *Archives of General Psychiatry*. https://doi.org/10.1001/archgenpsychiatry.2007.48

Smyth, D. J., Plagnol, V., Walker, N. M., Cooper, J. D., Downes, K., Yang, J. H. M., Howson, J. M. M., Stevens, H., McManus, R., Wijmenga, C., Heap, G. A.,

Dubois, P. C., Clayton, D. G., Hunt, K. A., Van Heel, D. A., and Todd, J. A. (2008). Shared and distinct genetic variants in type 1 diabetes and celiac disease. *New England Journal of Medicine*. https://doi.org/10.1056/NEJMoa0807917

Snow, B. E., Antonio, L., Suggs, S., Gutstein, H. B., and Siderovski, D. P. (1997). Molecular cloning and expression analysis of rat Rgs12 and Rgs14. *Biochemical and Biophysical Research Communications*. https://doi.org/10.1006/bbrc.1997.6537

Sotelo, C., and Dusart, I. (2009). Intrinsic versus extrinsic determinants during the development of Purkinje cell dendrites. In *Neuroscience*. https://doi.org/10.1016/j.neuroscience.2008.12.035

Sotelo, Constantino. (2004). Cellular and genetic regulation of the development of the cerebellar system. In *Progress in Neurobiology*. https://doi.org/10.1016/j.pneurobio.2004.03.004

Squires, K. E., Montañez-Miranda, C., Pandya, R. R., Torres, M. P., and Hepler, J. R. (2018). Genetic analysis of rare human variants of regulators of G protein signaling proteins and their role in human physiology and disease. *Pharmacological Reviews*, *70*(3), 446–474. https://doi.org/10.1124/pr.117.015354

Steinmayr, M., André, E., Conquet, F., Rondi-Reig, L., Delhaye-Bouchaud, N., Auclair, N., Daniel, H., Crépel, F., Mariani, J., Sotelo, C., and Becker-André, M. (1998). staggerer Phenotype in retinoid-related orphan receptor α-deficient mice. *Proceedings of the National Academy of Sciences of the United States of America*. https://doi.org/10.1073/pnas.95.7.3960

Stoyas, C. A., Bushart, D. D., Switonski, P. M., Ward, J. M., Alaghatta, A., Tang, M. bo, Niu, C., Wadhwa, M., Huang, H., Savchenko, A., Gariani, K., Xie, F., Delaney, J. R., Gaasterland, T., Auwerx, J., Shakkottai, V. G., and La Spada, A.

R. (2020). Nicotinamide Pathway-Dependent Sirt1 Activation Restores Calcium Homeostasis to Achieve Neuroprotection in Spinocerebellar Ataxia Type 7. *Neuron*. https://doi.org/10.1016/j.neuron.2019.11.019

Tanaka, J., Nakagawa, S., Kushiya, E., Yamasaki, M., Fukaya, M., Iwanaga, T., Simon, M. I., Sakimura, K., Kano, M., and Watanabe, M. (2000). Gq protein α subunits Gαq and Gα11 are localized at postsynaptic extra-junctional membrane of cerebellar Purkinje cells and hippocampal pyramidal cells. *European Journal of Neuroscience*, *12*(3), 781–792. https://doi.org/10.1046/j.1460-9568.2000.00959.x

Taylor, V. G., Bommarito, P. A., and Tesmer, J. J. G. (2016). Structure of the regulator of G protein signaling 8 (RGS8)-Gαq complex: Molecular basis for Gα selectivity. *Journal of Biological Chemistry*, *291*(10), 5138–5145. https://doi.org/10.1074/jbc.M115.712075

Toyoshi, E., Shigeru, K., and Toshimasa, O. (1985). Immunochemical and immunohistochemical localization of parvalbumin in rat nervous tissues. *Neuroscience Research Supplements*. https://doi.org/10.1016/s0921-8696(85)80029-3

Trzesniewski, J., Altmann, S., Jäger, L., and Kapfhammer, J. P. (2019). Reduced Purkinje cell size is compatible with near normal morphology and function of the cerebellar cortex in a mouse model of spinocerebellar ataxia. *Experimental Neurology*, *311*(June 2018), 205–212. https://doi.org/10.1016/j.expneurol.2018.10.004

Van De Leemput, J., Chandran, J., Knight, M. A., Holtzclaw, L. A., Scholz, S., Cookson, M. R., Houlden, H., Gwinn-Hardy, K., Fung, H. C., Lin, X., Hernandez, D., Simon-Sanchez, J., Wood, N. W., Giunti, P., Rafferty, I., Hardy, J., Storey, E., Gardner, R. J. M. K., Forrest, S. M., … Singleton, A. B. (2007). Deletion at ITPR1 underlies ataxia in mice and spinocerebellar ataxia 15 in humans. *PLoS Genetics*. https://doi.org/10.1371/journal.pgen.0030108

Vecellio, M., Schwaller, B., Meyer, M., Hunziker, W., and Celio, M. R. (2000). Alterations in Purkinje cell spines of calbindin D-28 k and parvalbumin knock-out mice. *European Journal of Neuroscience*. https://doi.org/10.1046/j.1460-9568.2000.00986.x

Vig, P. J. S., Wei, J., Shao, Q., Lopez, M. E., Halperin, R., and Gerber, J. (2012). Suppression of calbindin-D28k expression exacerbates SCA1 phenotype in a disease mouse model. *Cerebellum*. https://doi.org/10.1007/s12311-011-0323-9

Wagner, W., Brenowitz, S. D., and Hammer, J. A. (2011). Myosin-Va transports the endoplasmic reticulum into the dendritic spines of Purkinje neurons. *Nature Cell Biology*, *13*(1), 40–47. https://doi.org/10.1038/ncb2132

Wagner, W., McCroskery, S., and Hammer, J. A. (2011). An efficient method for the long-term and specific expression of exogenous cDNAs in cultured Purkinje neurons. *Journal of Neuroscience Methods*, *200*(2), 95–105. https://doi.org/10.1016/j.jneumeth.2011.06.006

Wang, D., Chan, C. C., Cherry, S., and Hiesinger, P. R. (2013). Membrane trafficking in neuronal maintenance and degeneration. In *Cellular and Molecular Life Sciences*. https://doi.org/10.1007/s00018-012-1201-4

Wang, J., Ducret, A., Tu, Y., Kozasa, T., Aebersold, R., and Ross, E. M. (1998). RGSZ1, a G(z)-selective rgs protein in brain: Structure, membrane association, regulation by Gα(z) phosphorylation, and relationship to a G(z) gtpase-activating protein subfamily. *Journal of Biological Chemistry*. https://doi.org/10.1074/jbc.273.40.26014

Wang, Q., Liu, X., Zhou, J., Yang, C., Wang, G., Tan, Y., Wu, Y., Zhang, S., Yi, K., and Kang, C. (2019). The CRISPR-Cas13a Gene-Editing System Induces Collateral Cleavage of RNA in Glioma Cells. *Advanced Science*, *6*(20). https://doi.org/10.1002/advs.201901299

Wang, S., Xu, L., Lu, Y. T., Liu, Y. F., Han, B., Liu, T., Tang, J., Li, J., Wu, J., Li, J. Y., Yu, L. F., and Yang, F. (2017). Discovery of benzofuran-3(2H)-one derivatives as novel DRAK2 inhibitors that protect islet β-cells from apoptosis. *European Journal of Medicinal Chemistry*, *130*, 195–208. https://doi.org/10.1016/j.ejmech.2017.02.048

Wang, Y., Wang, J., Zhang, L., Karatas, O. F., Shao, L., Zhang, Y., Castro, P., Creighton, C. J., and Ittmann, M. (2017). RGS12 is a novel tumor-suppressor gene in African American prostate cancer that represses AKT and MNX1 expression. *Cancer Research*. https://doi.org/10.1158/0008-5472.CAN-17-0669

Waters, M. F., Minassian, N. A., Stevanin, G., Figueroa, K. P., Bannister, J. P. A., Nolte, D., Mock, A. F., Evidente, V. G. H., Fee, D. B., Müller, U., Dürr, A., Brice, A., Papazian, D. M., and Pulst, S. M. (2006). Mutations in voltage-gated potassium channel KCNC3 cause degenerative and developmental central nervous system phenotypes. *Nature Genetics*. https://doi.org/10.1038/ng1758

Watson, L. M., Bamber, E., Schnekenberg, R. P., Williams, J., Bettencourt, C., Lickiss, J., Fawcett, K., Clokie, S., Wallis, Y., Clouston, P., Sims, D., Houlden, H., Becker, E. B. E., and Németh, A. H. (2017). Dominant Mutations in GRM1 Cause Spinocerebellar Ataxia Type 44. *American Journal of Human Genetics*, *101*(3), 451–458. https://doi.org/10.1016/j.ajhg.2017.08.005

Watson, N., Linder, M. E., Druey, K. M., Kehrl, J. H., and Blumer, K. J. (1996). RGS family members: GTPase-activating proteins for heterotrimeric G- protein α-subunits. *Nature*. https://doi.org/10.1038/383172a0

Weiner, J. L., Guttierez-Steil, C., and Blumer, K. J. (1993). Disruption of receptor-G protein coupling in yeast promotes the function of an SST2-dependent adaptation pathway. *Journal of Biological Chemistry*.

White, J. J., and Sillitoe, R. V. (2013). Development of the cerebellum: From gene expression patterns to circuit maps. *Wiley Interdisciplinary Reviews:*

Developmental Biology. https://doi.org/10.1002/wdev.65

White, M. R., Mitrea, D. M., Zhang, P., Stanley, C. B., Cassidy, D. E., Nourse, A., Phillips, A. H., Tolbert, M., Taylor, J. P., and Kriwacki, R. W. (2019). C9orf72 Poly(PR) Dipeptide Repeats Disturb Biomolecular Phase Separation and Disrupt Nucleolar Function. *Molecular Cell*. https://doi.org/10.1016/j.molcel.2019.03.019

Wilke, C., Bender, F., Hayer, S. N., Brockmann, K., Schöls, L., Kuhle, J., and Synofzik, M. (2018). Serum neurofilament light is increased in multiple system atrophy of cerebellar type and in repeat-expansion spinocerebellar ataxias: a pilot study. *Journal of Neurology*. https://doi.org/10.1007/s00415-018-8893-9

Willars, G. B. (2006). Mammalian RGS proteins: Multifunctional regulators of cellular signalling. *Seminars in Cell and Developmental Biology*, *17*(3), 363–376. https://doi.org/10.1016/j.semcdb.2006.03.005

Wong, M. M. K., Hoekstra, S. D., Vowles, J., Watson, L. M., Fuller, G., Németh, A. H., Cowley, S. A., Ansorge, O., Talbot, K., and Becker, E. B. E. (2018). Neurodegeneration in SCA14 is associated with increased PKCγ kinase activity, mislocalization and aggregation. *Acta Neuropathologica Communications*. https://doi.org/10.1186/s40478-018-0600-7

Woods, N. B., Muessig, A., Schmidt, M., Flygare, J., Olsson, K., Salmon, P., Trono, D., Von Kalle, C., and Karlsson, S. (2003). Lentiviral vector transduction of NOD/SCID repopulating cells results in multiple vector integrations per transduced cell: Risk of insertional mutagenesis. *Blood*. https://doi.org/10.1182/blood-2002-07-2238

Yalcin, B., Willis-Owen, S. A. G., Fullerton, J., Meesaq, A., Deacon, R. M., Rawlins, J. N. P., Copley, R. R., Morris, A. P., Flint, J., and Mott, R. (2004). Genetic dissection of a behavioral quantitative trait locus shows that Rgs2 modulates anxiety in mice. *Nature Genetics*. https://doi.org/10.1038/ng1450

Yamazaki, T., Igarashi, J., Makino, J., and Ebisuzaki, T. (2019). Real-time simulation of a cat-scale artificial cerebellum on PEZY-SC processors. *International Journal of High Performance Computing Applications*. https://doi.org/10.1177/1094342017710705

Yang, A. W., Sachs, A. J., and Nystuen, A. M. (2015). Deletion of Inpp5a causes ataxia and cerebellar degeneration in mice. *Neurogenetics*, *16*(4), 277–285. https://doi.org/10.1007/s10048-015-0450-4

Yang, J., Huang, J., Maity, B., Gao, Z., Lorca, R. A., Gudmundsson, H., Li, J., Stewart, A., Swaminathan, P. D., Ibeawuchi, S. R., Shepherd, A., Chen, C. K., Kutschke, W., Mohler, P. J., Mohapatra, D. P., Anderson, M. E., and Fisher, R. A. (2010). RGS6, a modulator of parasympathetic activation in heart. *Circulation Research*. https://doi.org/10.1161/CIRCRESAHA.110.224220

Yang, L., Lee, M. M. K., Leung, M. M. H., and Wong, Y. H. (2016). Regulator of G protein signaling 20 enhances cancer cell aggregation, migration, invasion and adhesion. *Cellular Signalling*. https://doi.org/10.1016/j.cellsig.2016.07.017

Yang, S. H., Li, C. F., Chu, P. Y., Ko, H. H., Chen, L. T., Chen, W. W., Han, C. H., Lung, J. H., and Shih, N. Y. (2016). Overexpression of regulator of G protein signaling 11 promotes cell migration and associates with advanced stages and aggressiveness of lung adenocarcinoma. *Oncotarget*. https://doi.org/10.18632/oncotarget.8860

Yang, S., and Li, Y. P. (2007). RGS12 is essential for RANKL-evoked signaling for terminal differentiation of osteoclasts in vitro. *Journal of Bone and Mineral Research*. https://doi.org/10.1359/jbmr.061007

Yang, S., Li, Y. P., Liu, T., He, X., Yuan, X., Li, C., Cao, J., and Kim, Y. (2013). Mx1-Cre mediated Rgs12 conditional knockout mice exhibit increased bone mass phenotype. *Genesis*. https://doi.org/10.1002/dvg.22373

Yang, Y., Sun, K., Liu, W., Zhang, L., Peng, K., Zhang, S., Li, S., Yang, M., Jiang, Z., Lu, F., and Zhu, X. (2018). Disruption of Tmem30a results in cerebellar ataxia and degeneration of Purkinje cells. *Cell Death and Disease*, *9*(9). https://doi.org/10.1038/s41419-018-0938-6

Yoshida, Y., Huang, F. L., Nakabayashi, H., and Huang, K. P. (1988). Tissue distribution and developmental expression of protein kinase C isozymes. *Journal of Biological Chemistry*.

You, M., Wang, D., Liu, P., Vikis, H., James, M., Lu, Y., Wang, Y., Wang, M., Chen, Q., Jia, D., Liu, Y., Wen, W., Yang, P., Sun, Z., Pinney, S. M., Zheng, W., Shu, X. O., Long, J., Gao, Y. T., … Anderson, M. W. (2009). Fine mapping of chromosome 6q23-25 region in familial lung cancer families reveals RGS17 as a likely candidate gene. *Clinical Cancer Research*. https://doi.org/10.1158/1078-0432.CCR-08-2335

Yvert, G. (2000). Expanded polyglutamines induce neurodegeneration and trans-neuronal alterations in cerebellum and retina of SCA7 transgenic mice. *Human Molecular Genetics*. https://doi.org/10.1093/hmg/9.17.2491

Zhang, K., Howes, K. A., He, W., Bronson, J. D., Pettenati, M. J., Chen, C. K., Palczewski, K., Wensel, T. G., and Baehr, W. (1999). Structure, alternative splicing, and expression of the human RGS9 gene. *Gene*. https://doi.org/10.1016/S0378-1119(99)00393-5

Zhang, P., and Mende, U. (2011). Regulators of g-protein signaling in the heart and their potential as therapeutic targets. *Circulation Research*, *109*(3), 320–333. https://doi.org/10.1161/CIRCRESAHA.110.231423

Zhang, S., Watson, N., Zahner, J., Rottman, J. N., Blumer, K. J., and Muslin, A. J. (1998). RGS3 and RGS4 are GTPase activating proteins in the heart. *Journal of Molecular and Cellular Cardiology*. https://doi.org/10.1006/jmcc.1997.0591

Zhang, Y., Snider, A., Willard, L., Takemoto, D. J., and Lin, D. (2009). Loss of Purkinje cells in the PKCγ H101Y transgenic mouse. *Biochemical and Biophysical Research Communications*. https://doi.org/10.1016/j.bbrc.2008.11.082

Zhao, X., Liu, L., Lang, J., Cheng, K., Wang, Y. Y., Li, X., Shi, J., Wang, Y. Y., and Nie, G. (2018). A CRISPR-Cas13a system for efficient and specific therapeutic targeting of mutant KRAS for pancreatic cancer treatment. *Cancer Letters*, *431*(May), 171–181. https://doi.org/10.1016/j.canlet.2018.05.042

Zhuchenko, O., Bailey, J., Bonnen, P., Ashizawa, T., Stockton, D. W., Amos, C., Dobyns, W. B., Subramony, S. H., Zoghbi, H. Y., and Lee, C. C. (1997). Autosomal dominant cerebellar ataxia (SCA6) associated with small polyglutamine expansions in the α(1A)-voltage-dependent calcium channel. In *Nature Genetics*. https://doi.org/10.1038/ng0197-62

Zu, T., Duvick, L. A., Kaytor, M. D., Berlinger, M. S., Zoghbi, H. Y., Clark, H. B., and Orr, H. T. (2004). Recovery from polyglutamine-induced neurodegeneration in conditional SCA1 transgenic mice. *Journal of Neuroscience*. https://doi.org/10.1523/JNEUROSCI.2978-04.2004

Acknowledgements

I would like to take this opportunity to thank my supervisor and the members of my dissertation committee, Prof. Josef Kapfhammer, Prof. Markus Rüegg and Prof. Beat Schwaller.

The knowledge and experience in developmental neurobiology and regeneration of my supervisor Josef Kapfhammer were essential and he gave me the guidance I needed to pursue my research. His patience and constant encouragement during my studies have helped me to keep on track in challenging times. Thank you to Prof. Markus Rüegg for being my official supervisor of the Faculty of Natural Sciences and thank you to Prof. Beat Schwaller for being the external expert of my dissertation committee. Their knowledge and perspective were very constructive and helpful and inspired me to have some new idea. They pointed out the limitations and provided advice during my studies to improve my project in each of my PhD committee meetings.

Thank you to Dr. Etsuko Shimobayashi for introducing me in biological technologies, especially cerebellar dissociated culture, which play an important role in my research. Thank you to Markus Saxer and Aleksandar Kovacevic for their technical assistance. Thank you to Prof. Eline Pecho-Vrieseling, for sharing the transfection device with me. I would like to thank the people in the lab for their help and friendship: Sabine Winkler, who sometimes shares interesting things to create a happy office atmosphere. The former graduate student Dr. Pradeep Sherkhane shared his experience of PhD studies. Thanks to the collaborator of our laboratory, Dr. Xinzhou Zhu, who recommended Prof. Josef Kapfhammer to me. Thanks to all the nice people I meet in the anatomy institute.

I would also like to thank my mother and my relatives for their love, understanding and support. Thanks for their help with my father's funeral. At last, I dedicate this

thesis to my late father Zhong-Liang Wu who taught me to be an independent and determined person.

P.S. The contribution to the printing cost of this dissertation is granted by the University of Basel dissertation fund or the Basel Scholarship Foundation.